Structure and Spectroscopy of Copper–Dioxygen Complexes

Liviu M. Mirica, Xavier Ottenwaelder, and T. Daniel P. Stack*

Department of Chemistry, Stanford University, Stanford, California 94305

Received August 15, 2003

Contents

1. Introduction

The reactions of Cu(I) complexes with O_2 and the oxidative properties of the resulting Cu/O_2 complexes have attracted much interest during the past decades because of their potential relevance to biochemical systems[1−3] and synthetic catalysis.[4−9] Different aspects of this field have been reviewed recently.[10−13] The oxidation of Cu(I) by O_2 in homogeneous solutions is a deceptively simple reaction. Many structurally diverse species form, most of which are thermally unstable even under optimal reaction conditions. The substitution lability of Cu(I) and Cu(II) ions makes the role of ligation paramount in controlling which species form and how stable they are. Seemingly minor ligand alterations can dramatically affect the oxygenation reactions, thus providing an incisive mechanistic probe if ligand variation is systematic. More efficient Cu-based oxidants and greater insights into biochemical O_2 activation processes will surely result from such investigations.

This review focuses on the structures and spectroscopic properties of well-characterized Cu/O_2 species formed by the reaction of Cu(I) complexes with O_2.[5] The number of such synthetic species now far exceeds those characterized in biochemical systems. Yet each new structural/spectroscopic type provides additional insights into the nuances of Cu/O_2 reactions that are fundamental to aerobic life and represents an energetically plausible intermediate in Cu-mediated biochemical oxidation processes. A bewildering array of Cu(I) complexes with ligands of variable nucleating and chelating abilities has served as precursors to different Cu/O_2 species. Our objective is to highlight the ligand attributes that create O_2-reactive Cu(I) complexes and lead to specific types of Cu/O_2 species.[14]

2. General Considerations

2.1. Role of Cu in Biology

Beyond the potential industrial applications of Cu/O_2-based oxidants,[15−17] understanding the fundamental aspects of the reactions between Cu(I) complexes and O_2 finds great inspiration in biochemical systems. In metalloenzymes, Cu exists in mononuclear and coupled multinuclear configurations that have evolved to facilitate redox processes. The predominant roles of most Cu enzymes are O_2 activation and subsequent substrate oxidation. Conventional wisdom suggests that biological Cu serves exclusively as a 1e$^-$ shuttle, alternating between Cu(I) and Cu(II). The Cu(III) oxidation state is generally considered to be inaccessible because of the highly positive Cu(III)/Cu(II) redox potentials that result from ligation of typical amino acid side chains such as imidazoles and phenolate ions.[18]

10.1021/cr020632z CCC: $48.50
Published on Web 01/29/2004

Liviu M. Mirica, a native of Romania, transferred in 1996 from the University of Bucharest to California Institute of Technology. He obtained his B.S. degree in chemistry in 1999, performing research in the laboratories of Professor H. B. Gray. He then started his graduate studies at Stanford University in the Department of Chemistry under the supervision of Professor T. D. P. Stack, as a John Stauffer Stanford Graduate Fellow. His thesis investigations are focused on the hydroxylation mechanism of binuclear copper complexes similar to that observed in tyrosinase.

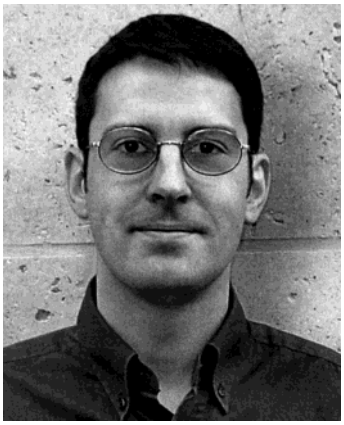

Xavier Ottenwaelder, a native of Champagne and Burgundy regions, France, pursued his undergraduate studies at the Ecole Normale Supérieure of Lyon. In 2001, he obtained his Ph.D. degree from the University Paris XI (Orsay) under the supervision of Dr. Y. Journaux and Dr. A. Aukauloo for work on molecular magnetism and radical-metallo-complexes. He is currently a postdoctoral fellow in the group of Professor T. D. P. Stack with interests in biomimetic inorganic chemistry.

Professor T. Daniel P. Stack obtained his undergraduate degree at Reed College and his Ph.D. degree from Harvard University working with Professor R. H. Holm. After completing a NSF postdoctoral fellowship with Professor K. N. Raymond at the University of California, Berkeley, he joined the faculty at Stanford University. He is currently an Associate Professor of Chemistry developing bio-inspired oxidation catalysts containing copper, iron, and manganese.

Cu-containing enzymes that activate O_2 function as dioxygenases, monooxygenases, and oxidases (Figure 1),[1,2,19] yet the nuclearity of the active site does not correlate directly with the type of reactivity, e.g., mononuclear Cu enzymes perform all three types of reactions. Quercetin 2,3-dioxygenase is currently the only firmly established mononuclear Cu dioxygenase, and it is thought to activate O_2 only after substrate reduction of the resting-state Cu(II) center.[20] Dopamine β-hydroxylase (DβH)[1] and peptidylglycine α-hydroxylating monooxygenase (PHM)[1,21,22] are mononuclear Cu monooxygenases capable of hydroxylating weak C−H bonds (ca. 88 kcal mol^{-1}) using a second reducing equivalent from a distant Cu center (Cu···Cu $\approx$ 10 Å). All mononuclear Cu oxidases have associated organic factors created by Cu-dependent post-translational oxidative modifications of an endogenous amino acid side chain (amine oxidase (AmO),[1,23] galactose oxidase (GOase),[24,25] glyoxal oxidase,[24,26] lysyl oxidase[27−29]). While it does not activate O_2, the enzyme Cu/Zn superoxide dismutase (SOD) is proposed to perform the microscopic reverse of this reaction by binding superoxide to Cu(II) to produce O_2 and Cu(I).[30]

The binuclear Cu protein hemocyanin (Hc)[2] and the binuclear Cu enzymes tyrosinase (Ty)[2] and catechol oxidase (CO)[31,32] bind O_2 reversibly by forming spectroscopically similar peroxide species. Yet the oxygenated form of the O_2 transport protein Hc (oxyHc) does not oxidize catechols to quinones as oxyTy or oxyCO do nor can oxyCO duplicate the monooxygenase activity of oxyTy. Accessibility of substrates to the oxygenated active site is thought to be responsible for these differences in reactivity.[33−35]

Multinuclear blue oxidase enzymes—laccase, ascorbate oxidase (AO), ceruloplasmin, FET3—couple the 4e$^-$ reduction of O_2 to water with the oxidation of a variety of electron-rich substrates.[2] A mononuclear Cu center, the so-called blue-copper that gives these enzymes their distinctive colors, is positioned ca. 12 Å from the trinuclear Cu O_2-binding site and provides the fourth reducing equivalent in the reaction.[36−40] The other enzyme capable of performing the 4e$^-$ reduction of O_2 to water is cytochrome *c* oxidase,[41] which contains a mononuclear Cu site associated with an Fe heme center (see Karlin's and Collman's reviews in this issue). Other multinuclear configurations of Cu active sites are thought to exist in particulate methane monooxygenase (pMMO)[42,43] and ammonia monooxygenase,[44] two enzymes capable of activating strong C−H and N−H bonds (>93 kcal mol^{-1}), respectively. More extensive descriptions of Cu/O_2 enzymes are available in recent biology-focused reviews.[1,2]

The coordination environments of Cu in these enzymes and proteins provide important insights into the structural attributes that are required for function. More structural data exist for the reduced than the oxygenated forms of these enzymes and proteins, yet it is the correlation between the two forms that is most informative. Trigonal ligation of Cu(I) by uncharged ligands is common for these reduced Cu enzymes and proteins (Figure 2).[45−51] The ligands are predominantly imidazoles from histidine residues,

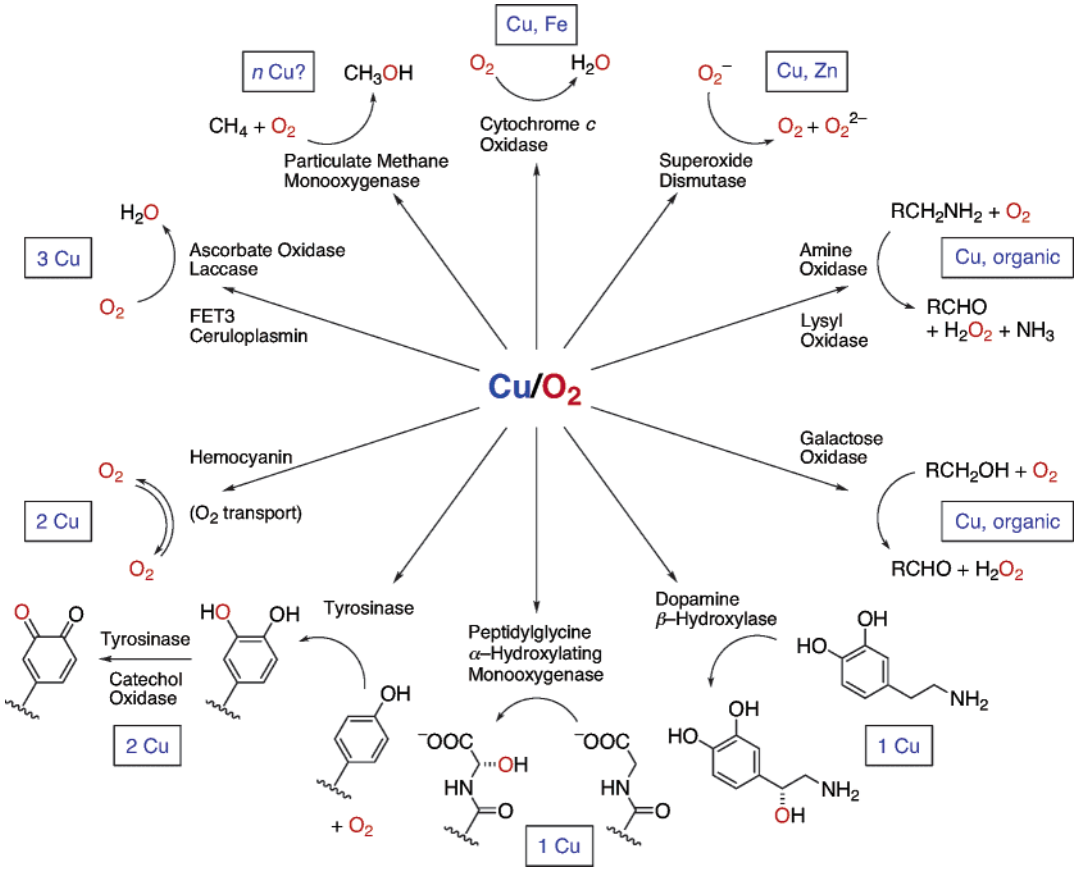

Figure 1. Selected Cu enzymes and proteins that activate O_2.[18]

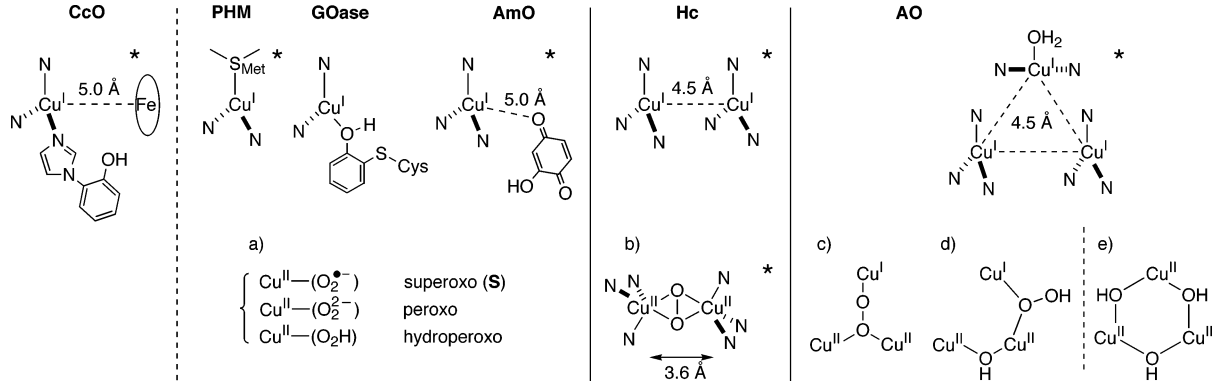

Figure 2. Active sites of Cu enzymes and proteins in their reduced state (top) and proposed oxygenated forms generated by reaction with O_2 (bottom, a−e). Species noted with an asterisk (*) have been crystallographically characterized.

but other ligands such as a water molecule, a methionine thioether, or a tyrosine phenol may occupy a single position.[45,50,51] For mononuclear Cu/O_2 enzymes, none of the proposed intermediates has yet been spectroscopically characterized (Figure 2a).

Hemocyanin is the only Cu protein that is crystallographically characterized in both reduced (redHc) and oxygenated (oxyHc) forms. In both forms of the protein, tris(imidazole) ligation is found at each Cu center. In redHc, the trigonally ligated Cu(I) ions are separated by ca. 4.5 Å;[52,53] in oxyHc, O_2 is reduced by 2e$^-$ to form the peroxide ion, which is ligated in a μ-η^2:η^2 configuration (i.e., bridging and side-on) (Figure 2b).[47,53−55] Each five-coordinated Cu(II) center has a distorted square-pyramidal geometry with one histidine nitrogen atom that is weakly associated (Figure 15c and d); the Cu···Cu separation of ca. 3.6 Å is significantly contracted relative to that in redHc. The spectroscopic congruency of oxyTy and oxyCO with oxyHc suggests similar ligation environments in all three oxygenated forms.[2]

The trinuclear Cu site in the blue oxidases from mammals, plants, and bacteria creates an efficient catalyst for reducing O_2 to H_2O. In reduced ascorbate oxidase (redAO), each Cu center of the trinuclear core bears three ligands from a total of eight imidazole ligands and a single water molecule; the Cu···Cu separations are ca. 4.5 Å. Extensive structural, spectroscopic, and kinetic studies provide a consensus mechanism for the 4e$^-$ reduction of O_2 to H_2O that involves two consecutive 2e$^-$ steps. The rate-limiting formation of a peroxide-level intermediate (Figure 2c or d)[56] is followed by a concerted transfer of two electrons, one from the Cu(I) ion of the trinuclear core

and one from the remote blue Cu site. This faster second step creates a postulated tris(hydroxy) trinuclear species (Figure 2e).[3,57]

In biochemical systems, tris-ligation of Cu(I) is undoubtedly purposeful for O_2 reactivity. Three-coordinated Cu(I) complexes with neutral ligands are weak reducing agents, which precludes fast outer-sphere reduction of O_2 to superoxide ion[3,58] and makes an associative, inner-sphere O_2 activation mechanism more favorable.[59] Therefore, a three-coordinated Cu center affords unfettered access for O_2, an impotent ligand intrinsically, and coordination flexibility necessary to accept the nascent reduced-O_2 ligand(s). Oxidation of Cu triggers significant changes of its structural preferences, such as those observed upon oxygenation of Hc. In the case of Hc, the proximity of the Cu(I) centers creates the possibility for the simultaneous $2e^-$ reduction of O_2, a process supported by recent DFT calculations.[58] Overall, these consistent structural trends observed for Cu in biochemical systems have guided the design of ligands for studying Cu/O_2 reactivity.

2.2. Synthetic Approach

Designing small-molecule models for O_2-activating metalloenzymes is difficult at best and leaves one with a profound appreciation for nature's subtle use of macromolecular engineering to develop metal-binding active sites. These sites exhibit remarkable levels of substrate selectivity and oxidative stability to survive multiple redox turnovers. Due to the lability and coordination flexibility of Cu(I) and Cu(II) complexes, the ligand dictates the pathway for Cu/O_2 reactivity. Ligands must approximate particular active site geometries yet retain the flexibility to accommodate the multiple oxidation states of the metal, all the while limiting unwanted side reactions and unintended oligomerization processes that can dominate in homogeneous solutions. The design of appropriate ligands for this chemistry is thus greatly aided by an appreciation of the geometric preferences of Cu in each oxidation state.

2.2.1. Geometric Preferences of Cu Centers

Cu(I). Univalent Cu has a d^{10} electronic configuration and is relatively indifferent to coordination topology. Its geometry is dominated by steric factors and/or structural constraints in the case of polydentate ligands. The high lability and geometric flexibility of Cu(I) complexes allow numerous geometries. Even though tetrahedral or trigonal-monopyramidal four-coordinated complexes are most common, T- or Y-shaped three-coordinated and linear two-coordinated complexes are frequently observed. Five-coordinated Cu(I) complexes are rare and in all cases have at least one Cu−ligand bond that is significantly longer than the others.[60−67]

Cu(II). The d^9 configuration of Cu(II) in an octahedral field leads to a significant Jahn−Teller distortion that usually manifests itself as an axial elongation, consistent with the lability and geometric flexibility of Cu(II) complexes. Hence, Cu(II) compounds commonly have square-planar or square-pyramidal geometries with ligands weakly associated in the axial position(s) at distances of 2.3−2.6 Å. In such complexes, the single unpaired electron is localized in the $d_{x^2-y^2}$ orbital. Trigonal-bipyramidal coordination of Cu(II) is also possible, in which case the electronic ground state has usually the unpaired electron in the d_{z^2} orbital. In either case, bridged compounds in which two or more Cu(II) ions are linked by anionic ligands (e.g., oxide, hydroxide) are commonplace; either an antiferromagnetic or a ferromagnetic coupling between the Cu(II) ions is observed.[68,69]

Cu(III). Discrete complexes of Cu(III) are much less common than those of Cu(I) and Cu(II). Such complexes are generally stabilized by strongly basic, anionic ligands that accommodate a square-planar geometry;[70−77] axial ligation to these square-planar complexes generally increases their oxidizing potentials.[71] While a d^8 Cu(III) center can exist in a high-spin state ($S = 1$),[78,79] all discrete Cu(III) complexes with oxygen ligation are low-spin and diamagnetic.

2.2.2. Biomimetic Cu/O_2 Chemistry

The expanded research efforts during the past two decades to stabilize and characterize Cu/O_2 species formed by the oxygenation of Cu(I) complexes can be attributed partly to a greater accessibility of appropriate spectroscopic tools and to a better appreciation of the appropriate reaction conditions. Low temperatures (ca. 200 K), aprotic solvents (e.g., CH_2Cl_2, THF, acetone), and weakly coordinating anions are now standard conditions. This approach contrasts with the earlier studies that relied on using ambient temperatures and coordinating anions (e.g., chloride, nitrate, or acetate); under these conditions, most Cu(I) complexes react with O_2 in a 4:1 stoichiometry without any measurable accumulation of intermediates. The ensuing products are Cu(II) complexes ligated by oxide-level ligands—oxide, hydroxide, or water—created by O_2 reduction.[80] Lower reaction temperatures enhance the lifetime of the initially formed Cu/O_2 species by reducing the entropic costs of formation and by attenuating subsequent reactions. This strategy has yielded well-characterized thermally sensitive species with Cu:O_2 reaction stoichiometries of 1:1, 2:1, and 3:1.

The formation of Cu/O_2 species is obviously contingent upon starting with O_2-reactive Cu(I) complexes, a property ensured through use of appropriate ligation. The Cu(I)/Cu(II) oxidation potential of a complex does not correlate necessarily with O_2 reactivity; redox potentials measure the energy associated with outer-sphere electron transfer, but the activation of O_2 through an inner-sphere process must also include the binding energy of the reduced-O_2 ligand. Many Cu(I) complexes with oxidation potentials greater than 1 V versus SCE readily react with O_2 because the reduced-O_2 moiety is accommodated in a favorable binding mode on the oxidized Cu center.

As found in biochemical systems, the reaction of Cu(I) with O_2 most reasonably proceeds through either a three-coordinated (T or Y shape) or four-coordinated monopyramidal Cu(I) complex. Associative addition of O_2 to a tetrahedral complex is less probable, even though many of the O_2-reactive Cu(I)

complexes are four-coordinated. In such cases, the complex presumably adopts either a monopyramidal geometry that is allowed by ligand flexibility and makes an axial position accessible or a trigonal geometry through the loss of a labile auxiliary ligand (e.g., acetonitrile, ethylene) from the initial tetrahedral geometry. Indeed, a recent study of a tridentate calixarene-based ligand clearly shows that formation of a three-coordinated Cu(I) ion by dissociation of a MeCN ligand from a tetrahedral complex is rapid and energetically viable; the large enthalpic costs from the loss of the MeCN ligand are offset by entropic gains.[81]

The diversity of Cu/O_2 species results from the formal oxidation state tunability of the Cu centers and the O_2-derived ligands; Cu(II) or Cu(III) can be ligated to superoxide ($1e^-$), peroxide ($2e^-$), or oxide ($4e^-$) ions. While X-ray crystal structures provide decisive atom-connectivity information, the metrical parameters are not definitive for making oxidation state assignments. The assignment of formal oxidation states creates an important classification that facilitates comparisons of complexes and their reactivity patterns. Such assignments, if they are to be meaningful, must be based on a direct probe of the electronic arrangements; this can be performed with Cu K-edge X-ray absorption spectroscopy (XAS).[82] A weak pre-edge absorption feature corresponding to the 1s → 3d transition is diagnostic of the Cu oxidation state: 8979 ± 0.5 eV for Cu(II) and 8981 ± 0.5 eV for Cu(III).[83,84] Within the past decade, arguably the most far-reaching advance has been the appreciation for the facile accessibility of Cu(III) in Cu/O_2 reactions. A direct spectroscopic probe of the reduced-O_2 ligand is possible through infrared (IR) and/or resonance Raman (rR) vibrational spectroscopies. The latter method is particularly advantageous for studying Cu/O_2 complexes because the Cu−O and O−O vibrational modes can be selectively enhanced and symmetric vibrational modes may be detected. Vibrational frequencies that shift appropriately upon $^{18}O_2$ substitution provide strong evidence for the specific reduction level of the O_2-derived ion: 1000−1150 cm^{-1} ($\Delta[^{18}O_2] \approx 50$ cm^{-1}) for superoxide and 750−850 cm^{-1} ($\Delta[^{18}O_2] \approx 50$ cm^{-1}) for the peroxide ion.[85]

Even though X-ray crystallography is the best technique for confirming the structures of these complexes, its limited success in the Cu/O_2 area is commensurate with the difficulty of working with thermally sensitive complexes. The Cu K-edge extended X-ray absorption fine structure (EXAFS) analysis of Cu/O_2 complexes, both in solution and in the solid state, provides an alternative approach to obtain key structural parameters such as the Cu···Cu and Cu−O/N distances.[82,86,87] In cases where comparisons between X-ray crystallography and solution EXAFS data have been made, the correlation is excellent.[88−90]

The UV−vis spectra of many Cu/O_2 species exhibit intense oxygen to Cu charge transfer (CT) absorptions, which are consistent with the presence of highly covalent Cu−O bonds. These transitions are often characteristic and in such cases portend distinct topological Cu/O_2 arrangements. The sensitivity of these absorption features to subtle structural changes, together with the simplicity of this technique, makes UV−vis spectroscopy a powerful experimental tool. A firm understanding of the electronic origins of these features allows one to predict structural distortions in Cu/O_2 complexes.

While many classifications of Cu/O_2 species are possible, for this review the $Cu:O_2$ ratio will be the primary determinant, with the Cu_nO_2 core topology and the Cu oxidation state as secondary and tertiary criteria, respectively (Figure 3).

$Cu:O_2$ = 1:1. Two different binding topologies of the reduced-O_2 moiety are observed in 1:1 Cu/O_2 complexes (section 3): end-on O_2 in the Cu(II)−superoxo ^{E}**S**[91−93] and side-on O_2 in both the Cu(II)−superoxo ^{S}**S**[94,95] and the Cu(III)−peroxo ^{M}**P**.[96−98] The electronic description of ^{M}**P** is currently being debated.

$Cu:O_2$ = 2:1. Five different structural types of 2:1 Cu/O_2 complexes are known, three of which are structurally characterized: end-on peroxodicopper(II) (^{T}**P**, section 4.3), side-on peroxodicopper(II) (^{S}**P**, section 4.4), and bis(μ-oxo)dicopper(III) (**O**, section 4.5). The first Cu/O_2 species to be structurally characterized was a ^{T}**P** species by Karlin et al. in 1988.[99] Beyond the structure itself, this work demonstrated that thermally sensitive, labile Cu/O_2 complexes could be characterized by standard techniques for inorganic complexes. Kitajima et al. reported the structure of a ^{S}**P** complex only a year later.[100] This structure revealed for the first time the μ-η^2:η^2 binding mode of the peroxide ion to transition metals, a structural arrangement generally overlooked prior to its publication. The subsequent structural characterization of oxyHc showed the same mode for O_2 binding. The last type of structurally characterized 2:1 Cu/O_2 species, **O**, was first reported in 1996 by Tolman et al.[101,102] Experimental evidence for the presence of Cu(III) centers in **O** came from Cu K-edge XAS investigations.[87] Despite being the most recent 2:1 archetype to be structurally characterized, more examples of **O** complexes now exist than for all other Cu/O_2 species. This proliferation correlates with the diversity of ligands capable of stabilizing **O** species. Interestingly, ^{T}**P**, ^{S}**P,** and **O** complexes are isoelectronic isomers, yet each exhibits distinct and characteristic spectroscopic features (Table 1).

$Cu:O_2$ = 3:1. The 3:1 species, **T**, results from the $4e^-$ reduction of O_2 by three Cu(I) complexes (section 5). The two oxide ligands that are formed connect the three Cu centers in a compact, valence-localized Cu(III)Cu(II)Cu(II) cluster. The 3:1 $M:O_2$ reactivity ratio is known only to occur for Cu among the transition metals, a result attributable to the ability of both Cu(III) and Cu(II) ions to adopt a square-planar geometry.

$Cu:O_2$ = 4:1. The tetranuclear peroxide complexes differ from the species listed above because their $Cu:O_2$ composition does not equal the Cu(I) and O_2 stoichiometry needed to generate such complexes (section 6). Unlike most other Cu/O_2 species, these complexes are stable indefinitely at ambient temperatures.

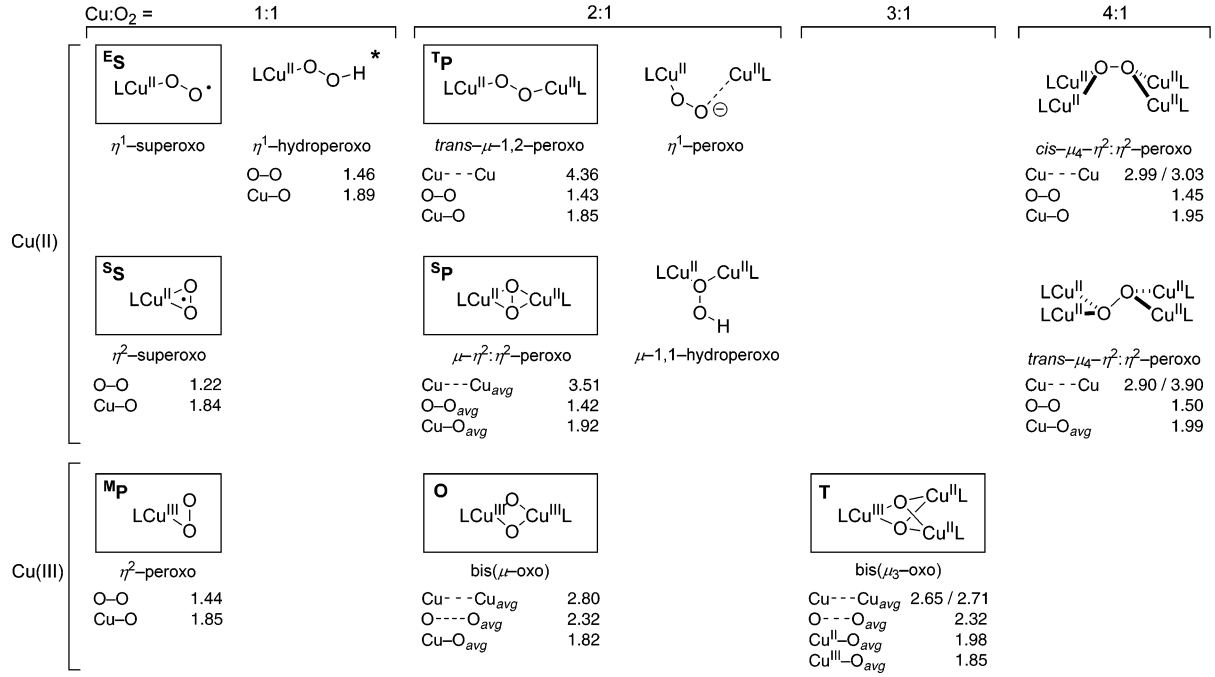

Figure 3. Cu/O_2 species formed by reaction of a Cu(I) complex with O_2 (except *, section 3.1). For crystallographically characterized species, significant metrical parameters (Å) are given. The seven framed structural types are the species that are most extensively discussed in this review: ^{E}**S**, end-on superoxocopper(II); ^{S}**S**, side-on superoxocopper(II); ^{M}**P**, mononuclear peroxocopper(III); ^{T}**P**, *trans*-1,2-peroxodicopper(II); ^{S}**P**, side-on peroxodicopper(II); **O**, bis(μ-oxo)dicopper(III); **T**, bis(μ_3-oxo)tricopper(II,II,III).

Table 1. Spectroscopic Features of 2:1 Cu/O_2 Species

species	UV−vis: λ, nm (ϵ, mM^{-1} cm^{-1})	rR: ν, cm^{-1} (Δ[$^{18}O_2$])
^{T}**P**	530 (10), 600 (sh, 7)	830 (46)
^{S}**P**	360 (24), 520 (1)	740 (40)
O	300 (20), 400 (24)	600 (28)

2.2.3. Ligand Attributes

The ligands that generate well-characterized Cu/O_2 species upon oxygenation of their Cu(I) complexes are presented in Figures 4−7. Systematic variation of the steric and electronic properties within a *family of ligands* is an incisive probe of Cu/O_2 chemistry. For this review, a family of ligands is defined as a set of ligands in which only the peripheral substituents/groups of a given position are varied (Figure 26). Thus, ligands of a particular family possess identical backbone structures (i.e., identical atom compositions) and the same overall charge. While restrictive, this definition provides a method to differentiate between electronic and steric effects. Ligands that differ by donor atoms, chelate ring sizes, or their overall formal charges can yield profound changes on Cu/O_2 reactivity patterns; attempts to distinguish between influences from electronic versus steric effects are usually unproductive in these cases.

Donor Atoms. The majority of O_2-reactive Cu(I) complexes used in biomimetic studies contain aromatic nitrogen ligands (pyrazole, pyridine, and imidazole), following biological precedence. Though ligands with aliphatic amine groups were initially dismissed, they form every major type of Cu/O_2 species, including several types that have yet to be observed using only aromatic nitrogen ligands. Oxygen ligation from phenols or phenolate ions, sulfur ligation from thioethers or disulfides, and phosphorus ligation from phosphines are less common. Sulfur and phosphorus donors tend to form very stable Cu(I) complexes that are inert to O_2.

Denticity. Cu(I) oxygenation studies with monodentate nitrogen ligands are generally very complicated because of the lability and geometric plasticity of Cu centers.[103,104] Polydentate ligation restricts the Cu speciation, thereby biasing oxygenation reactions toward well-defined Cu/O_2 complexes. While O_2-reactive Cu(I) complexes ligated by a pentadentate ligand are uncommon,[61] analogues that adopt a trigonal-monopyramidal geometry with a tetradentate ligand are well-known. Given the inclination of Cu(II) to be five-coordinated, tetradentate ligation of Cu(I) limits the binding of the reduced-O_2 species to the end-on mode. In contrast, Cu(I) complexes containing bi- and tridentate ligands have greater coordination flexibility and allow side-on ligation of the reduced-O_2 species. Since the Cu(III) ion prefers to be square-planar, bidentate ligands predominate in formed Cu(III)/O_2 complexes.

Charge. While neutral ligands are most common, monoanionic ligands create Cu(I) complexes that are more reducing, exhibit enhanced O_2 reactivity, and yield less oxidizing Cu/O_2 products. The structural characterization of 1:1 Cu/O_2 species is currently limited to those with monoanionic ligands, even though such species can form with neutral ligands.

Chelate Rings. The energetic advantage of a metal chelate is generally optimized with five- or six-membered rings. Dramatic changes in the oxygenation behavior of a Cu(I) complex are possible by changing a single chelate ring within a polydentate

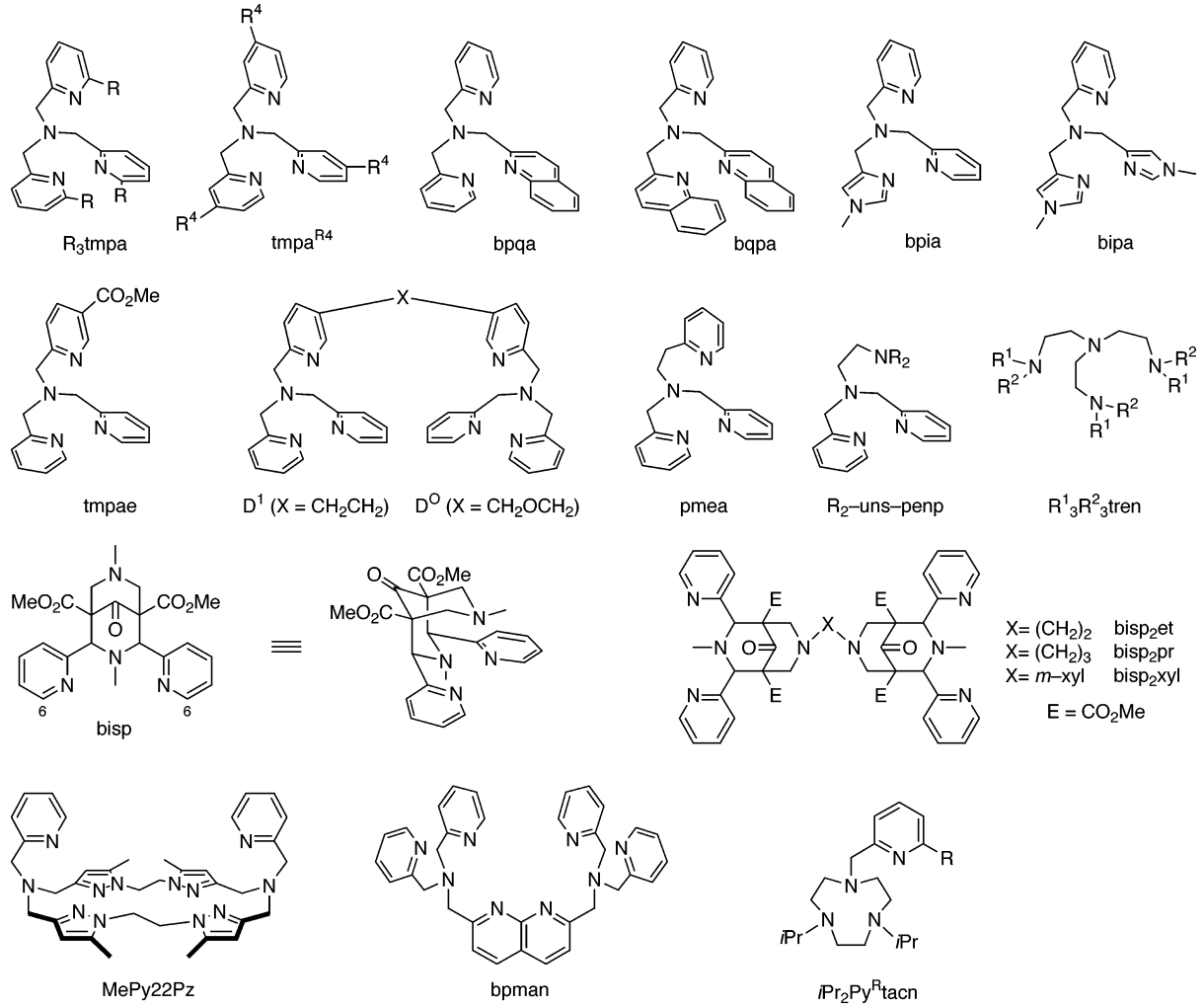

Figure 4. Tetradentate ligands (sections 3.2, 4.3, and 4.5).

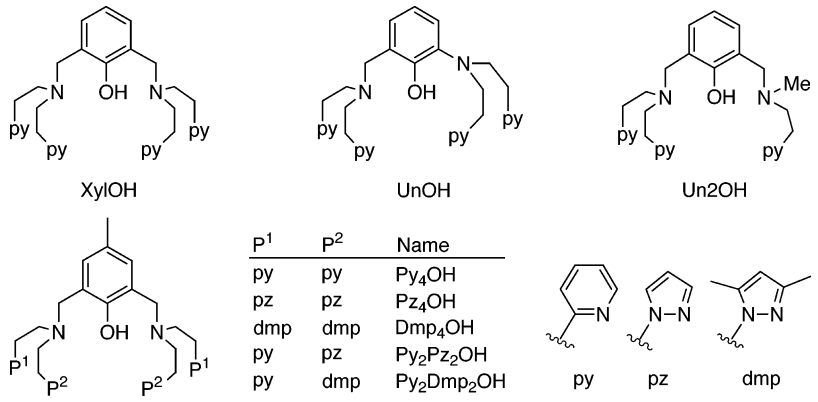

Figure 5. Ligands derived from XylOH (section 4.2).

ligand. Frequently, as the chelate ring size is increased from 5 to 6, the reactivity of the Cu(I) complex toward O_2 is attenuated or even obliterated. Whether this results from stabilization of the Cu(I) complex or destabilization of the Cu/O_2 species is not always obvious. At parity of peripheral substituents, the larger bite angle of a six-membered chelate ring will create a more sterically demanding ligand than its five-membered analogue.

Steric Demands. Steric crowding is the most extensively studied ligand property, partly because the substituents are readily varied and their influences on products are readily interpreted. More sterically demanding ligands yield more elongated Cu/O_2 structures, whereas compact Cu/O_2 cores are obtained with the ligands containing the smallest substituents. Additionally, steric effects alone can control the nuclearity of the Cu/O_2 product.

A vast amount of data exists for the reactions of Cu(I) complexes with O_2, and we collected the examples that have structurally and spectroscopically well-characterized Cu/O_2 products. Of course, this criterion is subjective, and we apologize for any omissions. Our goal has been to gather sufficient

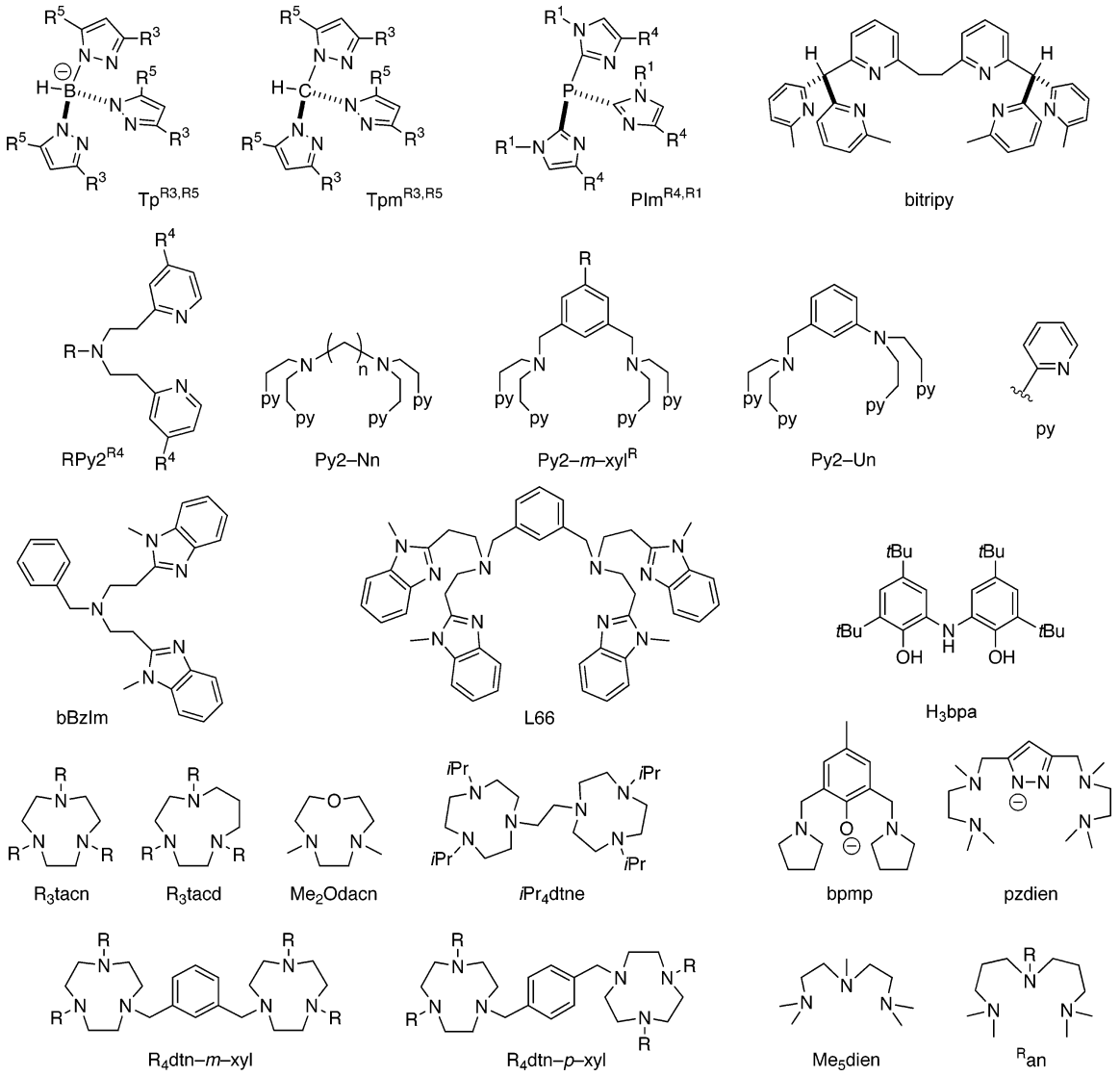

Figure 6. Tridentate ligands (sections 3.3.1 and 4.4−4.6).

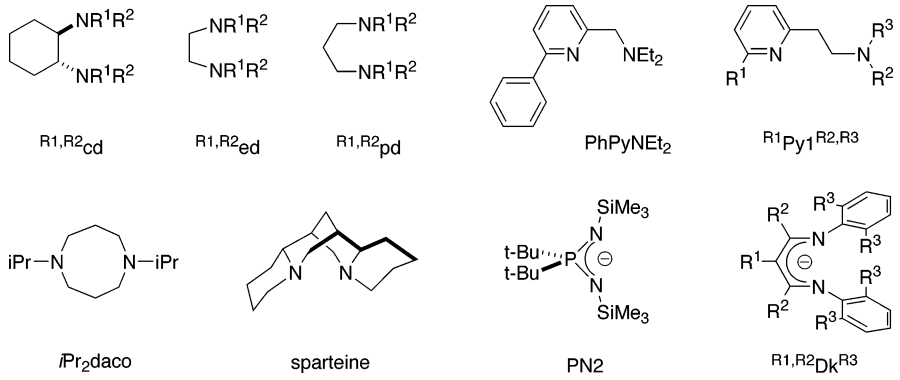

Figure 7. Bidentate ligands (sections 3.3.2 and 4.4−4.6).

information to propose a composite mechanistic scheme that interrelates the various Cu/O_2 species (Figure 27).

3. 1:1 Cu/O_2 Complexes

3.1. Introduction

Most experimental data suggest that oxygenations of Cu(I) complexes proceed via formation of a Cu(II)−superoxo species (**S**, eq 1). In several cases, the existence of this intermediate has been confirmed by structural and/or spectroscopic means. Though not yet detected in a biochemical system, a **S** species is commonly proposed as an intermediate in enzymatic cycles, particularly for mononuclear Cu enzymes such as DβH or PHM. Further reduction may occur to form a Cu(II)−peroxo species or a hydroperoxo form, Cu(II)−OOH, after protonation (eq 1).[1,24,105] To date,

Table 2. Spectroscopic Features of ^{E}S Complexes[a]

ligand[b]	solvent	UV–vis: λ, nm (ϵ, mM^{-1} cm^{-1})[c]	rR: ν, cm^{-1}	ref
tmpa	EtCN	410 (4.0), 580 (1.1), 747 (1.0)		92, 116, 117
tmpa	EtCN	414 (4.8), 586 (1.2)		91
tmpa^{R}	EtCN	410–413		92
	acetone, THF	420–422		92
tmpae	EtCN	415 (3.5), 591 (0.9), 760 (1.0)		118
D^{1}	EtCN	416 (4.5),[d] 583 (1.0),[d] 755 (1.1)[d]		118, 120
Me$_6$tren	EtCN	412 (4.8), 587 (1.7)	1122	91, 119
Bz$_3$tren	acetone	406		129
tren[e]	EtCN	400		13, 119
uns-penp	acetone	426		130
Me$_2$-uns-penp	EtCN	412		67
bisp	EtCN	404 (8.0), 599		93
bisp$_2$et	acetone	405, 487, 605		93

[a] Typical weakly coordinating anions, ca. −90 °C. [b] See Figure 4. [c] Extinction coefficients usually deduced from kinetic modeling of stopped-flow experiments. [d] Extinction coefficients per Cu. [e] This ^{E}**S** species is not stable and does not further react to form a stable ^{T}**P** complex.

all well-characterized mononuclear Cu–OOH model complexes are formed by reactions of H_2O_2 with Cu(II) complexes, a topic not covered by this review.[106–114]

$$Cu^{I} + O_2 \rightleftharpoons \underset{\text{superoxo (S)}}{Cu^{II}\text{–}(O_2^{\bullet -})} \xrightarrow{e^-} \underset{\text{peroxo}}{Cu^{II}\text{–}(O_2^{2-})} \xrightarrow{H^+} \underset{\text{hydroperoxo}}{Cu^{II}\text{–}OOH} \quad (1)$$

In solution, the **S** species tends to react with a second equivalent of the Cu(I) complex. Low-temperature stopped-flow UV–vis spectroscopy is a powerful technique for characterizing such transient species.[67] Experiments carried out on complexes with tetradentate ligands have revealed the presence of transient **S** species, leading to the overall two-step oxygenation mechanism shown in eqs 2a and 2b.[91–93,115–119] The presence of a labile monodentate ligand (e.g., acetonitrile), initially coordinated to the Cu(I) center, accounts for the dramatic solvent effects observed.[92,93,120] A close examination of kinetic and thermodynamic data for these reactions suggests that the superoxide ion is bonded end-on (^{E}**S**), though definitive structural or spectroscopic (rR) evidence supporting this assignment is currently lacking. Interestingly, both ^{E}**S** and ^{T}**P** species are favored enthalpically but strongly disfavored entropically, accounting for their instability at higher temperatures.[91–93,115,121]

With bi- and tridentate ligands, although a transient **S** species has yet to be observed, the overall oxygenation rate is generally first-order with respect to the Cu(I) complex. This observation is consistent with a mechanism similar to that given in eq 2 in which the formation of a **S** species is rate-determining.[115,121–126] A second-order dependence with respect to Cu(I) has been reported for two particular examples.[127] In complexes with bi- and tridentate ligands, the binding mode of the transient superoxide is unknown, yet side-on ligation is presumed.

$$LCu^{I}\text{–}Y^{\urcorner 1+} + O_2 \rightleftharpoons \underset{^{E}S}{LCu^{II}\text{-}O_{\diagdown}O^{\bullet}\,^{\urcorner +}} + Y \quad (2a)$$

$$\underset{^{E}S}{LCu^{II}\text{-}O_{\diagdown}O^{\bullet}\,^{\urcorner +}} + LCu^{I}\text{–}Y^{\urcorner +} \rightleftharpoons \underset{^{T}P}{LCu^{II}\text{-}O_{\diagdown}O\text{-}Cu^{II}L^{\urcorner 2+}} + Y \quad (2b)$$

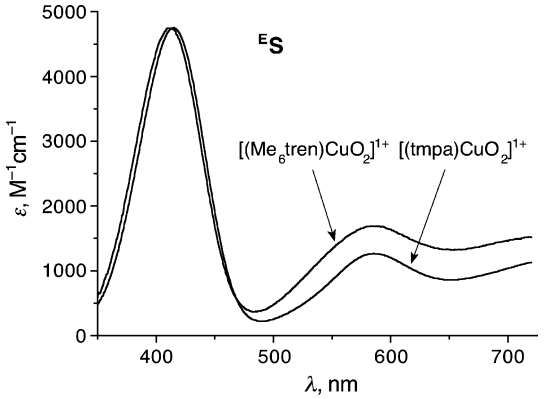

Figure 8. Spectra of the ^{E}**S** species $[(tmpa)Cu(II)(O_2)]^+$ and $[(Me_6tren)Cu(II)(O_2)]^+$ (EtCN, −90 °C).[91]

Despite the predilection of **S** complexes to form higher nuclearity Cu/O_2 products, an increase in the steric demands of the ligand can sufficiently attenuate the bimolecular step (eq 2b) such that 1:1 complexes can be isolated.[128] The use of an anionic rather than neutral ligand diminishes the oxidizing ability of the 1:1 species and hence its reactivity.[94–97] Exploiting the combination of appropriate steric demands and anionic ligation has led to the isolation of two crystallographically characterized 1:1 complexes.[94,97]

3.2. End-on Superoxocopper(II) Species, ^{E}S

3.2.1. Characterization

All transient ^{E}**S** complexes have characteristic spectral features (Table 2) that include an intense CT absorption band at ca. 410 nm (ϵ = 3000–8000 M^{-1} cm^{-1}) and two weaker features at ca. 600 and 750 nm (Figure 8). These three features vary little with the nature of the tetradentate nitrogen ligand. The lack of structural data has precluded detailed electronic analyses, but the ca. 410 nm absorption band is tentatively assigned as a $\pi_\sigma^* \rightarrow$ d CT transition, in which the in-plane π_σ^* orbital of the superoxide ion overlaps in σ fashion with a d orbital of the Cu(II) ion (Figure 9). The one case for which a rR spectrum is reported[91] exhibits a feature at 1122

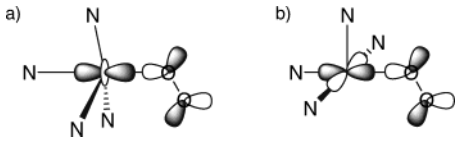

Figure 9. Overlap between the π_σ* orbital of the superoxide ion and the corresponding Cu d_{z^2} or $d_{x^2-y^2}$ orbital for a trigonal-bipyramidal or a square-pyramidal geometry, respectively.

cm^{-1}, consistent with the reduced-O_2 moiety being a superoxide ion.[85]

3.2.2. Effects of Ligand Structure

The oxygenation of the Cu(I) complex of tmpa is one of the most extensively studied Cu/O_2 reactions and provides spectroscopic data to support the formation mechanism given in eq 2.[91,92,115−117] The derived transient **ES** species, which converts to the thermodynamically more stable **TP** product at −90 °C in EtCN, serves as an archetype for all other end-on superoxide complexes (Table 2). Modification of tmpa to influence only the electronic properties of the donor atoms ($tmpa^R$ ligands) evidences an energetic stabilization of the **ES** species with more electron-donating R substituents.[92] With the related bqpa ligand, containing two quinolyl subunits, what was initially described as a 1:1 superoxo adduct[117,131] is now recognized as a bis(μ-oxo)dicopper(III) complex, **O**.[132] With binucleating ligands (D^1, D^O) created with flexible bridges linking two tmpa units, transient **ES** intermediates are also observed.[64,115,118,120]

tren and its derivatives are tripodal tetraamine ligands related to tmpa but possess only aliphatic amine groups. Amazingly, this nonconservative alteration of the ligand donors not only generates Cu/O_2 species of the same type, but also produces nearly identical spectroscopic features. With tren or Me_3-tren, **ES** complexes are observed but readily decay without yielding any other detectable Cu/O_2 species.[13,119] The slightly more sterically demanding Bz_3-tren[129] and Me_6tren[91] ligands yield **ES** species that ultimately form **TP** complexes (Table 2, Figure 8). Comparing kinetic measurements obtained at various temperatures reveals that the **ES** intermediate is enthalpically more stabilized with Me_6tren than with tmpa,[91] a difference attributed to the greater coordinating ability of aliphatic versus aromatic nitrogen ligands.

The bisp ligand and its derivatives are predisposed tetradentate ligands with two aliphatic amine and two pyridine donors. Their Cu(I) complexes react with O_2 through transient **ES** species en route to **TP** complexes.[93,133] Despite the semirigid square-pyramidal constraints of this type of ligand,[66] the **ES** species exhibit spectral features similar to those of tmpa- or Me_6tren-ligated **ES** complexes (Table 2).

In a chemical model of GOase, a 1:1 Cu/O_2 species employing a ligand of a very different type has been isolated. The oxygenation of a Cu(I) complex of ligand H_3bpa (Figure 6) in basic MeOH at −70 °C affords a diamagnetic, crystalline compound described as a mononuclear **ES** species.[134] Its absorption bands at ca. 400 nm (Table 3) are not as intense as those for other **ES** species. Through mixed oxygen-isotope studies, rR experiments reveal unsymmetric binding of O_2 with an O−O stretching vibration at 964 cm^{-1} ($\Delta[^{18}O_2]$ = 55 cm^{-1}), intermediate between those of peroxide and superoxide complexes.[85]

3.3. Side-on Mononuclear Species

3.3.1. Side-on Superoxocopper(II) Complexes, **SS**

A mononuclear Cu/O_2 species can be isolated by precluding its subsequent reaction with another Cu(I) complex (eq 2b) through proper ligand modifications. Kitajima et al. used this strategy with monoanionic tris(pyrazolyl)borate ligands[135] (Tp, Figure 6) bearing bulky R^3 substituents.[136] With $Tp^{tBu,iPr}$, a neutral, diamagnetic **SS** complex was selectively crystallized (Figure 10a).[94] Its X-ray crystal structure shows a Cu(II) ion with a distorted square-pyramidal coordination environment, a weakly associated axial nitrogen ligand, and a side-on-bonded superoxide ion with an O−O bond length of 1.22 Å. This bond length, determined at room temperature, may underestimate the true O−O distance because of librational motion within the CuO_2 core.[98] Other crystallographically characterized η^2-superoxo metal complexes (Co, Cr, Sm)—all with tris(pyrazolyl)borate ligands—have O−O bond lengths of 1.32−1.36 Å.[98,137−139]

Solutions of the **SS** complex formed with $Tp^{tBu,iPr}$ contain small amounts of the related binuclear **SP** complex, as revealed by its characteristic rR features (Table 1). With the more sterically demanding ligand $Tp^{Ad,iPr}$, bearing peripheral adamantyl substituents, no amount of **SP** is detected and only the **SS** complex forms.[95] IR spectra (Table 3) of the two **SS** complexes generated with $Tp^{tBu,iPr}$ and $Tp^{Ad,iPr}$ display O−O stretching vibrations at 1112 and 1058 cm^{-1} ($\Delta[^{18}O_2]$ = 50 cm^{-1}), respectively, establishing their formulation as superoxide complexes.[85] Theoretical calculations suggest that strong covalency exists between the Cu $d_{x^2-y^2}$ and the superoxide π_σ* orbitals and that the ground state is highly delocalized.[95] This cova-

Table 3. Spectroscopic Features of Isolated 1:1 Adducts

ligand [a]	species	solvent	UV−vis: λ, nm (ϵ, mM^{-1} cm^{-1})	rR or IR: ν, cm^{-1} ($\Delta[^{18}O_2]$) O−O	Cu−O	ref
H_3bpa	**ES**	CH_2Cl_2	391 (2.1), 423 (1.8) 524 (2.1), 649 (1.6)	964 (55)[b,c]		134
$Tp^{tBu,iPr}$	**SS**	toluene	510 (sh, 0.2), 660 (0.09)	1112 (50)[d]	550 (18)[d], 554 (20)[c]	94,95
$Tp^{Ad,iPr}$	**SS**	CH_2Cl_2	452 (0.3), 700 (sh, 0.04) 975 (0.02), 2380 (0.22)	1058 (50)[d]	542 (24)[d]	95
$^{H,tBu}Dk^{iPr}$	**MP**	THF	~420 (~2.3), ~600 (br)	961 (49)[c]		96,97
$^{H,Me}Dk^{iPr}$	**MP**	THF	~400 (sh, ~2.4), 600 (0.22, br)	968 (51)[c]		96,97

[a] See Figures 6 and 7. [b] Unsymmetrically bonded. [c] rR. [d] IR.

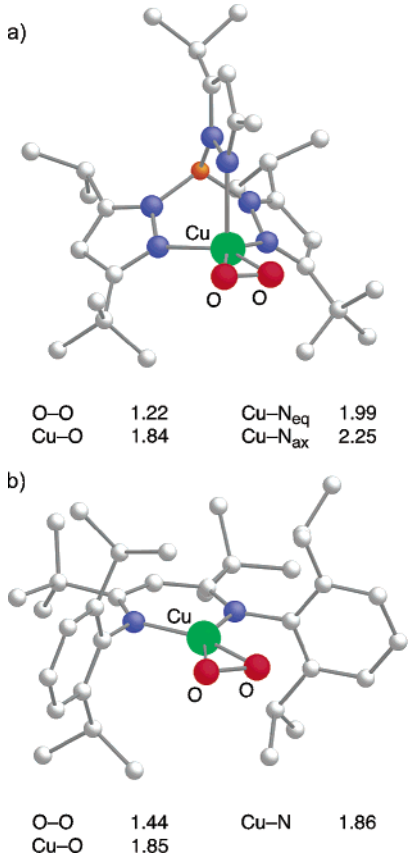

Figure 10. X-ray structures and metrical parameters (Å) of 1:1 Cu:O_2 complexes: (a) [(Tp^{tBu,iPr})Cu(II)(O_2)] ^{E}**S** species (Me groups on the upper *t*Bu group have been omitted for clarity)[94] and (b) [(^{H,tBu}Dk^{iPr})Cu(III)(O_2)] ^{M}**P** species.[97]

lency shifts the in-plane $\pi_\sigma^* \rightarrow d_{x^2-y^2}$ CT transition to high energy (>32 500 cm^{-1}; λ < 300 nm). The $\pi_v^* \rightarrow d_{x^2-y^2}$ CT band, in which π_v^* is the other π^* orbital of the superoxide moiety, appears at very low energy (4200 cm^{-1}; 2380 nm). Therefore, the UV–vis spectrum of this ^{S}**S** complex is dominated only by weak d → d transitions, unlike the ^{E}**S** complexes that exhibit strong CT absorptions at ca. 410 nm (section 3.2).

3.3.2. Side-on Peroxocopper(III) Complexes, ^{M}P

Similar to the Tp ligands described in the previous section, the bidentate β-diketiminate ligands Dk (Figure 7) also exploit charge and steric demands[140] to stabilize 1:1 Cu/O_2 species. The isolation of two diamagnetic 1:1 Cu/O_2 adducts with the ligands ^{H,Me}Dk^{iPr} and ^{H,tBu}Dk^{iPr} has been reported by Tolman et al.[96,97] In the structurally characterized example [(^{H,tBu}Dk^{iPr})Cu(O_2)] the O_2 moiety binds side-on and the Cu ion adopts a distorted square-planar geometry (Figure 10b). The 1.44 Å O–O bond length is typical of a metal–peroxo rather than a metal–superoxo adduct,[98,141] but the severe disorder within the crystal limits the interpretation of the metrical parameters. rR data reveal O–O stretching vibrations at ca. 965 cm^{-1} ($\Delta[^{18}O_2] \approx 50$ cm^{-1}) for both complexes (Table 3), intermediate between those of typical superoxide and peroxide complexes,[85] and the UV–vis spectra exhibit a feature at ca. 400 nm ($\epsilon \approx 2000$ M^{-1} cm^{-1}). These species are currently considered as hybrid species between a Cu(II)–superoxide, ^{S}**S**, and a Cu(III)–peroxide, ^{M}**P**, but for the purposes of this review, we classified them as ^{M}**P** complexes.

3.4. Summary

The paucity of well-characterized 1:1 Cu/O_2 species results from the demanding balance between creating an O_2-reactive Cu(I) complex and preventing its dimerization in solution. Ligands with large steric demands and a negative charge have been used to successfully isolate 1:1 species. The binding mode of the reduced-O_2 moiety is dictated primarily by the denticity of the ligand: end-on ^{E}**S** species with tetradentate ligands and side-on ^{S}**S** and ^{M}**P** species with bi- and tridentate ligands.

For biochemical systems, the inability to document a **S**-type species is consistent with its high reactivity. Because O_2-activating Cu proteins bind Cu(I) with three endogenous ligands, the studies of model complexes with tridentate ligands predicts that side-on ligation of superoxide, rather than end-on, should occur in these proteins.

4. 2:1 Cu/O_2 Complexes

4.1. Introduction

In 1878, hemocyanin (Hc) was reported as the Cu-containing O_2-transport protein in the blood of mollusks and arthropods,[142,143] raising a great deal of interest in reversible O_2 binding by Cu ions. The oxidative function of the related oxygenated binuclear enzymes, oxyTy and oxyCO, has been the dominant motivating force in synthetic Cu/O_2 chemistry. The reduction of O_2 to peroxide (2e$^-$) is more thermodynamically favorable than to superoxide (1e$^-$), which is mirrored by the fact that binuclear Cu_2O_2 adducts are the most abundant of all Cu/O_2 species. Many early attempts to reproduce the activity of the binuclear proteins arranged two Cu(I) centers within a binucleating ligand (section 4.2). With time, however, it became evident that many mononuclear Cu(I) complexes self-assemble into binuclear species upon oxygenation. The three structural types of 2:1 Cu/O_2 species, *trans*-1,2-peroxodicopper(II) (^{T}**P**, section 4.3), μ-η^2:η^2-peroxodicopper(II) (^{S}**P**, section 4.4), and bis(μ-oxo)dicopper(III) (**O**, section 4.5), are isoelectronic isomers with distinct spectroscopic features. Note that ^{T}**P** complexes are generated exclusively from Cu(I) complexes with tetradentate ligands, whereas ^{S}**P** and **O** species are obtained from precursors with bi-, tri, and tetradentate ligands. With certain ligands, mixtures of ^{S}**P** and **O** complexes are also possible (section 4.6).

4.2. Phenoxo-Bridged Dicopper Complexes

One of the first well-characterized Cu/O_2 systems is based on the binucleating ligand XylO– (Figure 5).[115,144–149] Oxygenation of its dicopper(I) complex affords a species with intense optical absorption bands at 505 nm (ϵ = 6300 M^{-1} cm^{-1}) and 610 nm (sh, $\epsilon \approx 2400$ M^{-1} cm^{-1}), ascribed to $\pi_\sigma^* \rightarrow$ d and $\pi_v^* \rightarrow$ d peroxide to Cu(II) CT transitions, respectively (Table 4). These optical features are analogous to those of ^{T}**P** complexes (section 4.3). Combined rR (803

Table 4. Spectroscopic Features of Complexes with XylO⁻ and Related Ligands[a]

ligand[b]	UV−vis: λ, nm (ϵ, mM^{-1} cm^{-1})	rR: ν, cm^{-1} ($\Delta[^{18}O_2]$) O−O	rR: Cu−O	EXAFS Cu···Cu, Å	ref
Peroxo Adducts, $Cu_2L(O_2)^+$					
XylO⁻[c]	505 (6.0), 610 (2.1)[d]	803 (53)	488 (24)	3.31	144, 145, 151, 153
Py_4O^-[c]	500 (6.5), 630 (0.8)[d]				154
$Py_2pz_2O^-$[c]	505 (4.9), 630 (1.2)[d]				154
$Py_2Dmp_2O^-$[c]	510 (6.7), 630 (1.6)[d]				154
UnO⁻[c]	510 (5.4), 642 (2.7)[d]			3.28	65, 155
Hydroperoxo Adducts, $Cu_2L(OOH)^{2+}$					
XylOH	395 (8.0), 450 (2.2)[d]			3.04	144, 145, 151, 153
Py_4OH	396 (8.3), 480 (3.7)[d]				154
Py_2pz_2OH	400 (8.4), 490 (3.3)[d]				154
Py_2Dmp_2OH	395 (5.5), 470 (1.3)[d]				154
Pz_4OH	402 (4.4), 458 (0.9)[d]				154
Dmp_4OH	404 (7.6), 506 (1.0)[d]				65, 154
UnOH	395 (7.0), 475 (2.0)[d]	892 (55)	506 (15)	2.95	65, 155
Un2OH	290 (4.2), 450 (1.6)[d]				156
Superoxo Adduct, $Cu_2L(O_2)^{2+}$					
UnO⁻[c,e]	404 (5.4)				157

[a] PF_6^-, CH_2Cl_2 −80 °C. [b] See Figure 5. Ligands are written in the form in which the Cu(I) complex reacts with O_2 to yield the mentioned species. [c] Reversible O_2 binding. [d] Shoulder. [e] Starting from the mixed-valence Cu(I)-Cu(II) complex.

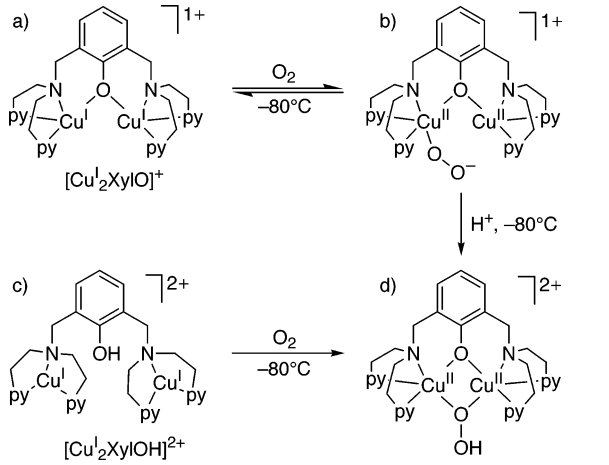

Figure 11. General O_2 reactivity of Cu(I) complexes of XylO− and XylOH ligands.

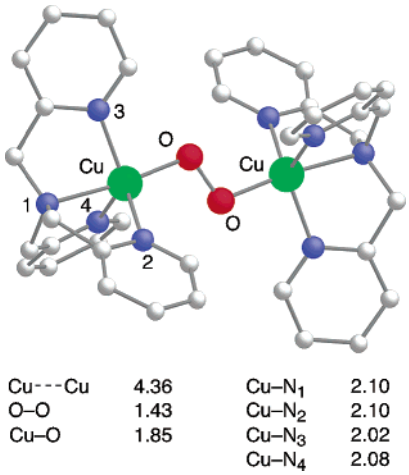

Figure 12. X-ray structure of the ^{T}**P** species $[(tmpa)_2Cu(II)_2(O_2)]^{2+}$ and metrical parameters (Å).[99]

cm^{-1}, $\Delta[^{18}O_2] = 53$ cm^{-1}) and EXAFS (Cu···Cu ≈ 3.3 Å) data are consistent with unsymmetric binding of a peroxide ion to a single Cu(II) center, even though both Cu(I) ions are necessary for the 2e⁻ reduction of O_2 to the peroxide ion (Figure 11b).[150,151] Oxygenation of the dicopper(I) complex of the protonated ligand XylOH produces a hydroperoxide species (Figure 11d) exhibiting a CT feature at 395 nm (ϵ = 8000 M^{-1} cm^{-1}) with a shoulder at 450 nm (Table 4).[152,153] The ca. 3.0 Å Cu···Cu distance measured by EXAFS is most consistent with a μ-1,1-hydroperoxide ion bridging the two Cu(II) ions. This species can also be generated by protonating the peroxide complex derived from XylO⁻ (Figure 11, b → d).

Similar peroxo and/or hydroperoxo species also form when binucleating ligands bearing pyrazoles or mixed pyrazole/pyridine subunits (Figure 5) are used.[154] The corresponding η^1-peroxo complexes have characteristic CT features in the ca. 510 and 620 nm regions and the μ-1,1-hydroperoxo species at ca. 400 nm (Table 4).[65] Similar complexes are generated from the unsymmetric UnOH[65,155,158] and Un2OH ligands,[156] as well as from a trinucleating derivative of XylOH.[159] A **S**-type complex can be generated with UnO⁻, either by oxidation of the peroxo intermediate or by reaction of the mixed-valence Cu(I)−Cu(II) complex with O_2, but vibrational spectra are currently lacking.[157] Similar to the results obtained on transient mononuclear ^{E}**S** intermediates, this binuclear **S** species displays an intense absorption band at 404 nm (ϵ = 5400 M^{-1} cm^{-1}) ascribed to a superoxo to Cu(II) CT transition.

These early examples illustrate the complexity of the Cu/O_2 reactivity patterns. A full understanding of the nature and binding mode of the reduced-O_2 moiety in a metal complex necessitates the use of several complementary techniques (UV−vis, rR, XAS), an approach that forms the basis for an accurate description of the properties of Cu/O_2 species.

4.3. *trans*-1,2-Peroxodicopper(II) Complexes, ^{T}P

4.3.1. Characterization

The 1,2-peroxodicopper(II) complex, ^{T}**P**, with the tmpa ligand was the first Cu/O_2 species to be crystallographically characterized (Figure 12).[63,99] The structure shows end-on trans binding of the peroxide

Table 5. Spectroscopic Features of ^{T}P Complexes[a]

ligand[b]	solvent	UV–vis: λ, nm (ϵ, mM^{-1}cm^{-1})[c]	rR: ν, cm^{-1} ($\Delta[^{18}O_2]$) O–O	Cu–O	ref
tmpa[d]	EtCN	525 (11.5), 590 (7)	832 (44)	561 (26)	63, 91, 99, 117, 131, 160
tmpa[d]	Et_2O	520 (~14)	827 (44)	561 (26)	92, 171
tmpa^{MeO}	Et_2O	520 (~15)	822 (43)	557 (24)	92, 171
tmpa^{Me_2N}	Et_2O	523 (~11)	812 (43)	551 (20)	92, 171
tmpae[d]	EtCN	532 (9.4), 590 (7)			118
Metmpa	acetone	537 (>5), 610			172
bpqa[d]	EtCN	535 (8.6), 600			63, 118, 131
bqpa[d,e]	EtCN	545			63, 118, 131
D^{1}	EtCN, acetone	540 (11.1), 600 (9)			64, 118, 120
D^{O}	EtCN, acetone	535			120
pmea	EtCN, acetone	536 (~5)			173
bpia	EtCN	535 (11.5), 600 (8)			174
*i*Pr$_2$Py^{H}tacn	THF/MeCN 10:1	550 (10.2), 600 (10)	822 (51)	530 (24)	175
*i*Pr$_2$Py^{5-Me}tacn[f]	THF	550 (11.5), 594 (11)	823 (51)	530 (28)	176
Me$_6$tren[d]	EtCN	552 (13.5), 600 (10)	825 (48)		91, 119
Bz$_3$tren	acetone	506			129
uns-penp	acetone	535			130
Me$_2$-uns-penp	EtCN	528			67
bisp[g]	EtCN	504 (8.0), 630 (6)	840		93, 133
bisp$_2$et[g]	EtCN	486 (3.0), 6499 (2)	824		93, 133
bisp$_2$pr[g]	EtCN	499 (6.8), 650	837		93
bisp$_2$xyl[g]	EtCN	503 (6.0), 650 (3)	847		93
MePy22Pz	MeCN	525 (4.0), 625 (2)	844 (46)	558 (26)	177
bpman	CH_2Cl_2	505 (10.5), 620 (5)	831 (44)	561	178

[a] Typical noncoordinating anions, ca. −90 °C. [b] See Figure 4. [c] The ca. 600 nm band is a shoulder of the ca. 520 nm absorption feature. A weak band at ca. 440 nm is also present. [d] Reversible O_2 binding. [e] Transient species. [f] Methyl substituent on the 5-position of the pyridine ring. [g] Irreversible O_2 binding.

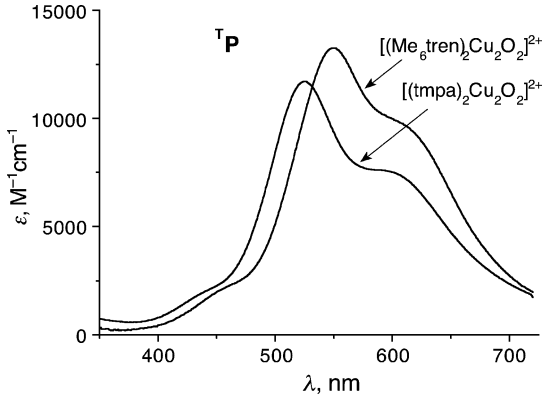

Figure 13. UV–vis spectra of the ^{T}**P** species $[(tmpa)_2Cu(II)_2(O_2)]^{2+}$ and $[(Me_6tren)_2Cu(II)_2(O_2)]^{2+}$ (EtCN, −90 °C).[91]

ion, requiring a Cu···Cu separation of 4.36 Å. Each Cu(II) ion has a distorted trigonal-bipyramidal coordination geometry with one oxygen atom of the peroxide ion in an axial position. While numerous other ^{T}**P** complexes are spectroscopically well-characterized, no other has been crystallographically characterized. Their assignment as ^{T}**P** species is based primarily on distinctive intense UV–vis features (Table 5, Figure 13) that are responsible for their purple colors: ca. 530 nm ($\epsilon \approx 10\,000$ M^{-1} cm^{-1}) and ca. 600 nm (shoulder). These absorptions are respectively ascribed to $\pi_\sigma^* \rightarrow$ d and $\pi_v^* \rightarrow$ d peroxo to Cu(II) CT transitions (Figure 14).[160,161] rR spectra of ^{T}**P** complexes generally have two oxygen-isotope-sensitive bands: an O–O stretching vibration at ca. 830 cm^{-1} ($\Delta[^{18}O_2] \approx 45$ cm^{-1}) and a Cu–O stretching vibration at ca. 555 cm^{-1} ($\Delta[^{18}O_2] \approx 24$ cm^{-1}) (Table 5). Interestingly, all ^{T}**P** species have very similar spectroscopic features, despite varied ligand characteristics. Other complexes are reported to form transient ^{T}**P** species, yet full characterization is lacking.[162−170]

4.3.2. Effects of Ligand Structure

Chelate Ring Size. The extensive structural and spectroscopic data for $[(tmpa)_2Cu(II)_2(O_2)]^{2+}$ serve as the benchmark for other ^{T}**P** complexes with tetradentate nitrogen ligands.[63,99,160] The effects of contraction or expansion of each chelate ring have been explored. Stepwise reduction of each chelate ring from five to four atoms leads to Cu(I) complexes that oxygenate slowly but form no observable Cu/O_2 intermediates.[179] Stepwise expansion of each chelate ring from five to six atoms also affects the Cu/O_2 reaction chemistry: a very unstable ^{T}**P** complex forms with pmea (5,5,6), no intermediate accumulates in the case of pmap (5,6,6), and no reaction occurs between O_2 and the Cu(I) complex of tepa (6,6,6) (the numbers in parentheses refer to the sizes of the chelate rings formed upon metal complexation).[173] Similar behavior is found for tren derivatives with elongated arms.[13] These observations lead to the conclusion that tripodal ligands with five-membered chelate rings are best for sustaining ^{T}**P** species.

Donor Atoms and Electronic Effects. Dramatic reactivity differences result from serial substitution of the pyridine groups of tmpa with imidazoles, yielding ligands bpia and bipa.[174] The Cu(I) complex of bpia behaves in a manner similar to tmpa, generating a ^{T}**P** species; the Cu(I) complex of a related ligand in which the imidazole is further substituted with a noncoordinating phenol to mimic the Cu coordination site in C*c*O reacts in like fashion.[180] While a single pyridine-to-imidazole substitution leads to few electronic/geometric/steric differences

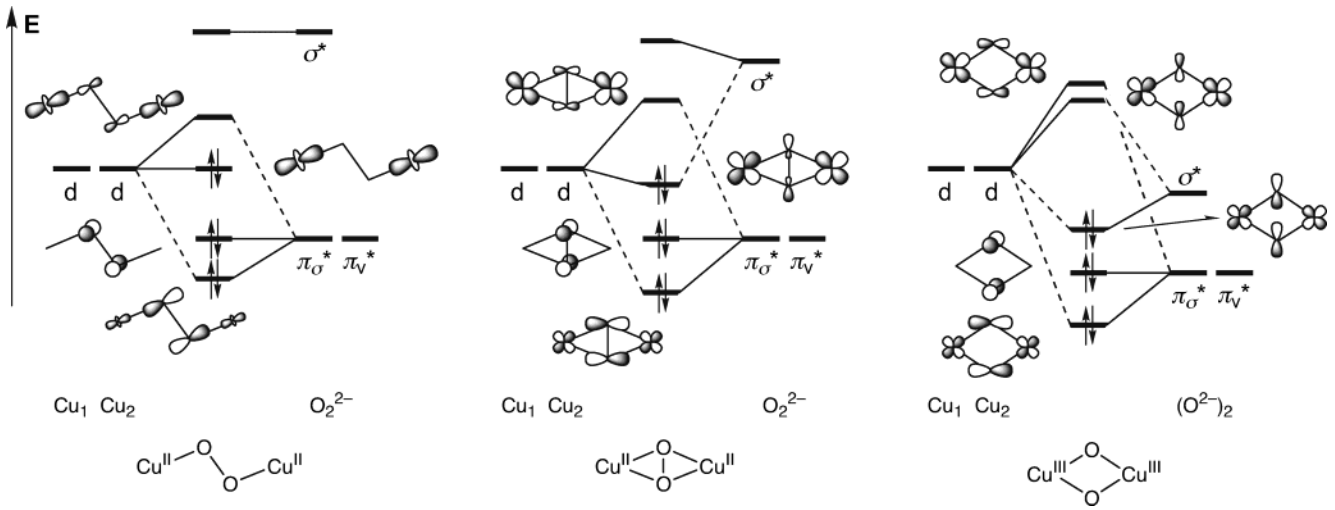

Figure 14. Approximate MO diagrams for the 2:1 Cu/O_2 ^{T}**P**, ^{S}**P**, and **O** isomers. The Cu d orbitals are drawn at the same energy.

between the systems, the ligand bipa, bearing two imidazole subunits, yields unstable and unidentified Cu/O_2 species.

The examples above demonstrate how ostensibly simple changes of the ligand donors can dramatically alter the Cu/O_2 reactivity characteristics, yet the change from pyridine to alkylamine donors, a seemingly large modification, does not affect the generation of well-defined ^{T}**P** complexes and their spectroscopic features.[13] The oxygenation of Cu(I) complexes of tetraamine ligand Me_6tren[91,119,181] and mixed ligands uns-penp and Me_2-uns-penp[67,130] generates ^{T}**P** adducts through the intermediacy of ^{E}**S** species, as reported by Schindler et al. Despite the presence of secondary amine donors in both Bz_3tren and Me_3tren ligands, the Cu(I) complex of the former yields a ^{T}**P** species, while that of the latter forms only an unstable ^{E}**S** species.[129] The Cu/O_2 species (^{E}**S** and ^{T}**P**) using the most thoroughly investigated tren-based ligand, Me_6tren, are enthalpically more stable than those prepared with tmpa,[91] reflecting the greater donating ability of aliphatic amine groups compared with pyridine groups.

A family of tmpa-derived ligands, tmpa^{R}, in which only the *para* substituent of the pyridine groups is varied, has been used to assess the direct influence of electronic parameters on the properties of ^{T}**P** complexes at parity of steric and geometric parameters.[92] Electron-donating substituents enhance the thermodynamic stability of the Cu/O_2 intermediates (^{E}**S** or ^{T}**P**), in line with the comparison between Me_6-tren and tmpa (vide supra). As concluded from a rR study on the ^{T}**P** complexes with tmpa^{R} ligands, electron donation from the substituents decreases the peroxide π_σ* donation to Cu, thereby weakening the Cu−O and O−O bonds.[171]

Steric Demands. With tmpa as a reference, the stepwise replacement of pyridine subunits by more sterically demanding quinolyl groups gives ligands supporting different Cu/O_2 species.[117] With a single quinolyl arm, bpqa affords a ^{T}**P** complex similar to that formed with tmpa. The more sterically demanding bqpa, with two quinolyl subunits, yields a bis(μ-oxo)dicopper(III) complex **O**.[132] Interestingly, a transient ^{T}**P** species is observed in the formation of this **O** complex (section 7). The most sterically demanding ligand of the series, bearing three quinolyl subunits, forms a Cu(I) complex that is inert to O_2.

Analogous results are obtained by stepwise substitution of tmpa at the 6-position of the pyridine rings. Only the Cu(I) complex of the least crowded monosubstituted ligand, Metmpa, yields a ^{T}**P** species.[172] Additional crowding of the ligand (Me_2tmpa and Me_3tmpa) results in the formation of **O** species, as observed in the quinolyl ligand series.[172,182,183] The Cu(I) complex of the most sterically demanding Ph_3-tmpa is unreactive toward O_2.[184] Similar trends are observed with tacn ligands bearing a single substituted pyridine arm, iPr$_2$Py^{R}tacn (section 7).[175,176]

A correlation between the steric demands of the ligands and the energy of the absorption features of the ^{T}**P** complexes exists (Table 5): the ca. 530 nm CT band shifts to lower energies as the ligand becomes more sterically demanding. Whereas the energies of the CT transitions in the ^{E}**S** complexes of Me_6tren and tmpa are very close (Figure 8), the principal CT bands for their respective ^{T}**P** adducts are quite distinct: 552 nm with Me_6tren and 525 nm with tmpa (Figure 13). The existence of greater steric repulsions within the binuclear ^{T}**P** species of Me_6-tren is substantiated by thermodynamic and kinetic measurements.[91] The same trend is observed with the ligands uns-penp and Me_2-uns-penp that integrate both pyridine and amine donor groups.[67,130] In addition, the O−O stretching vibrations are also influenced by steric demands of the ligand (Me_6tren, 825 cm^{-1}; tmpa, 832 cm^{-1}). Together, these effects may be attributed to a decrease in the overlap between the Cu d orbitals and the peroxide ion π_σ* orbital and/or to a decrease in the d orbital energies as a result of weaker donation by the more sterically demanding donor subunit(s).

Geometry. Semirigid tetradentate ligands of the bispidine family (bisp) developed by Comba et al. yield well-defined ^{T}**P** species.[93,133] Molecular mechanics calculations suggest that the Cu(II) ions in these ^{T}**P** complexes have a square-pyramidal geometry rather than a trigonal-bipyramidal geometry as in

the ^{T}**P** complexes described above.[66] Despite these geometric differences (Figure 9), the energies of the $\pi_\sigma^* \rightarrow$ d and $\pi_v^* \rightarrow$ d CT transitions are similar in both cases. With the semirigid bispidine-based ligands, the binding of O_2 is irreversible, which is attributed to destabilization of the Cu(I) state.[185] When the pyridine subunits are substituted with 6-methyl groups (Figure 4), the rate of oxygenation decreases and no Cu/O_2 intermediate accumulates, suggesting that the methyl substituents preclude equatorial coordination of the reduced-O_2 moiety.[93] According to the authors, peroxo ligation in the axial position would be very labile toward substitution and would preclude formation of stable Cu/O_2 intermediates.[186,187]

Binucleating Ligands. Generally, the self-assembly of two mononuclear Cu(I) complexes with O_2 to form a ^{T}**P** complex is an entropically unfavorable process. The entropic costs can be reduced by tethering two mononuclear complexes together. For example, the ^{T}**P** complex of ligand D^1, constructed from two tmpa units linked by a $-CH_2CH_2-$ group (Figure 4), is entropically stabilized in comparison with that of tmpa.[118] This favorable effect is counter-balanced by a disfavorable enthalpic effect, however. Molecular mechanics calculations show that the $-CH_2CH_2-$ spacer induces considerable strain in the ^{T}**P** complex and that a 3-atom-linked binucleating tmpa-based ligand would be more appropriate to promote stability.[188] Binucleating ligand D^O, consisting of two tmpa components connected by a $-CH_2OCH_2-$ bridge, successfully yields a thermally stable ^{T}**P** species ($t_{1/2} \approx 1$ min, acetone, 25 °C).[120] For bispidine derivatives, a similar molecular mechanics approach predicts a $-CH_2CH_2-$ group as the most appropriate-sized spacer. The resulting ligand, bisp$_2$et, leads to the most thermally stable ^{T}**P** intermediate among all bispidine-type ligands, mono- or binucleating ($t_{1/2} =$ 50 min, MeCN, 25 °C).[93,133] The macrocyclic binucleating ligand MePy22Pz,[189] designed with the aid of theoretical calculations, yields a ^{T}**P** species which is the first example of a Cu/O_2 complex with a reasonable lifetime at room temperature in a protic solvent ($t_{1/2} = 4$ min, MeOH, 21 °C).[177]

A different type of Cu/O_2 species is formed using the binucleating ligand bpman, which places two tetradentate coordination sites in proximity (Figure 4).[178] Its dicopper(I) complex, which has a short Cu···Cu separation (ca. 2.6 Å), reacts with O_2 to form a species with spectroscopic features characteristic of a ^{T}**P** complex (UV–vis: 505 nm, $\epsilon = 10\,500$ M^{-1} cm^{-1} and 620 nm, $\epsilon = 5400$ M^{-1} cm^{-1}; rR: 831 cm^{-1}, $\Delta[^{18}O_2] = 44$ cm^{-1}, and 561 cm^{-1}). rR data support symmetrical binding of the peroxide ion. EXAFS data reveal a Cu···Cu distance of 2.84 Å, too short to be sustained by a *trans*-1,2-peroxide bridge; a *cis*-1,2-peroxodicopper(II) structure is plausible.

4.3.3. Summary

While ^{T}**P** complexes have no proven biochemical significance, their synthetic accessibility and rich spectroscopy highlight key factors that govern Cu/O_2 reactivity and the stability of the resulting species. The formation of a ^{T}**P** complex depends keenly on ligand attributes, the denticity being the most decisive factor. All well-characterized ^{T}**P** complexes are supported by tetradentate ligands, strong coordination of four donors discouraging the side-on binding of O_2. Inappropriate chelate ring sizes or donor atoms either preclude the formation of ^{T}**P** species or open pathways to other types of Cu/O_2 products. And while the steric demands of the ligand exert only minor perturbations on the formed ^{T}**P** complexes, more hindered ligands such as bqpa, Me$_2$tmpa, and *i*Pr$_2$-Py^{Ph}tacn yield complexes with more compact structures, **O**, a trend that will be discussed in section 7.

4.4. μ-η^2:η^2-Peroxodicopper(II) Complexes, ^{S}P

4.4.1. Introduction

The early examples of Cu/O_2 species generated with tetradentate ligands or binucleating phenolate-bridged ligands showed little spectroscopic correspondence with oxyHc (UV–vis:[190,191] 345 nm, $\epsilon = 21\,000$ M^{-1} cm^{-1} and 550 nm, $\epsilon = 800$ M^{-1} cm^{-1}; rR:[192,193] 741 cm^{-1}, $\Delta[^{18}O_2] = 44$ cm^{-1}). Extensive exploration of Cu/O_2 reactivity with tridentate ligands followed from the structures of redHc in which the Cu(I) centers are ligated by three imidazoles.[48,194] The significant distance between the Cu(I) centers (ca. 4.5 Å), along with the coordination flexibility of Cu(II) ions, led to much speculation about the binding mode of the peroxide ion in oxyHc.[195,196]

4.4.2. Structural Characterization

Compelling experimental evidence for the unique O_2 binding mode in oxyHc was obtained from the structural characterization of a Cu/O_2 species by Kitajima et al.[100,195,197,198] With sterically demanding, *fac*, monoanionic tris(pyrazolyl)borate ligands,[135] Tp^{R3,R5} (R^3 = Me, *i*Pr, Ph; R^5 = Me, *i*Pr), similar to those used previously,[199] moderately stable Cu/O_2 complexes can be obtained. These complexes exhibit spectroscopic features such as those of oxyHc (UV–vis: 338–350 nm, $\epsilon \approx 21\,000$ M^{-1} cm^{-1}; 530–550 nm, $\epsilon \approx 840$ M^{-1} cm^{-1}; rR: 730–760 cm^{-1}, $\Delta[^{18}O_2] \approx 40$ cm^{-1}). The similarity of these spectroscopic features to those of oxyHc strongly supports the notion that O_2 binding in oxyHc occurs in the same fashion. The structure of [(Tp^{iPr,iPr})$_2$Cu(II)$_2$(O_2)] shows a peroxide ion bridging the two Cu centers in a side-on fashion (Figure 15a),[100] a binding mode unprecedented for a binuclear transition-metal peroxide complex. The Cu···Cu separation in this μ-η^2:η^2-peroxodicopper(II) complex (^{S}**P**) is 3.56 Å, and the O–O bond length is 1.41 Å, typical for a peroxide ion bonded to a metal. Each Cu(II) center is ligated in a slightly distorted square-pyramidal geometry ($\tau = 0.03, 0.03$)[200] with two Cu–N equatorial bonds (2.00 Å) and an elongated Cu–N axial bond (2.25 Å); the peroxide ion occupies the other two equatorial positions with Cu–O distances of ca. 1.91 Å. The axial nitrogen atoms are arranged in an anti rather than a syn configuration.

Subsequent structural characterization of oxyHc from horseshoe crab (*Limulus polyphemus*)[53–55] and octopus (*Octopus dofleini*)[47] confirmed the side-on binding mode of O_2 (Figure 15c and d). The crab oxyHc structure at 2.2 Å resolution has metrical parameters that are similar to the unconstrained

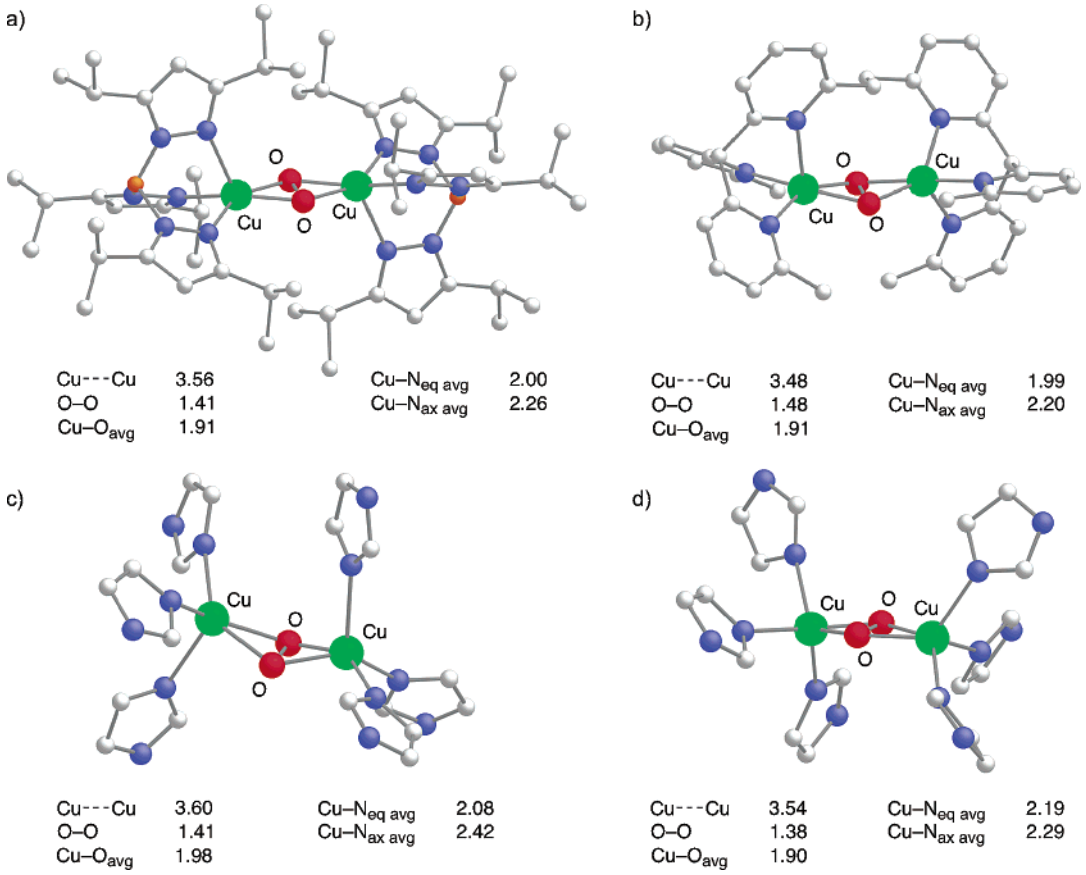

Figure 15. X-ray structures and metrical parameters (Å) of the well-characterized ^{S}**P** species (a) $[(Tp^{iPr,iPr})_2Cu(II)_2(O_2)]$[100,198] and (b) $[(bitripy)Cu(II)_2(O_2)]^{2+}$ [201] and the oxyHc active sites in (c) *Limulus polyphemus*[53−55] and (d) *Octopus dofleini*.[47]

complex reported by Kitajima; each Cu center is ligated in a distorted square-pyramidal geometry (τ = 0.10, 0.12) with the axial imidazole ligands positioned anti to one another. The Cu···Cu and O−O distances (3.60 and 1.41 Å, respectively) are typical, but the peroxide is unsymmetrically positioned between the Cu centers. The octopus oxyHc structure at 2.3 Å resolution has a more symmetric Cu_2O_2 core with a 3.54 Å Cu···Cu distance and a 1.38 Å O−O bond length. Yet, the geometry at each Cu center is more distorted from a square-pyramidal geometry (τ = 0.21, 0.37), possibly due to constraints of the protein structure.[35]

While many synthetic systems exhibit the characteristic spectroscopic features of the ^{S}**P** species (Table 6), only a limited number are crystallographically characterized.[201−203] Of these structures, only those reported by Kitajima et al. (vide supra)[100] and Kodera et al.[201] are sufficiently well-ordered to provide an interpretable O−O bond length. For the latter report, the sterically demanding, binucleating bitripy ligand with six pyridine subunits organizes two Cu(I) centers in proximity. $[(bitripy)Cu(I)_2(MeCN)_2]^{2+}$ reacts rapidly with O_2 to form a thermally robust ^{S}**P** species ($t_{1/2}$ = 25 h, CH_2Cl_2, 25 °C). Release of O_2 from $[(bitripy)Cu(II)_2(O_2)]^{2+}$ is achieved by heating at 80 °C under vacuum. The metrical parameters (Cu···Cu: 3.48 Å, O−O: 1.48 Å, Figure 15b), UV−vis bands, and rR features are commensurate with those of other ^{S}**P** complexes (Table 6). Although the bitripy ligand has 2-fold symmetry, the distortions at each Cu center are different; one Cu ion adopts a square-pyramidal coordination (τ = 0.15), while the other is distorted more toward a trigonal-bipyramidal geometry (τ = 0.44), suggesting that the connectivity within the bitripy ligand is not fully optimized to accommodate the Cu_2O_2 core. Additionally, the two pyridine groups connected by the $-CH_2CH_2-$ bridge are not positioned in the anticipated syn diaxial configuration; the more distorted Cu center has a bridging pyridine coordinated in an equatorial position. Such distortions are reminiscent of those observed in the structure of octopus oxyHc. The enhanced thermal stability of $[(bitripy)Cu(II)_2(O_2)]^{2+}$ relative to ^{S}**P** complexes formed with most mononucleating ligands is attributed to the reduced entropic costs of binding O_2 with a binuclear Cu(I) precursor. Additionally, the 6-Me substituents of the ligand create a protective environment for the peroxide ion.

The tris(pyrazolyl)borate Cu(I) complex $[(Tp^{CF_3,Me})Cu(I)]$ oxygenates to form a ^{S}**P** complex that is stable in solution for days at 25 °C.[204] Its enhanced stability relative to the ^{S}**P** species of the nonfluorinated analogue[195] $Tp^{Me,Me}$ is attributed to the inertness of the CF_3 groups to oxidation; the greater steric bulk and/or the electron-withdrawing nature of the CF_3 groups may also significantly contribute to the thermal stability of this ^{S}**P** species. Structural characterization of $[(Tp^{CF_3,Me})_2Cu(II)_2(O_2)]^{2+}$ confirms the presence of a ^{S}**P** species; [203] each Cu center has square-pyramidal geometry and an anti disposition of the axial ligands, similar to $[(Tp^{iPr,iPr})_2Cu(II)_2(O_2)]^{2+}$.[100] Further interpretations are limited by the severe disorder of the molecules within the crystal.

Table 6. Spectroscopic Features of ^{S}P Complexes

ligand[a]	anion	solvent	Cu···Cu, Å	UV–vis: λ, nm (ϵ, mM^{-1}cm^{-1})	rR: ν, cm^{-1} ($\Delta[^{18}O_2]$)	ref
Tp^{Me,Me}	[b]	CH_2Cl_2		338 (21), 530 (0.8)	725 (39)	195, 197
Tp^{Ph,Ph}	[b]	acetone		345 (20), 542 (0.8)	759 (42)	198, 206
Tp^{iPr,iPr}	[b]	acetone	3.56[c]	349 (21), 551 (0.8)	741 (43)	100, 198, 206
Tp^{CF_3,Me} [d]	[b]	CH_2Cl_2	~ 3.5[c]	334, 550	765 (40)	203, 204
Tpm^{Me,Me} [d]	PF_6^-	CH_2Cl_2		332 (24), 518 (3)		210
PIm^{Me,Et} [d]	ClO_4^-	CH_2Cl_2	3.48[e]	338 (20), 519 (0.8)	738 (38)	208
PIm^{iPr,Et} [d]	ClO_4^-	MeOH		338 (16), 546 (0.9)		208
PIm^{iPr,iPr}	BF_4^-	MeOH		343 (20), 549 (0.8)	750 (40)	209
bitripy[d]	PF_6^-	CH_2Cl_2	3.48[c]	360 (25), 532 (1.5)	760 (41)	201
MePy2[f]	PF_6^-	CH_2Cl_2	~ 3.6[e]	360 (14), 410 (2), 654 (0.3), 530 (0.4)	730 (39), 577 (26)[f]	123, 171, 211, 212
PhPy2[f]	PF_6^-	CH_2Cl_2		350 (6), 680 (0.1), 485 (0.3)		211
BzPy2[f]	PF_6^-	acetone		365 (18), 518 (0.9)	746 (42), 581 (28)[f]	211, 213
PhePy2	PF_6^-	THF		362 (13), 526 (0.8)	746 (42)	213–215
Py2–*m*–xyl^{tBu} [d]	PF_6^-	CH_2Cl_2		362 (16), 440 (4), 530 (1.0)		216
Py2–*m*–xyl^{F} [d]	PF_6^-	CH_2Cl_2		360 (11), 436 (3), 530 (1.0)		216
Py2–*m*–xyl^{CN} [d]	PF_6^-	CH_2Cl_2		358 (16), 435 (4), 530 (1.0)		216
Py2–*m*–xyl^{NO_2} [d]	PF_6^-	CH_2Cl_2		358 (20), 435 (5), 530 (1.2)		216
Py2-Un[d]	PF_6^-	CH_2Cl_2		360 (11), 520 (1), 600 (sh)		158
Py2-N3[d,g]	ClO_4^-	CH_2Cl_2	3.22[e]	365 (15), 490 (5), 600 (1.2)	764 (41)	217–221
Py2-N4[d,g]	PF_6^-	CH_2Cl_2	3.37[e]	360 (16), 458 (5), 550 (1.2)	750	217–222
Py2-N5[d,g]	PF_6^-	CH_2Cl_2		360 (21), 423 (4), 520 (1.2)	741	217, 219–221
^{Me}an	BArF$^-$	CH_2Cl_2		360 (22), 540 (2.5)	721 (38)	124
bBzIm[d,h]	PF_6^-	acetone		356 (3), 560		223
L66[d,f]	PF_6^-	acetone		362 (15), 455 (2), 550 (0.9)	760 (41), 581 (28)[f]	224
*i*Pr$_3$tacn	ClO_4^-	CH_2Cl_2		366 (22), 510 (1.3)	713 (41)	101, 102, 202, 225
*i*Pr$_4$dtn–*m*–xyl [d]	SbF_6^-	CH_2Cl_2		320 (8), 366 (15), 410 (9)		202
*i*Pr$_3$tacd	SbF_6^-	CH_2Cl_2	~ 3.52[c]	380 (22), 520 (2.3)	739 (43)	202
^{H,tBu}ed	TfO$^-$	THF	3.45[e]	350 (36), 485 (1.2), 605 (0.9)	721 (40)	125
^{H,tBu}ed	SbF_6^-	THF		353 (38), 425 (1.7), 472 (2.1)	727 (40)	125
^{Me}Py1^{Et,Bz}	PF_6^-	acetone		365 (18), 518 (0.9)	737 (41)	226

[a] See Figures 6 and 7. [b] Neutral complexes. [c] From X-ray structure. [d] Reversible O_2 binding. [e] From EXAFS data. [f] The solution contains a small amount of the **O** isomer. [g] Bent Cu_2O_2 core. [h] Incomplete formation.

The fourth example of a structurally characterized ^{S}**P** complex uses *i*Pr$_3$tacd, a 10-membered macrocyclic, *fac*, triamine ligand.[202] While the quality of the structure is marginal, the detection of a 3.5 Å Cu···Cu separation and a short O–O bond length confirms the presence of a ^{S}**P** species. Of the four synthetic ^{S}**P** species that are structurally characterized, the Cu centers in this complex have the most distorted square-pyramidal geometries (τ = 0.29, 0.32). The anticipated 180° dihedral angle of the axial nitrogen donors is only 116°, a distortion almost certainly induced by the intraligand steric interactions among the six *i*Pr substituents.

4.4.3. Spectroscopic Characterization

The tetragonal geometry at each Cu(II) center in the ^{S}**P** structures leads to a d_{xy} electronic ground state; for binuclear ^{S}**P** and **O** species, the *x* and *y* axes are oriented along the Cu–Cu and O–O vectors, respectively. The ligand-induced distortions from a square-pyramidal geometry, while often severe, are not sufficient to enforce a trigonal-bipyramidal d_{z^2} electronic ground state in any known case.

The unique spectroscopic features of ^{S}**P** species are directly related to the side-on peroxide binding mode. The absorption spectra of ^{S}**P** species (Figure 16) exhibit a high-energy CT band (340–380 nm; $\epsilon \approx$ 18 000–25 000 M^{-1} cm^{-1}) and a weaker, lower energy band (510–550 nm; $\epsilon \approx$ 1000 M^{-1} cm^{-1}). As is the case for ^{T}**P** species, the two π^* of the peroxide ligand are differentiated as σ- and π-bonding orbitals when interacting with the Cu d orbitals. On the basis of

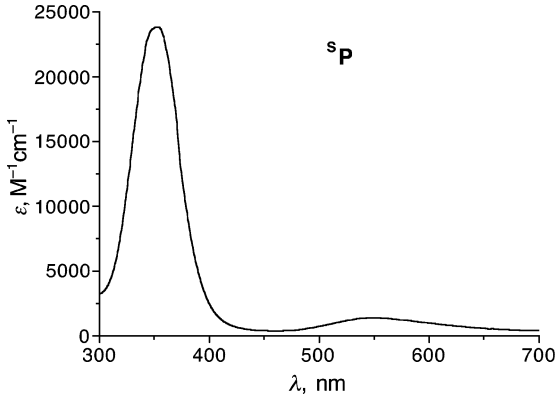

Figure 16. UV–vis spectrum of the $[(Tp^{iPr,iPr})_2Cu(II)_2(O_2)]$ ^{S}**P** complex (acetone, −80 °C).[206]

extensive spectroscopic and theoretical studies, the UV–vis absorption features were assigned by Solomon et al. as in-plane $\pi_\sigma^* \rightarrow d_{xy}$ and out-of-plane $\pi_v^* \rightarrow d_{xy}$ peroxo to Cu(II) CT transitions for the ca. 350 and 530 nm absorption bands, respectively (Figure 14).[3,161,196,205] The in-plane $\pi_\sigma^* \rightarrow d_{xy}$ feature is more intense, reflecting better orbital overlap than the out-of-plane $\pi_v^* \rightarrow d_{xy}$ feature (Figure 16). rR spectra display a low-energy O–O stretching vibration at 730–760 cm^{-1} ($\Delta[^{18}O_2] \approx$ 40 cm^{-1}) that is characteristic of ^{S}**P** species. Its lower O–O stretching frequency compared to that of a typical peroxide ion (ca. 850 cm^{-1}) is proposed to result from back-bonding from Cu(II) orbitals into the σ^* orbital of the peroxide ion (Figure 14).[206] This donation weakens the O–O bond and provides a pathway by which the O–O bond

can be cleaved. An isotope-insensitive feature at ca. 300 cm^{-1}, now assigned as the fundamental symmetric Cu_2O_2 core vibration, has a greater intensity than the ca. 740 cm^{-1} O−O stretching vibration and is a convenient rR feature for identifying a ^{S}**P** species.[207]

4.4.4. Other ^{S}P Complexes

Apart from the structurally characterized examples described above, more than 20 systems form ^{S}**P** species and almost all are temperature-sensitive. While bulk O_2 uptake experiments provide important information about the Cu:O_2 ratio, the large quantity of ligand required for precise manometric measurements has generally given way to the simpler spectroscopic characterization methods. Low-temperature UV−vis spectroscopy is the primary characterization technique, complemented more and more frequently by rR spectroscopy. This combination, with appropriate profiling or oxygen-isotope substitution in the rR experiments, allows almost unambiguous identification of a ^{S}**P** species. Whether complete formation of a single species occurs in these cases can be assessed generally by measuring the extinction coefficient of the intense CT features at ca. 350 nm.

In the following discussion, only the thoroughly characterized systems that form ^{S}**P** species will be covered, and classification will be made by ligand type.

Tridentate Aromatic Amine Ligands. Tridentate nitrogen ligands that provide *fac* coordination are the most successful class of ligands used to stabilize ^{S}**P** species. Numerous derivatives of the monoanionic tris(pyrazolyl)borate ligand $Tp^{R3,R5}$ have been employed, and their Cu(I) complexes bind O_2 irreversibly.[100,195,199,204] The tris(pyrazolyl)methane ligand $Tpm^{R3,R5}$ (Figure 6), a related ligand in which the boron atom of Tp is replaced by a carbon atom, is neutral. Although initially reported to be inert to O_2,[227] $[(Tpm^{Me,Me})Cu(I)(MeCN)]^+$ binds O_2 as a ^{S}**P** species, in a reversible manner (Table 6).[210] In these examples, the charge of the ligand does not impact the type of Cu/O_2 species that forms but only the energy difference between the reactants and products; the oxygenation of $[(Tp^{Me,Me})Cu(I)]$ is a more exothermic reaction.

Another class of neutral *fac* trinitrogen ligands comprises the tris(imidazolyl)phosphines, $PIm^{R4,R1}$, that provide more biologically relevant ligation. Similar to the $Tp^{R3,R5}$ systems, the Cu(I) complexes of $PIm^{R4,R1}$ generally include an exogenous labile ligand such as MeCN to give pseudo-tetrahedral coordination. Oxygenation of $[(PIm^{R4,R1})Cu(I)(MeCN)]^+$ in polar solvents (MeOH, acetone) at low temperatures gives a ^{S}**P** species (Table 6).[208,209] For one of these complexes, $[(PIm^{Et,Me})_2Cu(II)_2(O_2)]^{2+}$, metrical parameters from EXAFS data suggest that each Cu center has a square-pyramidal geometry (Cu···Cu: 3.48 Å, Cu−O: 1.94 Å, Cu−N_{eq}: 2.05 Å, and Cu−N_{ax}: 2.30 Å).[208] Varying the steric demands at the ligand periphery (R^4) from Me to *i*Pr to *t*Bu leads to less favorable reactions of $[(PIm^{R4,R1})Cu(I)]^+$ complexes with O_2. Thus, when R^4 = Me, irreversible O_2 binding occurs; for R^4 = *i*Pr, reversible O_2 binding is observed; for R^4 = *t*Bu, no reaction with O_2 is detected.[209] Interestingly, the O_2-inert $[(PIm^{tBu,Me})Cu(I)]^+$ forms a complex with carbon monoxide, indicating that the large *t*Bu substituents do not exclude exogenous ligand binding. Overall, the use of tris(pyrazolyl) and tris(imidazolyl) *fac* ligands clearly illustrates that the Cu_2O_2 peroxide core is stabilized by a variety of aromatic nitrogen donors, if the ligand is sufficiently flexible to accommodate square-pyramidal coordination; the peripheral ligand substituents can affect the degree of O_2 reactivity, however, by altering the enthalpy of the formation reaction.

Tridentate Mixed Aromatic/Aliphatic Amine Ligands. Bis[2-(2-pyridyl)ethyl]alkylamines (RPy2) represent another class of trinitrogen ligands extensively investigated in connection with Cu/O_2 chemistry (Figure 6). Their linear architecture that forms two six-membered chelate rings allows both *fac*ial and *mer*idional coordination, a flexibility not possible with the *fac* ligands described above. Coordination trends are evident from crystal structures of their Cu(I) and Cu(II) complexes. RPy2 ligate Cu(I) in the *mer* fashion, forming three-coordinated T-shaped complexes, even in the presence of excess MeCN.[211,222] Though exceptions exist,[228] RPy2 tend to ligate Cu(II) ions facially, as part of an overall square-pyramidal coordination; either the amine or pyridine group can be axially positioned.[123,229,230] Oxygenation of $[(RPy2)Cu(I)(MeCN)]^+$ (R = Ph, $PhCH_2$, $PhCH_2CH_2$) yield predominantly ^{S}**P** species,[127,211,214,215] while $[(MePy2)Cu(I)(MeCN)]^+$ forms a ca. 90:10 mixture of ^{S}**P** and **O** species both in solution and the solid state.[123,171,212,231] The crystal structure of $[(MePy2)_2Cu_2(O_2)]^{2+}$ reveals a 3.45 Å Cu···Cu distance and a long 1.67 Å O−O bond length that is atypical for a ^{S}**P** complex. These Cu/O_2 complexes are more thermally sensitive than those created with the *fac* ligands described above. Suitably deuterated derivatives of these ligands greatly enhance the thermal stabilities of their Cu/O_2 complexes, indicating that ligand oxidation is involved in the thermal decay process.[213,226]

The secondary amine group in HPy2 provides a convenient synthetic handle by which to create binucleating ligands with a wide variety of bridging groups. The resulting binuclear Cu(I) complexes are oxygenated to form ^{S}**P** species, the spectroscopy and stability of which are dependent on the nature of the bridge. The ^{S}**P** species formed using the Py2-*m*-xyl^R ligands (Figure 6, Table 6) are similar to those formed with RPy2, except that the arene ring of the former ligands are hydroxylated (see Tolman's review in this issue).[147,156,219,232] The stability of the ^{S}**P** species increases as the electron density of the arene bridge decreases, highlighting the importance of electronic effects on the thermal stability of such Cu/O_2 species.[233] Geometric considerations are also important.[220,234,235] Py2-Un, a ligand created by shortening the bridge of Py2-*m*-xyl^H by a single carbon atom, yields a more thermally stable ^{S}**P** species, which is thought to result from the suboptimal positioning of the Cu_2O_2 core near the C−H group that is oxidized. This increased thermal stability allows the observation of reversible O_2 binding.[158]

The binucleating Py2-Nn ligands with oxidatively more stable alkyl bridges, $-(CH_2)_n-$ ($n = 3-5$), are generally more flexible but span a shorter distance than their *m*-xylyl counterparts. Py2-Nn ligands are used to create ^{S}**P** species displaying unique spectroscopic and geometric features that vary with the bridge length.[217,220−222,234] EXAFS data for the Py2-N4 and Py2-N3 systems reveal Cu···Cu distances of 3.37 and 3.22 Å, respectively,[218] shorter than the typical distance of ca. 3.5 Å for a ^{S}**P** species. The Cu···Cu contraction correlates with a decrease in intensity of the high-energy CT band at ca. 350 nm as well as an increase in energy of the O−O stretching vibration (741, 751, 765 cm^{-1}; $n = 3, 4, 5$, respectively). Together, these data are consistent with a 'butterfly' bending of the Cu_2O_2 core. Such distortion from planarity gives rise to an additional absorption band in the 420−490 nm range, assigned as the second component of the $\pi_\sigma^* \rightarrow d_{xy}$ peroxo to Cu(II) CT band,[220] a transition not formally allowed in a planar ^{S}**P** complex.

bBzIm is a mononucleating ligand similar to Py2 except that benzimidazole rather than pyridine groups are the aromatic nitrogen donors.[236,237] The Cu(I) complexes of bBzIm and a binucleating analogue of Py2-*m*-xyl, L66, reversibly bind O_2 to yield ^{S}**P** species at low temperatures (Table 6).[224] While $[(L66)Cu(I)_2]^{2+}$ fully oxygenates at −85 °C, the mononuclear $[(bBzIm)Cu(I)]^{+}$ forms only ca. 30% of the anticipated ^{S}**P** species.[223] The greater steric demands of two benzyl substituents in $[(bBzIm)_2Cu(II)_2(O_2)]^{2+}$ versus the single bridging *m*-xyl group in $[(L66)Cu(II)_2(O_2)]^{2+}$ are probably responsible for this difference in the degree of oxygenation. Substituent groups within a ligand, often considered as structurally innocent, can significantly affect the formation of compact metal complexes. This is especially true when these groups are sterically demanding, as in bBzIm.

Tridentate Aliphatic Amine Ligands. Until the mid-1990s, most ligands used in Cu/O_2 chemistry contained at least one aromatic nitrogen donor.[238] The perceived inability of a purely aliphatic amine ligand to stabilize a ^{S}**P** species was attributed to the electronic differences between aromatic and aliphatic amines: the latter are σ-donors and cannot act as π-acceptors. The large peripheral *i*Pr substituents of *i*Pr_3tacn, a *fac* triamine ligand that forms three five-membered chelate rings (a 5,5,5-chelate), and the use of low temperatures proved to be necessary in generating a ^{S}**P** species. Smaller substituents lead to the exclusive formation of an **O** species (section 4.5). Even with *i*Pr substituents, a change in solvent or counteranion generates a measurable equilibrium mixture of ^{S}**P** and **O** species, indicating a nearly isoenergetic relationship between these isomers, as initially described by Tolman et al. (section 4.6).[101,102,239,240] The CT bands and rR features of the ^{S}**P** complex with *i*Pr_3tacn are somewhat distinct from those derived from aromatic nitrogen ligands (Table 6). The low 713 cm^{-1} O−O stretching vibration[202] suggests significant electron donation into the σ^* orbital of the peroxide ion, a presumed consequence of the strong σ donation of the ligand and its inability to act as a π-acceptor. The CT absorption band at 366 nm suggests a distortion of the Cu_2O_2 core (section 4.4.5).

Expansion of the macrocyclic ring of *i*Pr_3tacn by a single carbon atom gives the *fac* triamine ligand *i*Pr_3-tacd, a 5,5,6-chelate. Upon oxygenation, its Cu(I) complex generates a ^{S}**P** species whereas those of the less sterically demanding cognates (Me_3tacd, Bz_3tacd) form an **O** species.[202] *i*Pr_3tacd is more sterically demanding than *i*Pr_3tacn because of the larger N−Cu−N bite angle created by its six-membered chelate ring.[14] The distorted structure of $[(iPr_3\text{-tacd})_2Cu(II)_2(O_2)]^{2+}$ (vide supra) coincides with a red shift of its CT absorption band to 380 nm. Curiously, its rR feature at 739 cm^{-1} is higher in energy than that of any other ^{S}**P** species formed with ligands containing only aliphatic amine donors (^{Me}an, *i*Pr_3-tacn, ^{H,tBu}ed; Table 6). The related macrocyclic triamine ligand that is a 6,6,6-chelate binds Cu(I) in a nearly trigonal-planar rather than a facial manner, and it is inert to O_2.[202] The limited flexibility of the macrocyclic ring is presumably responsible for this inertness because its acyclic triamine analogue, ^{Me}an (a 6,6-chelate), readily forms a ^{S}**P** species (Table 6).[124]

Bidentate Ligands. The necessity for tridentate ligation to stabilize ^{S}**P** species is not justified by the reported structures, which show that one of the nitrogen atoms is always weakly associated to each Cu ion. Accordingly, bidentate nitrogen ligands were shown to suffice in stabilizing Cu/O_2 species, including the ^{S}**P** species. Their Cu(I) complexes are generally three-coordinated, by binding an additional labile ligand. Such complexes have been known for two decades to react with O_2 and form thermally sensitive Cu/O_2 species.[238] The vast majority of these ligands has been used to generate **O** species or equilibrium mixtures of ^{S}**P** and **O** species (vide infra), yet two examples have been reported in which measurable amounts of only ^{S}**P** species form.

$[(^{H,tBu}ed)Cu(I)(MeCN)]^{+}$ reacts with O_2 at −80 °C to form a ^{S}**P** species that exhibits an exceptionally intense CT band at 350 nm ($\epsilon \approx 36\,000$ M^{-1} cm^{-1}), blue-shifted relative to other aliphatic amine ^{S}**P** species (ca. 365 nm).[125] Yet the 3.46 Å Cu···Cu distance and $Cu-O/N_{avg}$ bond lengths of 1.96 Å obtained from EXAFS data are typical for ^{S}**P** species. A weak axial interaction with another O/N donor at ca. 2.5 Å, ascribed to an oxygen atom of a counteranion, creates a square-pyramidal geometry at each Cu center. Counteranion variation in solution shifts the CT bands and O−O rR features, confirming an intimate interaction of the couteranion with the complex. The ligand ^{H,tBu}ed, a secondary diamine, is an unconventional choice for Cu/O_2 chemistry, yet its ^{S}**P** species is more thermally stable ($t_{1/2} = 20$ days, THF, −80 °C) than that formed with ^{Me,tBu}ed, which has no N−H groups.[124,129] A reduction in the steric demands of the R group in ^{H,R}ed ligands diminishes the thermal stability of the resulting ^{S}**P** species.

^{Me}Py1^{Et,Bz} is the other bidentate ligand known to create a ^{S}**P** species exclusively.[226] Its optical and rR features are similar to those of the ^{S}**P** species formed with *i*Pr_3tacd, a structurally characterized complex with significant distortions from square-pyramidal coordination at each Cu center. The 6-methyl substituent of ^{Me}Py1^{Et,Bz} is essential for the generation

of a ^{S}**P** species, since the 6-H analogue, ^{H}Py1^{Et,Bz}, forms solely the more compact **O** species.

4.4.5. Summary

Systematic shifts are observed in the characteristic high-energy CT band of the ^{S}**P** species within a family of ligands; an increase in the steric demands of the ligand leads to a decrease in the energy of the CT transition (Table 6). For the $\pi_\sigma^* \rightarrow d_{xy}$ peroxo to Cu CT transition, any influence that affects either the accepting d_{xy} or the donating π_σ^* orbital would change the transition energy (Figure 14). A simple molecular orbital analysis suggests that elongation of the Cu−Cu vector and/or distortion of the equatorial amine ligands out of the Cu_2O_2 plane—either of which may be induced through steric interactions—should lead to a bathochromic shift of this CT feature.

The initial identification of the novel binding mode for O_2 in oxyHc from the characterization of a coordination compound is correctly recognized as a seminal achievement in bioinorganic chemistry. While the spectroscopic and structural fidelity of the models to the native systems is remarkable, this system clearly highlights some fundamental principles that underlie bioinorganic modeling endeavors. First is the correlation between unique spectroscopic features and unique structural features, in this particular case the unique O_2 binding mode. Second, structures obtained with simple model complexes under the abiological conditions of low temperatures and aprotic solvents provide chemically plausible species for mechanisms proposed for biochemical systems.

4.5. Bis(μ-oxo)dicopper(III) Complexes, O

4.5.1. Introduction

The bis(μ-oxo)dicopper(III) species (**O**) was the last 2:1 Cu/O_2 archetype to be discovered, and no evidence currently exists to support its biochemical relevance.[241] While initially observed in 1993 by two groups working with different but related ligand systems,[117,172] the **O** species was not properly identified until its first structural characterization in 1996.[101,242] During the past decade, the **O** species has been thrust into the limelight of Cu/O_2 chemistry as the most prevalent species, a prominence resulting in part from the great diversity of ligands that can be used in its formation, including bidentate,[96,97,127,140,226,242−247] tridentate,[101,102,124,239,248] and even tetradentate ligands.[176,182,183] The proclivity of Cu(III) to be square-planar with anionic ligands facilitates its formation when it is provided with two bridging oxide (O^{2-}) ligands from reduction of O_2 and bidentate nitrogen donors from the attendant ligand. Mixtures containing the ^{S}**P** and **O** isomers can be generated with several ligands (section 4.6). The differences in oxidation states of Cu and the O_2-derived moiety between ^{S}**P** and **O** manifest themselves in remarkably different structural and spectroscopic characteristics (Figure 3, Table 1) as well as different chemical reactivity patterns for the two isomers.[113,233,245]

4.5.2. Structural Characterization

Despite bearing diverse ligands, all six crystallographically characterized **O** complexes have short Cu−O bonds (1.79−1.86 Å) and exhibit a preference for square-planar coordination (Figure 17).[97,102,182,242,247,249] The structures also reveal that the Cu_2O_2 core is more compact in **O** than in ^{S}**P** species. Four of the structurally characterized **O** complexes are dications with neutral ligands, one is neutral with two monoanionic ligands, and one is a monocation with both a neutral and a monoanionic ligand.

The first structurally characterized **O** species, reported by Tolman et al. in 1996, was generated with the macrocyclic *fac* triamine ligand Bz_3tacn (Figure 17a).[101,102] The short Cu···Cu and Cu−O_{avg} distances (2.79 and 1.80 Å, respectively) and the long 2.23 Å O···O separation result from complete cleavage of the bond in O_2 to produce two oxide ligands, concomitant with oxidation of each Cu(I) center to Cu(III). Both Cu ions are square-pyramidal ($\tau = 0.02$, 0.02),[200] with axial nitrogen donors weakly associated at ca. 2.3 Å and arranged anti within the core, and with equatorial Cu−N bond lengths of ca. 1.99 Å. Metrical parameters for the **O** species formed with *i*Pr_4dtne, a binucleating version of *i*Pr_3tacn reported by the same group, are similar (Cu···Cu: 2.78 Å, Cu−O_{avg}: 1.83 Å, and O···O: 2.35 Å, Figure 17d).[249] The two nitrogen atoms linked by the $-CH_2CH_2-$ bridge are axial (Cu−N_{avg} = 2.31 Å) and complete the square-pyramidal coordination of each Cu center (τ = 0.08, 0.14). In contrast to those in $[(Bz_3tacn)_2Cu(III)_2(O)_2]^{2+}$, these axial nitrogen donors have a syn configuration within the core structure.

Simple bidentate aliphatic amine ligands such as ^{Me,Et}cd suffice to form **O** species, in line with the geometric preferences of Cu(III), as reported by Stack et al. The minimized peripheral substituents of the ligand ^{Me,Et}cd allow the **O** structure $[(^{Me,Et}cd)_2Cu(III)_2(O)_2]^{2+}$ to have one of the most compact Cu_2O_2 cores yet reported (Cu···Cu: 2.74 Å, Cu−O_{avg} 1.80, and O···O: 2.34 Å, Figure 17b).[242] The metrical parameters obtained from solid-state EXAFS data (Cu···Cu: 2.73 Å, Cu−O_{avg} 1.80 Å) agree closely with the crystallographic results.[87] Even though this complex is a dication, the counteranions do not bind to the square-planar Cu centers. The contraction in the Cu···Cu distance by 0.05 Å along with a similar expansion in the O···O distance in $[(^{Me,Et}cd)_2Cu(III)_2(O)_2]^{2+}$ compared with those in $[(Bz_3tacn)_2Cu(III)_2(O)_2]^{2+}$ can be attributed to lesser steric demands of the diamine ligand.

The intriguing **O** species prepared by Suzuki et al. uses the ligand Me_2tmpa, which is similar to the tmpa-based ligands used to generate ^{T}**P** species.[182] Yet, the tetradentate ligand Me_2tmpa acts de facto as a bidentate one in the **O** complex $[(Me_2tmpa)_2Cu(III)_2(O)_2]^{2+}$. The unsubstituted pyridine and the amine groups bind in equatorial positions (Cu−N_{eq} ≈ 1.94 Å), while the two 6-methylpyridine groups interact weakly in the axial positions of each Cu center (Cu−N_{ax} ≈ 2.5 Å, Figure 17c). The Cu···Cu and O···O distances of 2.76 and 2.32 Å, respectively, are consistent with those of the other structurally characterized **O** species. The remarkable and unique

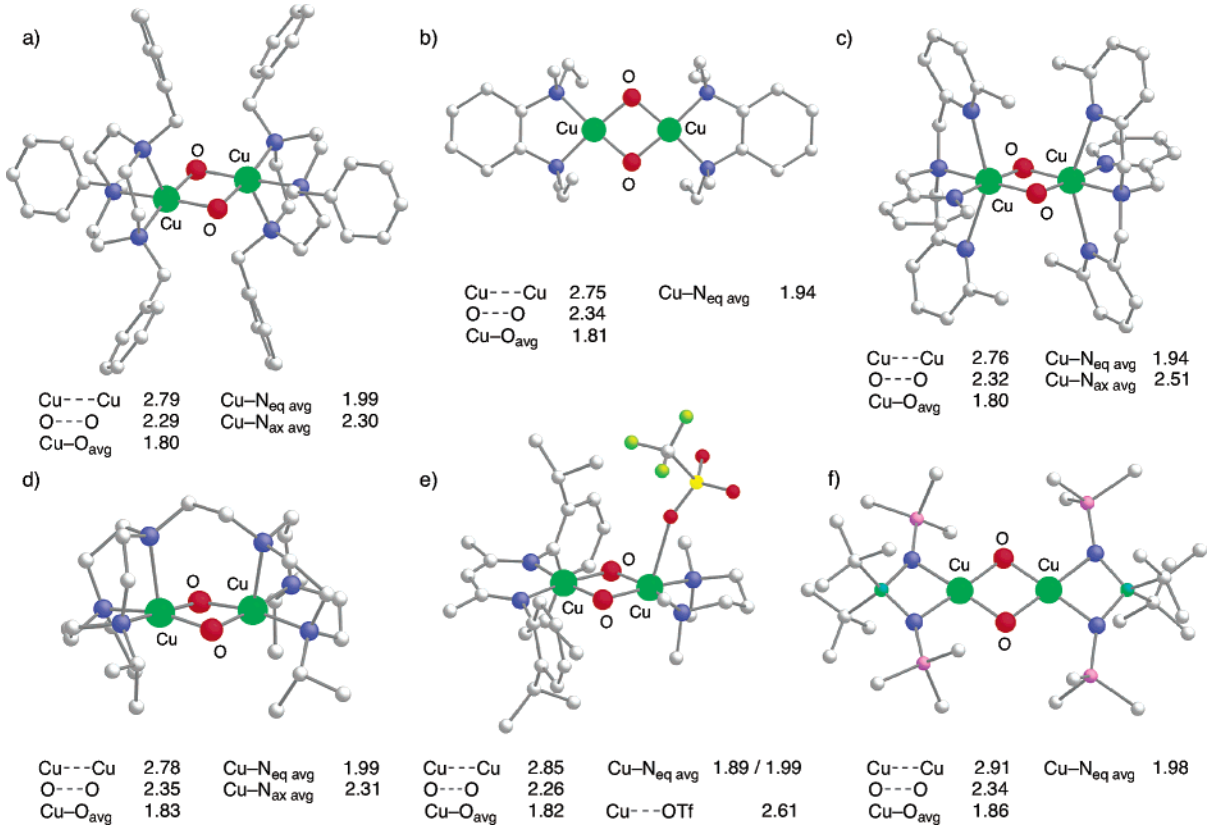

Figure 17. X-ray structures of **O** species with metrical parameters (Å): (a) $[(Bz_3tacn)_2Cu(III)_2(O)_2]^{2+}$,[101,102] (b) $[(^{Me,Et}cd)_2Cu(III)_2(O)_2]^{2+}$,[242] (c) $[(Me_2tmpa)_2Cu(III)_2(O)_2]^{2+}$,[182] (d) $[(iPr_4dtne)Cu(III)_2(O)_2]^{2+}$,[249] (e) $[(^{H,Me}Dk^{iPr})(^{Me,Me}pd)Cu(III)_2(O)_2]^{+}$ (one *i*Pr group removed for clarity),[97] (f) $[(PN2)_2Cu(III)_2(O)_2]$.[247]

attribute of this **O** complex is its ability to reversibly bind O_2 at low temperatures, a $4e^-$ process that requires reversible breaking and making of the bond in O_2.

While all cationic **O** species characterized to date are thermally unstable, an indefinitely stable neutral **O** species, reported by Hoffman et al., uses a monoanionic bidentate iminophosphanamide ligand, PN2.[247] The four-membered chelate ring of PN2 does not allow rigorously square-planar coordination around the Cu centers, but the crystal structure reveals a crystallographically imposed planar Cu_2O_2 core (Cu···Cu: 2.90 Å, O···O: 2.34 Å, and Cu−O$_{avg}$: 1.86 Å, Figure 17f). Though slightly longer than those in other **O** complexes, these distances are consistent with the presence of Cu(III) centers.

A series of monoanionic, bidentate β-diketiminate ligands, $^{R1,R2}Dk^{R3}$, that stabilize the Cu(III) ion has been reported recently by Tolman et al.[96,140] Depending on the steric demands of the ligand, either 1:1 ^{M}**P** or 2:1 **O** species form (section 7), akin to the reactivity pattern seen with monoanionic $Tp^{R3,R5}$ ligands. For those cases in which a ^{M}**P** complex can be formed (section 3.3.2), subsequent addition of one equivalent of a second Cu(I) complex with lesser steric demands creates a mixed-ligand **O** species (Figure 17e).[97] Structural characterization of one such complex reveals distinct Cu−N bond lengths for the two ligands (1.89 Å for $^{H,Me}Dk^{iPr}$, 1.99 Å for $^{Me,Me}pd$), yet the Cu−O bond lengths are similar. Each Cu ion in $[(^{H,Me}Dk^{iPr})(^{Me,Me}pd)Cu(III)_2(O)_2]^{+}$ is square-planar with typical metrical parameters for an **O** species with six-membered chelate rings (Cu···Cu: 2.85 Å, Cu−O: 1.82 Å, and O···O: 2.26 Å, Figure 17e).[97] The $^{Me,Me}pd$-ligated Cu center interacts weakly with one oxygen atom of the TfO^- counteranion (Cu···O$_{ax}$: 2.61 Å). This association is similar to that predicted from solution EXAFS data of $[(^{Me,Me}pd)_2Cu(III)_2(O)_2](CF_3SO_3)_2$, an **O** species with metrical parameters (Cu···Cu: 2.85 Å, Cu−O: 1.81 Å, and Cu···O$_{ax}$: 2.32 Å) that are remarkably similar to those of the mixed-ligand system.[243]

4.5.3. Spectroscopic Characterization

The dramatic structural differences between **O** and ^{S}**P** isomers portend different UV−vis and rR spectroscopic characteristics. **O** complexes generally exhibit two intense CT absorption bands at ca. 300 and 400 nm (Figure 18). rR experiments reveal a characteristic and intense vibration at ca. 600 cm^{-1} that shifts by ca. 25 cm^{-1} upon $^{18}O_2$ substitution and is assigned as a symmetric breathing mode of the Cu_2O_2 core.[241,250] An isotope-insensitive feature in the 120−135 cm^{-1} range is the fundamental symmetric vibration of the Cu_2O_2 core. The combination of UV−vis and rR spectroscopies along with DFT calculations were used by Solomon et al. to assign the two intense 300 and 400 nm absorptions bands as the $\pi_\sigma^* \rightarrow d_{xy}$ and $\sigma^* \rightarrow d_{xy}$ oxide to Cu(III) CT transitions, respectively (Figure 14).[250] The high intensities of these CT bands are consistent with a significant covalency in the Cu−O bonds. The ca. 300 nm in-plane $\pi_\sigma^* \rightarrow d_{xy}$ transition has similar origins to the ca. 350 nm transition in ^{S}**P** species, but the ca. 400 nm feature

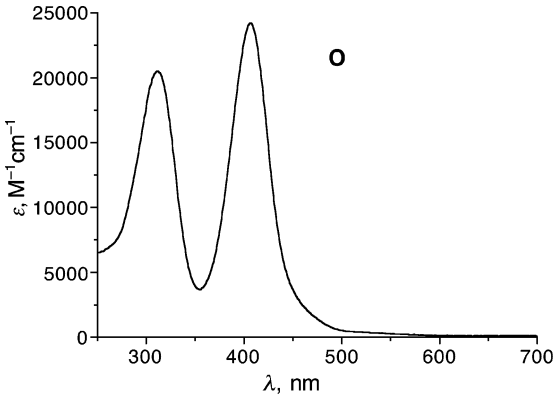

Figure 18. UV−vis spectrum of the **O** species $[(^{Me,iPr}ed)_2Cu(III)_2(O)_2]^{2+}$ (CH_2Cl_2, −80 °C, TfO^-).[251]

is unique to **O** species. Upon reduction of the peroxide ion and cleavage of the O−O bond, the σ^* orbital decreases dramatically in energy and becomes occupied (Figure 14). Good overlap of the filled σ^* orbital in the **O** species with the d_{xy} orbitals of the Cu centers gives rise to this intense ligand to Cu CT feature.

4.5.4. Other O Complexes

The characteristic UV−vis and rR spectroscopic features, combined with the Cu/O_2 reaction stoichiometry, provide a nearly unambiguous characterization of an **O** species. More than 40 different **O** complexes with a variety of ligands have been characterized to date, forming the most prevalent and diverse class of Cu/O_2 species (Table 7). No **O** species is currently known to have only aromatic nitrogen ligation, however. Most of the **O** species are stabilized with neutral aliphatic amine ligands, with a bias toward bidentate ligation.[241]

Almost all R_3tacn *fac* tridentate ligands (R = Me, Bz, *i*Pr) yield **O** complexes with characteristic UV−vis and rR optical features.[101,102,239,242,253] The **O** complex formed with Me_3tacn is the most thermally stable in this family ($t_{1/2}$ = 40 s, CH_2Cl_2, −10 °C) and is nearly 10 times more stable than the **O** species with Bz_3tacn.[126] The latter **O** species decomposes via oxidation at a benzylic carbon atom of the ligand. In fact, to obtain the crystal structure of $[(Bz_3tacn)_2Cu(III)_2(O)_2]^{2+}$, the ligand was perdeuterated at the benzylic positions to enhance the thermal stability

Table 7. Spectroscopic Features of O Complexes

ligand[a]	anion	solvent	Cu···Cu, Å	UV−vis: λ, nm (ε, mM^{-1} cm^{-1})	rR: ν, cm^{-1} (Δ[$^{18}O_2$])	ref
Me_3tacn	TfO^-	CH_2Cl_2	2.77[b]	307 (16), 412 (18)	604 (23)	126,242
Me_2Odacn	TfO^-	CH_2Cl_2		297 (16), 397 (15)		126
Bz_3tacn	ClO_4^-	CH_2Cl_2	2.79[c]	318 (12), 430 (14)	603, 595 (23)	102,248,252,253
$Bz3_3$tacn[d]	PF_6^-	CH_2Cl_2		302 (2.7[e]), 411 (3[e])	600 (31)	254
iPr_2Bztacn	ClO_4^-	CH_2Cl_2		322 (12), 436 (16)	594 (22)	102,253
iPr_3tacn	ClO_4^-	THF		324 (11), 448 (13)	589 (22)	102,252
*i*Prdtne	ClO_4^-	CH_2Cl_2	2.78[c]	316 (13), 414 (14)	600 (22)	249
iPr_4dtn-*m*-xyl[f]	TfO^-	CH_2Cl_2		320 (13), 430 (15)	595 (25)	122
iPr_4dtn-*p*-xyl[f]	ClO_4^-	CH_2Cl_2		320 (13), 430 (14)	594 (24)	122
Me_3tacd	SbF_6^-	CH_2Cl_2		304 (16), 404 (16)	595 (20)	202
Bz_3tacd	SbF_6^-	CH_2Cl_2		312 (14), 428 (14)	600 (25)	202
^{Me,Me}cd	TfO^-	CH_2Cl_2		301 (20), 399 (25)	605 (23)	242
^{EtMe_3}cd[g]	TfO^-	CH_2Cl_2	2.73[b]	305 (19), 402 (27)		242
^{Me,Et}cd	TfO^-	CH_2Cl_2	2.73[b], 2.74[c]	313 (21), 408 (28)	610 (23)	242
^{Et,Et}cd	TfO^-	CH_2Cl_2		319 (17), 413 (23)	616 (26)	242
^{Et,Et}ed	TfO^-	CH_2Cl_2	2.74[b]	309 (17), 407 (24)	603 (31)	126
^{Me,Et}ed	TfO^-	CH_2Cl_2		297 (23), 397 (25)		126
^{Me_2Et_2}ed[h]	TfO^-	CH_2Cl_2		297 (18), 397 (21)		126
^{Me,iPr}ed	TfO^-	CH_2Cl_2		311 (20), 407 (24)		251
^{Me,Me}pd	TfO^-	CH_2Cl_2	2.85[b]	297 (16), 397 (24)	609 (28)	243
^{Me,Et}pd	TfO^-	CH_2Cl_2		305 (14), 402 (23)		251
Me_5dien	PF_6^-	EtCN		405 (6)		13
^{H}an	$B(C_6F_5)_4^-$	CH_2Cl_2		293 (15), 393 (12)	608 (28)	124
iPr_2daco	SbF_6^-	CH_2Cl_2		330, 438	632/591 (24)	225
sparteine	TfO^-	CH_2Cl_2		330 (13), 427 (23)	619 (28)	246
$PhPyNEt_2$	SbF_6^-	THF		406 (13)	606 (28)	255
^{H}Py1^{Et,Bz}	PF_6^-	acetone		400 (17)	606 (29)	226,256,257
^{H}Py1^{Et,Phe}	PF_6^-	acetone		402 (18)	607 (29)	127,226
Me_2tmpa[i]	PF_6^-	acetone	2.76[c]	378 (22), 494 (0.3)	590 (26)	172,182
Me_3tmpa[j]	PF_6^-	acetone		517	583 (25)	183
PN2	[k]	pentane	2.91[c]	444 (10)		247
^{H,Me}Dk^{Me}	[k]	THF		328 (19), 422 (11)	608 (27)	140
^{H,Me}Dk^{Et}	[k]	THF		352 (11), 426 (10)	604 (27)	140
^{Ph,H}Dk^{Me}	[k]	THF		377 (10), 420 (12)	586/614 (27)	140
^{Ph,H}Dk^{Et}	[k]	THF		379 (10), 425 (17)	591/617 (30)	140
^{Ph,H}Dk^{iPr}	[k]	THF		369 (10), 433 (sh, 7)	580 (20)	96
^{H,Me}Dk^{iPr}/^{H,Me}Dk^{Me}	[k]	THF		435 (9[e])	598 (28)	97
^{H,Me}Dk^{iPr}/Me_3tacn	TfO^-	THF		406 (20[e])	647 (23)	97
^{H,Me}Dk^{iPr}/^{Me,Me}pd	TfO^-	THF	2.85[c]	398 (17[e])	653 (28)	97

[a] See Figures 6 and 7. [b] From EXAFS data. [c] From X-ray structure. [d] A tacn-based dendrimer. [e] Approximate value. [f] Intermolecular complex (dimer of dimers). [g] *N*-ethyl-*N*,*N*′,*N*′-trimethyl-1*R*,2*R*-cyclohexanediamine. [h] *N*,*N*-diethyl-*N*′,*N*′-dimethyl-1,2-ethanediamine. [i] Reversible O_2 binding. [j] Incomplete formation. [k] Neutral complexes.

of its **O** complex.[101,102] Dendritic extension of the Bz_3-tacn ligand leads to formation of more thermally stable **O** species, yet this strategy is limited because the rate of formation of the dimeric **O** species is adversely affected by the size of the dendritic groups.[254] Within these dendritic environments, the CT features are significantly blue-shifted relative to those of $[(Bz_3\text{-tacn})_2Cu(III)_2(O)_2]^{2+}$ (Table 7). Binucleating tacn ligands, created by connecting two iPr$_2$tacn units through *m*-xylyl, *p*-xylyl, or $-CH_2CH_2-$ bridges, also generate **O** complexes. The iPr$_4$dtn-*p*-xyl ligand yields a tetranuclear **O** species, an *inter*molecular "dimer-of-dimers".[122,225] The analogous iPr$_4$dtn-*m*-xyl forms such an intermolecular **O** species only at high Cu concentrations, while an *intra*molecular ^{S}**P** species forms at low Cu concentrations, yet no interconversion between these complexes was observed.

Similar to those of R_3tacn, the Cu(I) complexes of R_3tacd (R = Me, Bz), tridentate macrocyclic ligands (5,5,6-chelates), generate **O** complexes upon oxygenation.[202] With the same peripheral substituents, an increase in the macrocyclic ring size by one atom raises the thermal stability of the **O** species by one order of magnitude at −10 °C,[126,202] but the spectroscopic features are not altered significantly. Combined, these data suggest that one of the five-membered chelate rings of Me_3tacd binds in the equatorial plane of each Cu center, a ligation mode observed in the crystal structure of the thermal decay product $[(Me_3tacd)_2Cu(II)_2(OH)_2]^{2+}$.[202] The presence of a six-membered chelate ring weakens the axial nitrogen interaction, possibly reducing the oxidizing ability of the Cu(III) centers.[71] The open-chain analogue of Me_3tacn, Me_5dien (a 5,5-chelate), forms an **O** species that is not stable even at −80 °C.[13] However, the open-chain ligand, ^{H}an (a 6,6-chelate), leads to the formation of a stable **O** species.[124]

Alkylated diamines constitute the largest class of ligands that generate **O** complexes (Table 7). They are generally less sterically demanding than the macrocycles, and their bidentate structures ideally match the square-planar ligation preference of each Cu(III) center within the Cu_2O_2 core. While only limited data exist, a five- rather than a six-membered chelate ring seems to confer higher thermal stability to the **O** species, at parity of peripheral substituents.[126] Changing the N-alkyl substituents (R = Me, Et, iPr, tBu) as well as the diamine backbones (ed, cd, pd) allows the steric demands within the series of ligands to be varied smoothly, a convenient variation for investigating the thermodynamic and kinetic properties of Cu/O_2 species (section 7).[242,243]

Bidentate ligands with both aliphatic and aromatic nitrogen donors lead preferentially to **O** species (Table 7). For example, the Cu(I) complex of PhPy-NEt_2 oxygenates to yield an **O** complex, [255] as do the homologue ligands with six-membered chelate rings, ^{R1}Py1^{R2,R3}.[127,226,256−258] However, ligands that are more sterically demanding, such as ^{Me}Py1^{Et,Bz}, can yield ^{S}**P** species (section 4.4).[226]

4.5.5. Summary

The subtle variation of the peripheral substituents of ligands within a family creates a continuum of steric effects that provides a systematic probe of the structure of **O** species through a smooth shift of the characteristic spectroscopic features. Generally, the intense CT features shift to lower energies as the steric demands of the ligands increase, as observed in four different families (Table 8). These examples highlight the sensitivity of the electronic features of these complexes to seemingly minor structural distortions. Increased steric interactions between the peripheral substituents of the two ligands and/or between the ligand substituents and the oxide ligands may create a distortion within the Cu_2O_2 core. Because the Cu−O bonds do not lengthen significantly in these dicationic **O** complexes, this distortion is associated with an increase of the Cu···Cu distance and a decrease of the O···O distance. The energy of the σ_u* orbital, the donor orbital involved in the ca. 400 nm CT transition, should be especially sensitive to the O···O distance, and thus a decrease in the absorption energy is predicted for such a distortion of the Cu_2O_2 core. Other **O** species with sterically demanding ligands such as the diazacyclononane ligand iPr$_2$daco[225] and the polycyclic diaza ligand sparteine[246] also have low-energy CT features, consistent with an increase of the Cu···Cu separation. In those cases, however, additional distortions of the Cu coordination geometry from square-planar toward tetrahedral could affect the d-orbital manifold and therefore the energy levels of the accepting orbitals (Figure 14). The rR data do not reveal systematic trends beyond the fact that the ca. 600 cm^{-1} feature appears generally at higher energy with bidentate than with tridentate ligands.

Table 8. Low Energy CT Band of O Complexes for Four Families of Ligands (λ_{max}, nm)

^{Me,Me}cd	399	^{Me,Me}ed	398	^{Me,Me}pd	397	Me_3tacn	412
^{Me_3Et}cd	402	^{Et,Et}ed	407	^{Me,Et}pd	402	Bz_3tacn	430
^{Me,Et}cd	408	^{Me,iPr}ed	407	^{Me,iPr}pd	411	iPr$_2$Bztacn	436
^{Et,Et}cd	413	^{Me,tBu}ed	452	^{Et,Et}pd	415	iPr$_3$tacn	448

4.6. Mixtures of ^{S}P and O Complexes

The two most prevalent binuclear Cu/O_2 species, ^{S}**P** and **O**, are isomers that can exist in measurable quantities in equilibrium with each other. Recent theoretical investigations, in contrast to previous reports,[259,260] suggest that the **O** complex is more enthalpically stable than the corresponding ^{S}**P** isomer in model compounds, while the ^{S}**P** species appears to be favored in biochemical systems.[261,262] However, a ^{S}**P**/**O** equilibrium mixture can be obtained under specific conditions. This equilibrium is influenced primarily by the steric demands of the ligand, although counteranion, solvent, and electronic features of the ligand can also affect its position (vide infra). Varying the temperature induces a reversible change in the equilibrium position, which provides evidence for a facile ^{S}**P**/**O** isomerization, an intrinsic property of these isomers.

For each of the well-characterized systems currently known to exist as equilibrium mixtures of dicationic ^{S}**P** and **O** complexes,[240,245,251] the **O** species is stabilized enthalpically while the ^{S}**P** species is stabilized entropically, as determined from the ther-

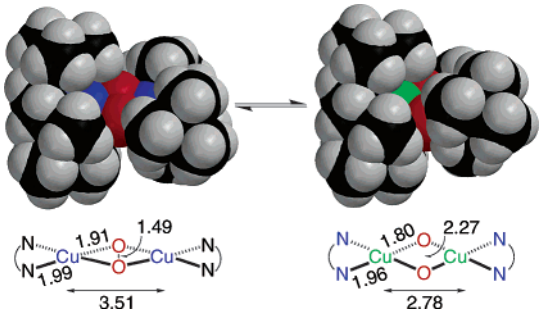

Figure 19. DFT-calculated ^{S}**P** and **O** species with ^{Me,tBu}ed, and selected metrical parameters (Å).[14]

modynamic parameters for the ^{S}**P** ⇔ **O** equilibrium ($\Delta H° = -0.9$ kcal mol^{-1}, $\Delta S° = -6$ cal mol^{-1} K^{-1};[240] and $\Delta H° = -0.6$ kcal mol^{-1}, $\Delta S° = -2$ cal mol^{-1} K^{-1},[245] respectively). As anticipated, the small entropic differences reflect the isomeric relationship of these species, and the equilibrium constants are only weakly temperature dependent. In cases with large enthalpic differences between the two isomers (sections 4.4 and 4.5), large temperature variations would be required to achieve detectable mixtures, which is not commensurate with the thermal instability of Cu/O_2 species. In addition, the difficulty to deconvolute their broad overlapping absorption features limits the number of mixtures detectable by UV−vis spectroscopy. For these reasons, only a limited number of ligands possess the appropriate attributes to generate such mixtures. While not observed in every case, a rapid equilibrium is assumed. In one particular case, the rate of isomer interconversion is diminished and the two species react independently.[245]

Steric Demands of the Ligands. The more compact structure of **O** versus ^{S}**P** (Cu···Cu: ca. 2.8 Å for **O**, ca. 3.6 Å for ^{S}**P**) implies that, for the same ligand, intramolecular steric interactions are greater for **O** than for ^{S}**P**, a characteristic in accord with estimates made using space-filling models of the two species (Figure 19).[14] Hence, increasing the steric demands within a family of ligands destabilizes **O** to a larger degree and biases the ^{S}**P**/**O** equilibrium position more toward ^{S}**P** (Table 9).

When steric interactions are minimized, tridentate and bidentate aliphatic amine ligands preferentially stabilize the **O** core, as evidenced by the exclusive formation of **O** species with the simplest ligands (Me_3-tacn, Me_3tacd, ^{Me,Me}cd, and ^{Me,Me}pd). DFT calculations on dicationic complexes that exclude counteranion effects predict an energetic preference for the **O** species in such systems greater than 20 kcal mol^{-1}.[262] This energetic bias is attenuated as the ligand steric interactions increase, through the attachment of larger peripheral substituents, until a measurable equilibrium is detected. Under such conditions, other energetic contributions—counteranion, solvent, and electronic features of the ligand—become comparable to the energy difference between the two isomers. For instance, at −80 °C, a change in the ^{S}**P**:**O** ratio from 10:90 to 90:10 requires only ca. 1.7 kcal mol^{-1}. Thus, the steric demands of the ligand provide coarse-tuning of the equilibrium position, while the other variables provide fine-tuning of the established equilibrium.

Counteranion. The position of the ^{S}**P**/**O** equilibrium for dicationic Cu_2O_2 species can be influenced by the identity of the weakly coordinating counteranions. With bidentate amine ligands, **O** species form predominantly when less coordinating anions (SbF_6^-, BF_4^-, BArF$^-$) are used while more coordinating anions (TfO$^-$, MsO$^-$) bias the equilibrium toward ^{S}**P** (Figure 20).[14,245,251] The apparently greater affinity of the ^{S}**P** species for better coordinating counteranions is in line with its more exposed Cu_2O_2 core and the greater proclivity of Cu(II) ions to bind axial ligands, in contrast with the Cu(III)-containing **O** species. Strongly coordinating anions such as chloride or acetate generally lead to rapid decay of the complexes by a yet unknown mechanism.

Solvent. Other conditions being equal, more polar solvents favor the formation of **O** species while less polar solvents favor the production of ^{S}**P** species (Fig-

Table 9. Spectroscopic Features of ^{S}P/O Mixtures

				UV−vis: λ, nm (ϵ, mM^{-1} cm^{-1})				rR: ν, cm^{-1} (Δ[$^{18}O_2$])		
ligand[a]	^{S}**P**:**O** ratio[b]	anion	solvent	**O**	^{S}**P**	**O**		^{S}**P**	**O**	ref
*i*Pr$_3$tacn	90:10	ClO_4^-	CH_2Cl_2		366 (23)		510 (1.3)	714 (41)		101, 102, 253
	10:90	ClO_4^-	THF	324 (11)		448 (13)			589 (20)	101, 102
	60:40	SbF_6^-	THF		364 (18)	418 (8)	510	711 (40)	589 (25)	240
MePy2	90:10	BArF$^-$	CH_2Cl_2		356 (15)	410 (3)	530 (0.6) 654 (0.5)	729 (40)	587 (26)	123, 171
MePy2^{MeO}	88:12	BArF$^-$	CH_2Cl_2		356 (20)	410 (4)	535 (1.0) 650 (0.8)	728 (39)	585 (26)	171
MePy2^{Me_2N}	86:14	BArF$^-$	CH_2Cl_2		360 (28)	410 (sh)	515 (1.4) 650 (0.7)	729 (40)	548 (25)	171
^{Me,tBu}ed	50:50	TfO$^-$	THF	327 (5)	369 (15)	455 (14)		730 (39)	617 (26)	245
	40:60	ClO_4^-	THF	334 (5)	370 (15)	452 (13)				245
	40:60	ClO_4^-	MeTHF	334 (6)	370 (12)	452 (17)				245
	10:90	SbF_6^-	THF	329 (11)	370 (sh)	451 (22)				14, 251
	90:10	MsO$^-$	THF		369 (24)	450 (sh)				14, 251
^{Et,Et}pd	10:90	TfO$^-$	acetone	325 (17)		421 (30)				14, 251
	50:50	TfO$^-$	THF	310 (sh)	362 (20)	416 (17)				14, 251
	70:30	TfO$^-$	MeTHF		362 (27)	415 (12)				14, 251
^{iPr,Me}pd	20:80	SbF_6^-	THF	328 (14)	365 (sh)	425 (25)				251
	40:60	TfO$^-$	THF	317 (10)	365 (16)	412 (20)				251
	90:10	MsO$^-$	THF		361 (24)					251

[a] See Figures 6 and 7. [b] Approximate value.

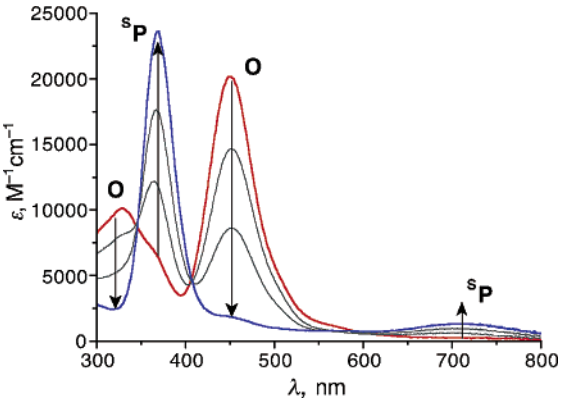

Figure 20. Titration of $[(^{Me,tBu}ed)Cu_2O_2](SbF_6)_2$ with 0 → 1 equiv of MsO^- increases the quantity of the ^{S}**P** in the mixture (THF, −80 °C).[14]

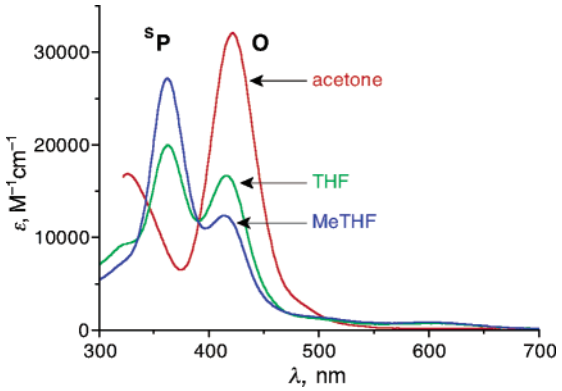

Figure 21. Influence of solvent on the ^{S}**P**/**O** equilibrium (^{Et,Et}pd, TfO^-, −85 °C).[14]

ure 21).[102,240,245] This trend is clear for systems using bidentate amine ligands (^{tBu,Me}ed, ^{Et,Et}pd, ^{iPr,iPr}pd)[245] or the tridentate amine ^{H}an[124] but not when iPr$_3$tacn is used.[240] The effect of the solvent polarity is likely coupled with the preferential counteranion association with the ^{S}**P** species, because such associated species would have a lower effective charge.

Electronic Effects. The impact of ligand electronic effects on the ^{S}**P**/**O** ratio has recently been investigated, using the MePy2^R family of ligands.[123,171,258] Varying the substituent at the 4-position of the pyridine rings affects the electron density of the ligand without significantly changing its steric demands, although coordination to the Cu center is potentially ambiguous because the aliphatic amine groups can bind in either an axial or an equatorial position. Slight changes in the equilibrium position are observed as the 4-substituent is varied, a change in energy that amounts to no more than 0.5 kcal mol^{-1}. Electron-donating substituents shift the equilibrium toward the **O** species, an effect attributed to the better stabilization of the Cu(III) oxidation state.

4.7. Summary

Biochemically relevant 2:1 Cu/O_2 complexes can be created using a variety of nitrogen-containing ligands, but 2:1 Cu/O_2 complexes having no analogues in biochemical systems have been discovered as a result of the greater diversity of ligands available to the synthetic chemist. The denticity of the ligand and its

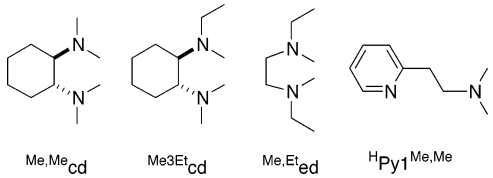

Figure 22. Ligands that stabilize **T** complexes.

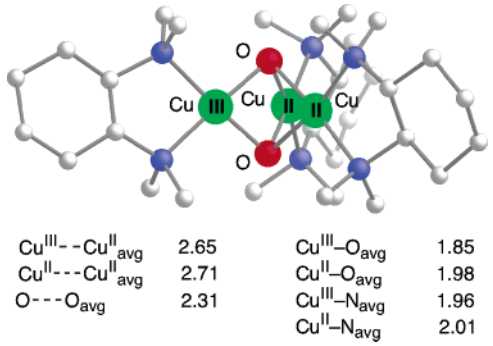

Figure 23. X-ray structure of the **T** species $[(^{Me,Me}cd)_3Cu_3(\mu_3\text{-}O)_2]^{3+}$ and averaged metrical parameters (Å) of the two independent trications in the unit cell.[263]

steric demands are most important in controlling the type of Cu/O_2 complexes formed. All 2:1 Cu/O_2 complexes have isoelectronic cores, but the diversity among their structures, which includes the coordination number of Cu and the geometric arrangements of their cores and ligands, reveals an elaborate web of Cu/O_2 reactivity patterns and is leading to a better understanding of Cu/O_2 chemistry.

5. 3:1 Cu/O_2 Complexes

Multi-copper oxidases (e.g., ascorbate oxidase, laccase, ceruloplasmin) couple the oxidation of various substrates to the complete 4e$^-$ reduction of O_2 to H_2O at a trinuclear Cu active site.[2] In these systems, the apparently incongruous match of a trinuclear Cu cluster with the 4e$^-$ reduction of O_2 is circumvented by the presence of a fourth reducing equivalent at a blue Cu site positioned ca. 12 Å away from the Cu_3 cluster. In synthetic chemistry, while a ratio of 1:1, 2:1, or 4:1 for the reaction between a metal complex and O_2 is well documented, the 3:1 stoichiometry is rare. Among model compounds known to date, only four ligands support a trinuclear Cu core bridged by oxide ligands (Figure 22).[226,263,264] The first example of a discrete 3:1 Cu/O_2 species was reported by Stack et al. in 1996. It was formed upon oxygenation of the Cu(I) complex of ^{Me,Me}cd in CH_2Cl_2 at −80 °C.[263] Manometric measurements confirmed the 3:1 $Cu:O_2$ stoichiometry, and structural characterization showed the presence of the trinuclear core $[Cu_3(\mu_3\text{-}O)_2]^{3+}$ (**T**). The O_2 molecule is fully cleaved to produce two μ_3-oxide ligands, and all three Cu centers have square-planar N_2O_2 coordination environments (Figure 23). One of the Cu centers is differentiated from the other two by its significantly shorter Cu−O bonds (Cu−O: 1.83 versus 1.98 Å for the other two centers), which is consistent with the Cu(III) oxidation state for this unique Cu center (Figure 3). These short Cu−O bonds are also detected by Cu K-edge EXAFS both in solution and the solid state,[84] indicating that this

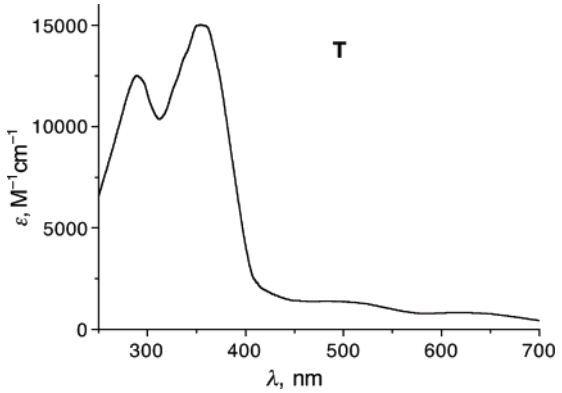

Figure 24. UV−vis spectrum of the **T** species $[(^{Me,Me}cd)_3Cu_3(\mu_3\text{-}O)_2]^{3+}$ ([Cu] ≈ 20 mM, CH_2Cl_2, TfO^-, −80 °C).[263]

distortion does not arise from crystal packing effects. Additionally, the pre-edge XAS region exhibits a feature characteristic of Cu(III).[84,87] The unsymmetric structure along with the XAS data fully support its formal description as a valence-localized Cu(III)−Cu(II)−Cu(II) cluster, which accounts for the four electrons needed to fully reduce one O_2 molecule. The anionic bis(oxide) ligation and square-planar environment, akin to that in the **O** species, are ideal to stabilize a Cu(III) center. In contrast with known 2:1 complexes, the **T** species is paramagnetic with a $S = 1$ electronic ground state that was confirmed by solid-state magnetic susceptibility, EPR, and magnetic circular dichroism,[265,266] as well as theoretical calculations.[267−269] The two Cu(II) centers are weakly ferromagnetically coupled ($J = +7$ cm^{-1}), in line with the acute Cu(II)−O−Cu(II) angle of 87°. The UV−vis spectrum of this **T** species exhibits four absorption bands (Figure 24): 290 nm ($\epsilon \approx 12\,500$ M^{-1} cm^{-1}), 355 nm ($\epsilon \approx 15\,000$ M^{-1} cm^{-1}), 480 nm ($\epsilon \approx 1400$ M^{-1} cm^{-1}), and 620 nm ($\epsilon \approx 800$ M^{-1} cm^{-1}). No rR data has been reported for this **T** species.

The formation of a **T** species is dependent upon the ligand structure and the initial concentrations of Cu(I) and O_2. If the concentration of $[(^{Me,Me}cd)Cu(I)(MeCN)]^+$ is significantly greater than that of dissolved O_2,[234] the **T** species forms preferentially. In the reversed situation, an **O** species forms instead. Intermediate concentration ratios of reactants generate mixtures of the **T** and **O** species. Yet, only a slight increase in the steric demands of the ligand changes the course of the reaction: $^{Me,Et}cd$ forms an **O** species at all concentrations examined (section 4.5). These results underscore the important role of the steric demands of the ligand in dictating the structure of the reaction product. Steric constraints are especially restrictive for the more compact **T** species.

As a rule, only the least sterically demanding ligands yield **T** species. Within the family of $^{R1}Py1^{R2,R3}$ ligands, $[(^{H}Py1^{Me,Me})Cu(I)]^+$ reacts with O_2 at a 3:1 ratio in acetone to yield a complex with UV−vis spectral features consistent with the formation of a **T** species: 342 nm ($\epsilon \approx 12\,000$ M^{-1} cm^{-1}), 515 nm ($\epsilon \approx 1000$ M^{-1} cm^{-1}), and 685 nm ($\epsilon \approx 800$ M^{-1} cm^{-1}).[226,258] Detailed spectroscopic analysis of the oxygenation reaction indicates a concentration dependence of the Cu/O_2 speciation similar to those described above: a **T** species is formed at higher initial Cu concentrations, and an **O** species is generated at high O_2 concentrations. The authors also demonstrate that addition of the $[(^{H}Py1^{Me,Me})Cu(I)]^+$ complex to an O_2-free solution of the related **O** species yields the **T** species, suggesting that **O** is a precursor of the **T** complex (section 7).

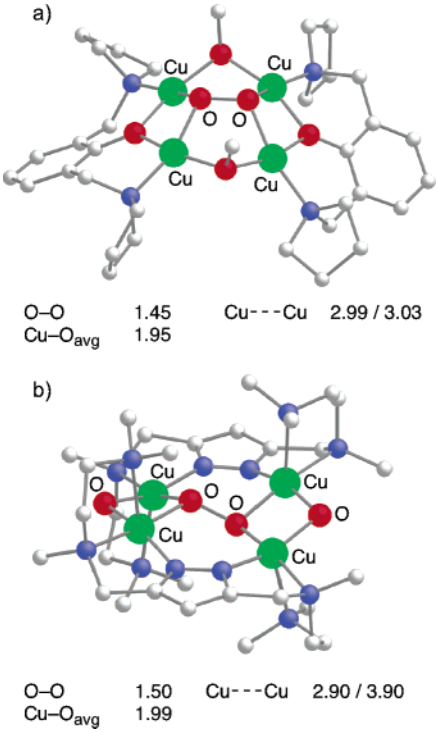

Figure 25. X-ray structures of the 4:1 Cu:O_2 species with metrical parameters (Å) of the $Cu_4(O_2)$ core: (a) $[(bpmp)_2Cu(II)_4(cis\text{-}\mu_4\text{-}O_2)(OMe)_2]^{2+}$ (the *p*-Me groups removed for clarity);[273] (b) $[(pzdien)_2Cu(II)_4(trans\text{-}\mu_4\text{-}O_2)(OH)_2]^{2+}$.[275]

6. 4:1 Cu/O_2 Complexes

Even though a tetranuclear Cu cluster is found at the active site of the enzyme N_2O reductase,[270−272] an O_2-activating tetranuclear Cu cluster is currently unknown in any biochemical context. This arrangement, however, is found in two structurally distinct, thermally robust synthetic complexes. Each tetranuclear unit is assembled from two Cu complexes of binucleating ligands that either cap or bridge a central μ_4-peroxide ligand. The formation of these complexes follows a presumably more complex mechanism than the Cu/O_2 reactions described in the previous sections since the 4e$^-$ provided by the Cu centers do not correlate with the 2e$^-$ reduction of O_2 to peroxide.

The first structurally characterized tetranuclear complex is best described as a *cis*-μ_4-peroxotetracopper(II) species. The complex is formed either by the in situ reduction of Cu(II) in oxygenated MeOH using 3,5-di-*tert*-butylcatechol in the presence of the binucleating monoanionic ligand bpmp or by treating Cu(I) with bpmp in basic MeOH followed by exposure to air.[273] The *cis*-μ_4-peroxo group binds to a rectangular arrangement of Cu(II) atoms that are also bridged in alternating fashion by methoxide and phenolate groups (Figure 25a). The two Cu centers ligated by bpmp cap the ends of the peroxide group.

The O−O bond length of 1.45 Å and the Cu−O_{avg} distance of 1.95 Å are typical for peroxo metal complexes. Ligands closely related to bpmp also form similar tetranuclear peroxo complexes.[274] These complexes exhibit similar absorption spectra with CT bands at ca. 390 nm ($\epsilon \approx 9500$ M^{-1} cm^{-1}) and ca. 580 nm ($\epsilon \approx 600$ M^{-1} cm^{-1}). These transitions are assigned to a combination of phenolate → Cu(II) and peroxo → Cu(II) CT transitions and to a peroxo → Cu(II) CT transition, respectively. The rR O−O stretching vibrations in the 880−900 cm^{-1} range support the presence of peroxo groups, and magnetic susceptibility measurements reveal strong antiferromagnetic coupling between the Cu(II) ions. A detailed mechanism for the formation of this complex is currently lacking.

Pzdien is a binucleating, hexadentate, nitrogen ligand with a pyrazolate ion that can bridge Cu centers in a *cis*-1,2 fashion. Oxygenation of $[(pzdien)Cu(I)_2]^{2+}$ at −80 °C creates a complex with four Cu atoms assembled around a μ_4-peroxide ligand, and each pzdien ligates two Cu(II) centers (Figure 25b).[275] The pyrazolate ion of each pzdien ligand links two Cu centers in a *cis*-1,2 coordination mode, yet the two ligand subunits ligate the peroxide core in a *trans*-orientation. Each Cu(II) center adopts a distorted square-pyramidal geometry with the binding pockets of the pzdien ligands providing *fac* coordination; the apical Cu−N_{avg} distance of 2.34 Å is typical. The equatorial coordination of each Cu ion is completed by a μ-hydroxide and the μ_4-peroxide ligand.[275] The O−O bond length of 1.50 Å is consistent with that of a peroxide ion, although it is the longest peroxide bond reported among structurally characterized Cu complexes. The absorption feature at 360 nm ($\epsilon \approx 3100$ M^{-1} cm^{-1}) is presumably a peroxide to Cu(II) CT band, and the feature at 630 nm ($\epsilon \approx 260$ M^{-1} cm^{-1}) is likely a d−d transition of a tetragonally distorted Cu(II) center. No rR data are currently available. The composition of this cluster and the modest yield of its formation (ca. 40%) are consistent with both $2e^-$ and $4e^-$ reduction reactions of O_2 to produce the necessary peroxide and hydroxide ions, respectively. Certainly, even more complicated formation schemes are possible.

7. Conclusion

Though exceptions are known,[92] most Cu/O_2 reactions generate a thermodynamic rather than a kinetic Cu/O_2 product, a predilection supported by the general lability and coordination flexibility of Cu centers. The prevalent formation of dimeric Cu/O_2 complexes in homogeneous solutions is consistent with the thermodynamic trends of O_2 reduction: $1e^-$ reduction is unfavorable relative to the $2e^-$ and $4e^-$ pathways. To isolate Cu/O_2 complexes that are not binuclear requires the use of ligands with specific attributes. 1:1 complexes are generally stabilized by very sterically demanding ligands, while 3:1 complexes are stabilized by the least sterically demanding ones. These trends are consistent through several *families* of ligands (Figure 26) and strongly suggest that O_2-reactive Cu(I) complexes yield the most compact Cu/O_2 complex permitted by the steric demands of the ligands. As described above, the modification of the steric demands of the ligands allows the stabilization of many types of Cu/O_2 species, which can be regarded as way-stations along the path of the $4e^-$ reduction of O_2. A possible reaction matrix for the Cu(I)-mediated reduction of O_2 is presented in Figure 27. While not comprehensive, it does succinctly integrate a vast amount of data from a diverse set of Cu/O_2 complexes.

Ligand denticity is of obvious importance in controlling Cu/O_2 reactivity patterns. For example, tetradentate ligands are the only ones known to form ^{T}**P** and ^{E}**S** species (Figure 27, top). In contrast, bi- and tridentate-ligated Cu(I) complexes all form more compact products (Figure 27, bottom). A comparison between the reactivity of the Cu(I) complexes of *i*Pr_3-tacn (tridentate ligand) and *i*Pr_2Py^Htacn (tetradentate ligand) is useful in this regard. The former yields a ^{S}**P**/**O** equilibrium mixture, while the latter, with an additional pyridine ligating arm, forms only a ^{T}**P** species.[175] Dissociation of the pyridine arm of *i*Pr_2-Py^Htacn would produce a tridentate ligand with steric demands comparable to those of *i*Pr_3tacn, yet the energetic stabilization provided by the two Cu(II)−pyridine bonds within a ^{T}**P** species is apparently more favorable than the formation of an **O** species with tridentate ligation.

For a given denticity, incremental steric escalation within a family of ligands tends to favor the formation of less compact Cu/O_2 species. Counterexamples exist with certain tetradentate amine ligands, but these cases are rationalized through a reduction of their effective denticity. Three families of tetradentate ligands—tmpa/Metmpa/Me_2tmpa, tmpa/bpqa/bqpa, and *i*Pr_2py^Htacn/*i*Pr_2py^{Ph}tacn—exhibit a decreased effective denticity in their most sterically demanding forms. The Cu(I) complex of tmpa, the parent ligand of the first two families, oxygenates to form a ^{T}**P** species, as do the Cu(I) complexes of Metmpa, bpqa, and *i*Pr_2py^Htacn. By contrast, the Cu(I) complexes of Me_2tmpa, bqpa, and *i*Pr_2py^{Ph}tacn oxygenate to form an **O** species (Figure 26, entry 1). As seen in the structure of $[(Me_2tmpa)_2Cu(II)_2(O)_2]^{2+}$, the ostensibly tetradentate Me_2tmpa ligand binds only in bidentate fashion, with the two hindered 6-Me-pyridine groups virtually dissociated from each Cu center (Figure 17c). Without these bonding interactions, contraction to an **O** core is energetically preferred. Interestingly, a transient ^{T}**P** species is observed during the formation of an **O** species from $[(bqpa)Cu(I)]^+$.[117,132] The bqpa ligand presumably binds in a tetradentate fashion to form a transient ^{T}**P** species that collapses to an **O** species, potentially through the intermediacy of a ^{S}**P** species. This property of "denticity reduction" endows certain tetradentate ligands with the ability to cross into the reactivity realm of bi- and tridentate ligands (Figure 27, step 3 or step 4) and leads, for example, to the remarkable ability of $[(Me_2tmpa)Cu(I)]^+$ to reversibly bind O_2 at low temperature through formation of an **O** species.

With tetradentate ligands, a transient ^{E}**S** species can react with another Cu(I) complex to yield a binuclear ^{T}**P** complex (Figure 27, steps 1 and 2). With

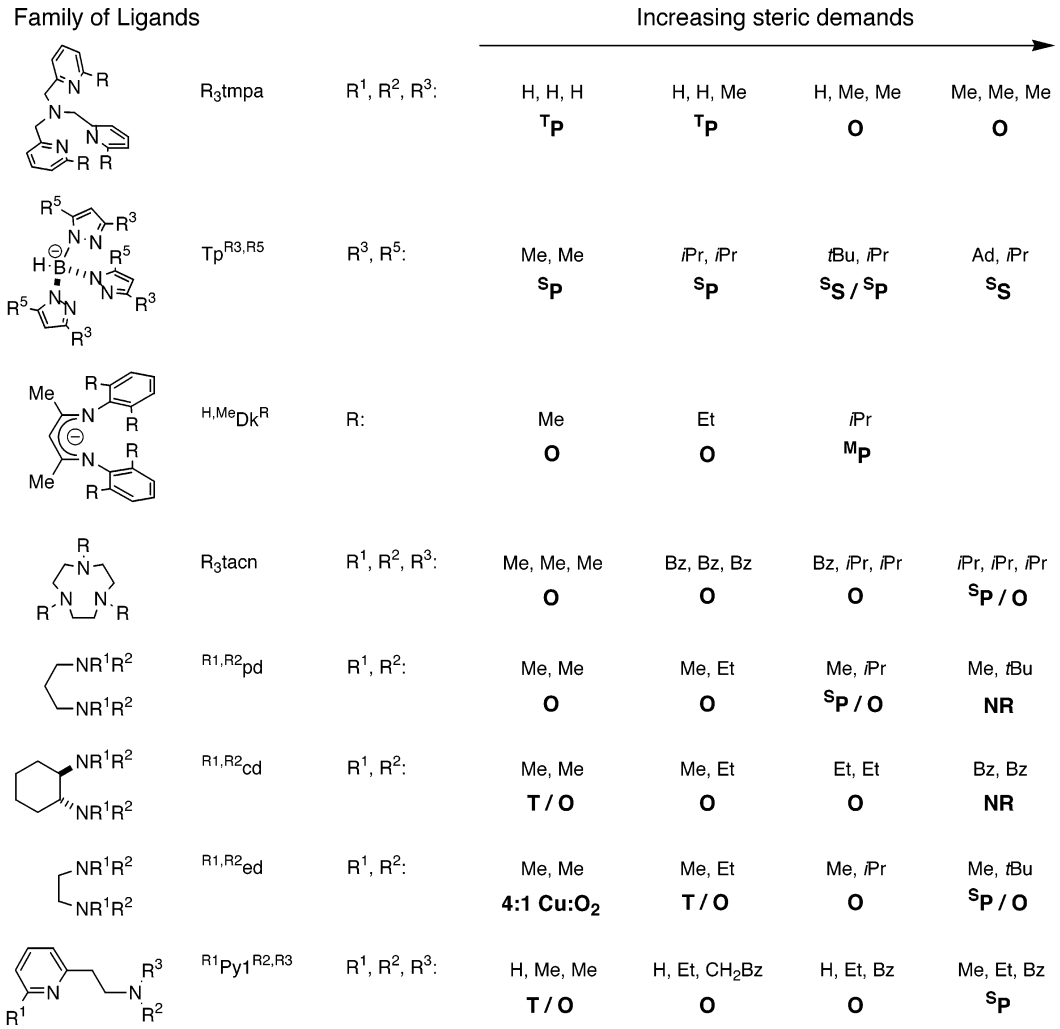

Figure 26. Principal families of ligands and their Cu/O_2 reactivity with respect to increasing steric demands (**NR**: not reactive).

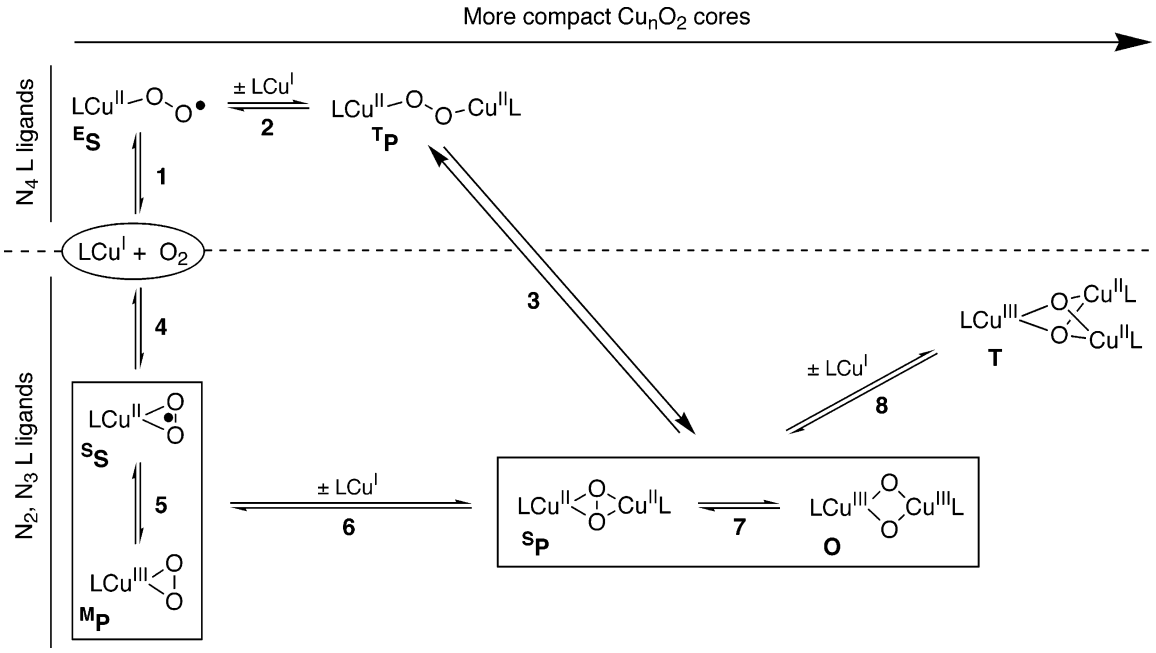

Figure 27. Formation reactions of Cu/O_2 species with bi-, tri-, and tetradentate ligands (N_2, N_3, and N_4 ligands, respectively).

bi- and tridentate ligands, however, no transient 1:1 Cu/O_2 intermediates have been detected *during the course* of the reactions leading to ^{S}**P** and **O** (Figure 27, steps 4 and 6). The existence of a 1:1 species is

inferred from the first-order dependence of the oxygenation rate on the Cu(I) concentration. Judiciously increasing the steric demands of the ligand can preclude the bimolecular step (Figure 27, step 6), resulting in formation of a "trapped" 1:1 species that can be regarded as a snapshot of the reaction intermediate preceding the ^{S}**P** and/or **O** species. Within the family of tris(pyrazolyl)borate ligands, $Tp^{R3,R5}$ (Figure 26, entry 2), only the ligand with bulky 1-adamantyl group in the R^3 position yields a pure 1:1 ^{S}**S** species.[95] A slight reduction in size of the R^3 substituent from adamantyl to *t*Bu leads to formation of a mixture of monomeric ^{S}**S** and dimeric ^{S}**P** species, significantly biased toward the former.[94] Use of smaller R^3 substituents produces measurable amounts of only ^{S}**P** species. Similar control of Cu/O_2 reactivity is observed using a series of β-diketiminate ligands, $^{R1,R2}Dk^{R3}$ (Figure 26, entry 3). While most Dk ligands yield dimeric **O** species, 1:1 ^{M}**P** species can be generated by using Dk ligands with substituents that increase the ligand bite angle (R^2) and the size of the peripheral aryl groups (R^3).[96,97] These "trapped" ^{M}**P** species can react with Cu(I) of lesser steric demands to form **O** species, proving that such 1:1 species are viable way-stations toward 2:1 complexes (Figure 27, step 6). Although undocumented, an equilibrium between the valence isomers ^{S}**S** and ^{M}**P** is postulated (Figure 27, step 5).

The rapid interconversion of the ^{S}**P** and **O** isomers (Figure 27, step 7) is now well documented for several ligand systems (section 4.6). Systematic variations within families of ligands clearly illuminate the dominant role of steric effects and the secondary role of electronic effects[171] on the position of the ^{S}**P**/**O** equilibrium (Figure 26, entries 4−8). For ligands with small tertiary amine groups, the bis(μ-oxo)dicopper(III) core of **O** is intrinsically more energetically stable than the μ-η^2:η^2-peroxodicopper(II) core of the isomeric ^{S}**P** species. The equilibrium between ^{S}**P** and **O** species is particularly sensitive to the steric demands of the ligand, given the short Cu···Cu separation in the **O** isomer (ca. 2.8 Å) that can be accommodated by the smaller substituents. Increasing the steric demands of the ligand by incorporating larger peripheral substituents and bite angles destabilizes the **O** isomer in preference for the ^{S}**P** species.

Only the least sterically demanding bidentate ligands can support the very compact Cu_3O_2 core of a **T** species (Figure 26, entries 6−8). Its structure provides an important snapshot in the progression toward complete reduction of O_2.[263] With the $^{H}Py1^{Me,Me}$ ligand, formation of the **T** species proceeds from the **O** species by titration with $[(^{H}Py1^{Me,Me})Cu(I)]^+$ under anaerobic conditions (Figure 27, step 8).[226] While direct conversion of **O** to **T** species is conceptually attractive, the intermediacy of a ^{S}**P** species cannot be dismissed, especially if the reaction is to proceed by an inner-sphere mechanism. By either pathway, a significant structural reorganization is required, based on the metrical parameters of each species. Use of the smallest ligand ^{Me,Me}ed affords a poorly understood species with a 4:1 $Cu:O_2$ reaction ratio, while the most sterically demanding ligands such as ^{Bz,Bz}cd and ^{Me,tBu}pd form unreactive Cu(I) complexes.

Directed ligand design is a powerful tool with which to investigate complex reactions such as the interaction of Cu(I) with O_2. Studies involving systematic ligand variations have proven to be productive in the Cu/O_2 area, highlighting key reactivity issues that would not be apparent from studies of a single complex. The ability to slow individual steps by ligand modification has allowed the characterization of "trapped" intermediates that dot the Cu/O_2 landscape. While the number of structural types of Cu/O_2 species now far exceeds those known in biochemical systems, other species undoubtedly remain undiscovered. If past investigations are any indication, these new structural types will be identified initially through their unique spectroscopic features that reflect unique binding modes of the O_2-derived ligands. The next decade of research will likely solidify the connections between the known Cu/O_2 species and uncover new structures with potential relevance to the oxidative processes that are operative in biochemical systems.

8. Acknowledgments

We thank Professor K. D. Karlin and Professor S. Schindler for providing unpublished information, A. P. Cole, R. C. Pratt, and P. Chen for helpful discussions, and Professor T. N. Sorrell for critical feedback on this manuscript.

9. Abbreviations

AO	ascorbate oxidase
AmO	amine oxidase
$BArF^-$	$B(C_6F_5)_4^-$
C*c*O	cytochrome *c* oxidase
CT	charge transfer
(oxy)CO	(oxy)catechol oxidase
DβH	dopamine β-hydroxylase
DFT	density functional theory
ϵ	molar absorptivity in M^{-1} cm^{-1}
EtCN	propionitrile
fac	facial
GOase	galactose oxidase
(oxy)Hc	(oxy)hemocyanin
LMCT	ligand to metal charge transfer
mer	meridional
MeCN	acetonitrile
MeOH	methanol
MeTHF	2-methyltetrahydrofuran
MO	molecular orbital
MsO^-	$CH_3SO_3^-$
PHM	peptidylglycine α-hydroxylating monooxygenase
pMMO	particulate methane monooxygenase
SCE	saturated calomel electrode
SOD	superoxide dismutase
SOMO	singly occupied molecular orbital
TfO^-	$CF_3SO_3^-$
THF	tetrahydrofuran
TsO^-	p-$CH_3C_6H_4SO_3^-$
(oxy)Ty	(oxy)tyrosinase

10. References

(1) Klinman, J. P. *Chem. Rev.* **1996**, *96*, 2541.
(2) Solomon, E. I.; Sundaram, U. M.; Machonkin, T. E. *Chem. Rev.* **1996**, *96*, 2563.
(3) Solomon, E. I.; Chen, P.; Metz, M.; Lee, S.-K.; Palmer, A. E. *Angew. Chem., Int. Ed.* **2001**, *40*, 4570.

(4) *Bioinorganic Chemistry of Copper*; Karlin, K. D., Tyeklár, Z., Eds.; Chapman & Hall: New York, 1993.
(5) Kitajima, N.; Moro-Oka, Y. *Chem. Rev.* **1994**, *94*, 737.
(6) Ito, M.; Fujisawa, K.; Kitajima, N.; Moro-Oka, Y. In *Oxygenases and Model Systems*; Funabiki, T., Ed.; Kluwer Academic Publishers: Dordrecht, 1997.
(7) Karlin, K. D.; Zuberbühler, A. D. In *Bioinorganic Catalysis*; Reedijk, J., Bouwman, E., Eds.; Marcel Dekker: New York, 1999.
(8) Blackman, A. G.; Tolman, W. B. *Struct. Bonding (Berlin)* **2000**, *97*, 179.
(9) Zhang, C. X.; Liang, H.-C.; Humphreys, K. J.; Karlin, K. D. In *Advances in Catalytic Activation of Dioxygen by Metal Complexes*; Simándi, L. I., Ed.; Kluwer: Dordrecht, Boston, London, 2003; Vol. 26.
(10) Fox, S.; Karlin, K. D. In *Active Oxygen in Biochemistry*; Valentine, J. S., Foote, C. S., Greenberg, A., Liebman, J. F., Eds.; Blackie Academic and Professional: London, 1995.
(11) Kopf, M.-A.; Karlin, K. D. In *Biomimetic Oxidations Catalyzed by Transition Metal Complexes*; Meunier, B., Ed.; Imperial College Press: London, 2000.
(12) Mahadevan, V.; Klein Gebbink, R. J. M.; Stack, T. D. P. *Curr. Opin. Chem. Biol.* **2000**, *4*, 228.
(13) Schindler, S. *Eur. J. Inorg. Chem.* **2000**, 2311.
(14) Stack, T. D. P. *Dalton Trans.* **2003**, *10*, 1881.
(15) Aycock, D.; Abolins, V.; White, D. M. *Encyclopedia of Polymer Science and Engineering*, 2nd ed.; John Wiley & Sons: New York, 1986.
(16) Parshall, G. W.; Ittel, D. D. *Homogeneous Catalysis, The Applications and Chemistry of Catalysis by Soluble Transition Metal Complexes*, 2nd ed.; John Wiley & Sons: New York, 1992.
(17) Sheldon, R. A.; Kochi, J. K. *Metal Catalyzed Oxidations of Organic Compounds*; Academic Press: New York, 1981.
(18) Kaim, W.; Rall, J. *Angew. Chem., Int. Ed. Engl.* **1996**, *35*, 43.
(19) Fontecave, M.; Pierre, J.-L. *Coord. Chem. Rev.* **1998**, *170*, 125.
(20) Steiner, R. A.; Kalk, K. H.; Dijkstra, B. W. *Proc. Natl. Acad. Sci. U.S.A.* **2002**, *99*, 16625.
(21) Prigge, S. T.; Mains, R. E.; Eipper, B. A.; Amzel, L. M. *Cell. Mol. Life Sci.* **2000**, *57*, 1236.
(22) Prigge, S. T.; Kolhekar, A. S.; Eipper, B. A.; Mains, R. E.; Amzel, L. M. *Nat. Struct. Biol.* **1999**, *6*, 976.
(23) Wilmot, C. M.; Hajdu, J.; Mcpherson, M. J.; Knowles, P. F.; Phillips, S. E. V. *Science* **1999**, *286*, 1724.
(24) Whittaker, J. W. *Chem. Rev.* **2003**, *103*, 2347.
(25) Rogers, M. S.; Dooley, D. M. *Curr. Opin. Chem. Biol.* **2003**, *7*, 189.
(26) Whittaker, M. M.; Kersten, P. J.; Cullen, D.; Whittaker, J. W. *J. Biol. Chem.* **1999**, *274*, 36226.
(27) Wang, S. X.; Mure, M.; Medzihradszky, K. F.; Burlingame, A. L.; Brown, D. E.; Dooley, D. M.; Smith, A. J.; Kagan, H. M.; Klinman, J. P. *Science* **1996**, *273*, 1078.
(28) Csiszar, K. *Prog. Nucleic Acid Res. Mol. Biol.* **2001**, *70*, 1.
(29) Rucker, R. B.; Mitchell, A. E.; Tchaparian, E.; Last, J. A. *Food Sci. Technol (NY, United States)* **2003**, *122*, 493.
(30) Hart, P. J.; Balbirnie, M. M.; Ogihara, N. L.; Nersissian, A. M.; Weiss, M. S.; Valentine, J. S.; Eisenberg, D. *Biochemistry* **1999**, *38*, 2167.
(31) Rompel, A.; Fischer, H.; Meiwes, D.; Buldt-Karentzopoulos, K.; Dillinger, R.; Tuczek, F.; Witzel, H.; Krebs, B. *J. Biol. Inorg. Chem.* **1999**, *4*, 56.
(32) Gerdemann, C.; Eicken, C.; Krebs, B. *Acc. Chem. Res.* **2002**, *35*, 183.
(33) Decker, H.; Rimke, T. *J. Biol. Chem.* **1998**, *273*, 25889.
(34) Decker, H.; Dillinger, R.; Tuczek, F. *Angew. Chem., Int. Ed.* **2000**, *39*, 1591.
(35) Decker, H.; Tuczek, F. *Trends Biochem. Sci.* **2000**, *25*, 392.
(36) Messerschmidt, A.; Luecke, H.; Huber, R. *J. Mol. Biol.* **1993**, *230*, 997.
(37) Messerschmidt, A.; Ladenstein, R.; Huber, R.; Bolognesi, M.; Avigliano, L.; Petruzzelli, R.; Rossi, A.; Finazzi-Agro, A. *J. Mol. Biol.* **1992**, *224*, 179.
(38) Lindley, P.; Zaitseva, I.; Zaitsev, V.; Ralph, A.; Card, G. *Biochemistry* **1996**, *35*, 109.
(39) Ducros, V.; Brzozowski, A. M.; Wilson, K. S.; Brown, S. H.; Ostergaard, P.; Schneider, P.; Yaver, D. S.; Pedersen, A. H.; Davies, G. J. *Nat. Struct. Biol.* **1998**, *5*, 310.
(40) Hakulinen, N.; Kiiskinen, L.-L.; Kruus, K.; Saloheimo, M.; Paananen, A.; Koivula, A.; Rouvinen, J. *Nat. Struct. Biol.* **2002**, *9*, 601.
(41) Ferguson-Miller, S.; Babcock, G. T. *Chem. Rev.* **1996**, *96*, 2889.
(42) Lieberman, R. L.; Shrestha, D. B.; Doan, P. E.; Hoffman, B. M.; Stemmler, T. L.; Rosenzweig, A. C. *Proc. Natl. Acad. Sci. U.S.A.* **2003**, *100*, 3820.
(43) Basu, P.; Katterle, B.; Andersson, K. K.; Dalton, H. *Biochem. J.* **2003**, *369*, 417.
(44) Berthe-Corti, L.; Fetzner, S. *Acta Biotechnol.* **2002**, *22*, 299.
(45) Prigge, S. T.; Kolhekar, A. S.; Eipper, B. A.; Mains, R. E.; Amzel, L. M. *Science* **1997**, *278*, 1300.
(46) Dooley, D. M.; Scott, R. A.; Knowles, P. F.; Colangelo, C. M.; Mcguirl, M. A.; Brown, D. E. *J. Am. Chem. Soc.* **1998**, *120*, 2599.
(47) Cuff, M. E.; Miller, K. I.; Vanholde, K. E.; Hendrickson, W. A. *J. Mol. Biol.* **1998**, *278*, 855.
(48) Volbeda, A.; Hol, W. G. J. *J. Mol. Biol.* **1989**, *209*, 249.
(49) Yoshikawa, S.; Shinzawaitoh, K.; Nakashima, R.; Yaono, R.; Yamashita, E.; Inoue, N.; Yao, M.; Fei, M. J.; Libeu, C. P.; Mizushima, T.; Yamaguchi, H.; Tomizaki, T.; Tsukihara, T. *Science* **1998**, *280*, 1723.
(50) Messerschmidt, A. *Struct. Bonding (Berlin)* **1998**, *90*, 37.
(51) Roberts, S. A.; Weichsel, A.; Grass, G.; Thakali, K.; Hazzard, J. T.; Tollin, G.; Rensing, C.; Montfort, W. R. *Proc. Natl. Acad. Sci. U.S.A.* **2002**, *99*, 2766.
(52) Hazes, B.; Magnus, K. A.; Bonaventura, V.; Dauter, Z.; Kalk, K. H.; Hol, W. G. J. *Protein Sci.* **1993**, *2*, 597.
(53) Magnus, K. A.; Ton-That, H.; Carpenter, J. E. *Chem. Rev.* **1994**, *94*, 727.
(54) Magnus, K.; Ton-That, H. *J. Inorg. Biochem.* **1992**, *47*, 20.
(55) Magnus, K. A.; Hazes, B.; Ton-That, H.; Bonaventura, C.; Bonaventura, J.; Hol, W. G. J. *Proteins: Struct., Funct., Genet.* **1994**, *19*, 302.
(56) Shin, W.; Sundaram, U. M.; Cole, J. L.; Zhang, H. H.; Hedman, B.; Hodgson, K. O.; Solomon, E. I. *J. Am. Chem. Soc.* **1996**, *118*, 3202.
(57) Lee, S.-K.; Debeer George, S.; Antholine, W. E.; Hedman, B.; Hodgson, K. O.; Solomon, E. I. *J. Am. Chem. Soc.* **2002**, *124*, 6180.
(58) Metz, M.; Solomon, E. I. *J. Am. Chem. Soc.* **2001**, *123*, 4938.
(59) Astruc, D. *Electron Transfer and Radical Processes in Transition-Metal Chemistry*; Wiley-VCH: New York, 1995.
(60) Divaira, M.; Mani, F. *J. Chem. Soc., Dalton Trans.* **1985**, 2327.
(61) Goodwin, J. A.; Stanbury, D. M.; Wilson, L. J.; Eigenbrot, C. W.; Scheidt, W. R. *J. Am. Chem. Soc.* **1987**, *109*, 2979.
(62) Goodwin, J.; Bodager, G.; Wilson, L.; Stanbury, D.; Scheidt, W. *Inorg. Chem.* **1989**, *28*, 35.
(63) Tyeklár, Z.; Jacobson, R. R.; Wei, N.; Murthy, N. N.; Zubieta, J.; Karlin, K. D. *J. Am. Chem. Soc.* **1993**, *115*, 2677.
(64) Wei, N.; Lee, D. H.; Murthy, N. N.; Tyeklár, Z.; Karlin, K. D.; Kaderli, S.; Jung, B.; Zuberbühler, A. D. *Inorg. Chem.* **1994**, *33*, 4625.
(65) Root, D. E.; Mahrooftahir, M.; Karlin, K. D.; Solomon, E. I. *Inorg. Chem.* **1998**, *37*, 4838.
(66) Börzel, H.; Comba, P.; Hagen, K. S.; Katsichtis, C.; Pritzkow, H. *Chem. Eur. J.* **2000**, *6*, 914.
(67) Weitzer, M.; Schatz, M.; Hampel, F.; Heinemann, F. W.; Schindler, S. *J. Chem. Soc., Dalton Trans.* **2002**, *5*, 686.
(68) Hodgson, D. J. *Prog. Inorg. Chem.* **1975**, *19*, 173.
(69) Macgregor, K. T.; Watkins, N. T.; Lewis, D. L.; Drake, R. F.; Hodgson, D. J.; Hatfield, W. E. *Inorg. Nucl. Chem. Lett.* **1973**, *9*, 423.
(70) Diaddario, L. L.; Robinson, W. R.; Margerum, D. W. *Inorg. Chem.* **1983**, *22*, 1021.
(71) Youngblood, M. P.; Margerum, D. W. *Inorg. Chem.* **1980**, *19*, 3068.
(72) Caira, M. R.; Koch, K. R.; Sacht, C. *Acta Crystallogr., Sect. C: Cryst. Struct. Commun.* **1991**, *47*, 29.
(73) Kanatzidis, M. G.; Baenziger, N. C.; Coucouvanis, D. *Inorg. Chem.* **1985**, *24*, 2680.
(74) Oliver, K. J.; Waters, T. N. *J. Chem. Soc., Chem. Commun.* **1982**, 1111.
(75) Ruiz, R.; Surville-Barland, C.; Aukauloo, A.; Anxolabehere-Mallart, E.; Journaux, Y.; Cano, J.; Muñoz, M. C. *J. Chem. Soc., Dalton Trans.* **1997**, 745.
(76) Hanss, J.; Krüger, H.-J. *Angew. Chem., Int. Ed. Engl.* **1996**, *35*, 2827.
(77) Will, S.; Lex, J.; Vogel, E.; Schmickler, H.; Gisselbrecht, J.-P.; Haybtmann, C.; Bernard, M.; Gross, M. *Angew. Chem., Int. Ed. Engl.* **1997**, *36*, 357.
(78) Klemm, W.; Huss, E. *Z. Anorg. Chem.* **1949**, *258*, 221.
(79) Krebs, C.; Glaser, T.; Bill, E.; Weyhermuller, T.; Meyer-Klaucke, W.; Wieghardt, K. *Angew. Chem., Int. Ed.* **1999**, *38*, 359.
(80) Sorrell, T. N.; Jameson, D. L. *J. Am. Chem. Soc.* **1983**, *105*, 6013.
(81) Rondelez, Y.; Rager, M.-N.; Duprat, A.; Reinaud, O. *J. Am. Chem. Soc.* **2002**, *124*, 1334.
(82) Scott, R. A. In *Physical Methods in Bioinorganic Chemistry*; Que, L., Jr., Ed.; University Science Books: Sausalito, CA, 2000.
(83) Kau, L. S.; Spira-Solomon, D. J.; Penner-Hahn, J. E.; Hodgson, K. O.; Solomon, E. I. *J. Am. Chem. Soc.* **1987**, *109*, 6433.
(84) Dubois, J. L.; Mukherjee, P.; Stack, T. D. P.; Hedman, B.; Solomon, E. I.; Hodgson, K. O. *J. Am. Chem. Soc.* **2000**, *122*, 5775.
(85) Nakamoto, K. *Infrared and Raman Spectra of Inorganic and Coordination Compounds*, 5th ed.; John Wiley & Sons: New York, 1997.
(86) Solomon, E. I. *Comm. Inorg. Chem.* **1984**, *3*, 227.
(87) Dubois, J. L.; Mukherjee, P.; Collier, A. M.; Mayer, J. M.; Solomon, E. I.; Hedman, B.; Stack, T. D. P.; Hodgson, K. O. *J. Am. Chem. Soc.* **1997**, *119*, 8578.
(88) Dubois, J. L. Ph.D. Thesis, Stanford University, 2000.
(89) Woolery, G. L.; Powers, L.; Winkler, M.; Solomon, E. I.; Spiro, T. G. *J. Am. Chem. Soc.* **1984**, *106*, 86.

(90) Woolery, G. L.; Powers, L.; Winkler, M.; Solomon, E. I.; Lerch, K.; Spiro, T. G. *Biochim. Biophys. Acta* **1984**, *788*, 155.
(91) Weitzer, M.; Schindler, S.; Brehm, G.; Schneider, S.; Hormann, E.; Jung, B.; Kaderli, S.; Zuberbühler, A. D. *Inorg. Chem.* **2003**, *42*, 1800.
(92) Zhang, C.; Kaderli, S.; Costas, M.; Kim, E.; Neuhold, Y.; Karlin, K.; Zuberbühler, A. D. *Inorg. Chem.* **2003**, *42*, 1807.
(93) Börzel, H.; Comba, P.; Hagen, K. S.; Kerscher, M.; Pritzkow, H.; Schatz, M.; Schindler, S.; Walter, O. *Inorg. Chem.* **2002**, *41*, 5440.
(94) Fujisawa, K.; Tanaka, M.; Moro-Oka, Y.; Kitajima, N. *J. Am. Chem. Soc.* **1994**, *116*, 12079.
(95) Chen, P.; Root, D. E.; Campochiaro, C.; Fujisawa, K.; Solomon, E. I. *J. Am. Chem. Soc.* **2003**, *125*, 466.
(96) Spencer, D. J. E.; Aboelella, N. W.; Reynolds, A. M.; Holland, P. L.; Tolman, W. B. *J. Am. Chem. Soc.* **2002**, *124*, 2108.
(97) Aboelella, N. W.; Lewis, E. A.; Reynolds, A. M.; Brennessel, W. W.; Cramer, C. J.; Tolman, W. B. *J. Am. Chem. Soc.* **2002**, *124*, 10660.
(98) Cramer, C. J.; Tolman, W. B.; Theopold, K. H.; Rheingold, A. L. *Proc. Natl. Acad. Sci. U.S.A.* **2003**, *100*, 3635.
(99) Jacobson, R. R.; Tyeklár, Z.; Farooq, A.; Karlin, K. D.; Liu, S.; Zubieta, J. *J. Am. Chem. Soc.* **1988**, *110*, 3690.
(100) Kitajima, N.; Fujisawa, K.; Moro-Oka, Y.; Toriumi, K. *J. Am. Chem. Soc.* **1989**, *111*, 8975.
(101) Halfen, J. A.; Mahapatra, S.; Wilkinson, E. C.; Kaderli, S.; Young, V. G.; Que, L., Jr.; Zuberbühler, A. D.; Tolman, W. B. *Science* **1996**, *271*, 1397.
(102) Mahapatra, S.; Halfen, J. A.; Wilkinson, E. C.; Pan, G. F.; Wang, X. D.; Young, V. G.; Cramer, C. J.; Que, L., Jr.; Tolman, W. B. *J. Am. Chem. Soc.* **1996**, *118*, 11555.
(103) Zuberbühler, A. D. In *Bioinorganic Chemistry of Copper*; Karlin, K. D., Tyeklár, Z., Eds.; Chapman & Hall: New York, 1993.
(104) Sanyal, I.; Karlin, K. D.; Strange, R. W.; Blackburn, N. J. *J. Am. Chem. Soc.* **1993**, *115*, 11259.
(105) Francisco, W. A.; Blackburn, N. J.; Klinman, J. P. *Biochemistry* **2003**, *42*, 1813.
(106) Wada, A.; Harata, M.; Hasegawa, K.; Jitsukawa, K.; Masuda, H.; Mukai, M.; Kitagawa, T.; Einaga, H. *Angew. Chem., Int. Ed.* **1998**, *37*, 798.
(107) Kodera, M.; Kita, T.; Miura, I.; Nakayama, N.; Kawata, T.; Kano, K.; Hirota, S. *J. Am. Chem. Soc.* **2001**, *123*, 7715.
(108) Ohta, T.; Tachiyama, T.; Yoshizawa, K.; Yamabe, T.; Uchida, T.; Kitagawa, T. *Inorg. Chem.* **2000**, *39*, 4358.
(109) Ohtsu, H.; Itoh, S.; Nagatomo, S.; Kitagawa, T.; Ogo, S.; Watanabe, Y.; Fukuzumi, S. *Chem. Commun.* **2000**, 1051.
(110) Ohtsu, H.; Itoh, S.; Nagatomo, S.; Kitagawa, T.; Ogo, S.; Watanabe, Y.; Fukuzumi, F. *Inorg. Chem.* **2001**, *40*, 3200.
(111) Osako, T.; Nagatomo, S.; Tachi, Y.; Kitagawa, T.; Itoh, S. *Angew. Chem., Int. Ed.* **2002**, *41*, 4325.
(112) Ohta, T.; Tachiyama, T.; Yoshizawa, K.; Yamabe, T. *Tetrahedron Lett.* **2000**, *41*, 2581.
(113) Chen, P.; Solomon, E. I. *J. Inorg. Biochem.* **2002**, *88*, 368.
(114) Chen, P.; Fujisawa, K.; Solomon, E. I. *J. Am. Chem. Soc.* **2000**, *122*, 10177.
(115) Karlin, K. D.; Kaderli, K.; Zuberbühler, A. D. *Acc. Chem. Res.* **1997**, *30*, 139.
(116) Karlin, K. D.; Wei, N.; Jung, B.; Kaderli, S.; Zuberbühler, A. D. *J. Am. Chem. Soc.* **1991**, *113*, 5868.
(117) Karlin, K. D.; Wei, N.; Jung, B.; Kaderli, S.; Niklaus, P.; Zuberbühler, A. D. *J. Am. Chem. Soc.* **1993**, *115*, 9506.
(118) Lee, D.-H.; Wei, N.; Murthy, N. N.; Tyeklár, Z.; Karlin, K. D.; Kaderli, S.; Jung, B.; Zuberbühler, A. D. *J. Am. Chem. Soc.* **1995**, *117*, 12498.
(119) Becker, M.; Heinemann, F. W.; Schindler, S. *Chem. Eur. J.* **1999**, *5*, 3124.
(120) Karlin, K. D.; Lee, D. H.; Kaderli, S.; Zuberbühler, A. D. *Chem. Commun.* **1997**, 475.
(121) Karlin, K. D.; Tolman, W. B.; Kaderli, S.; Zuberbühler, A. D. *J. Mol. Catal. A: Chem.* **1997**, *117*, 215.
(122) Mahapatra, S.; Kadereli, S.; Llobet, A.; Neuhold, Y. M.; Palanche, T.; Halfen, J. A.; Young, V. G.; Kaden, T. A.; Que, L.; Zuberbühler, A. D.; Tolman, W. B. *Inorg. Chem.* **1997**, *36*, 6343.
(123) Obias, H. V.; Lin, Y.; Murthy, N. N.; Pidcock, E.; Solomon, E. I.; Ralle, M.; Blackburn, N. J.; Neuhold, Y. M.; Zuberbühler, A. D.; Karlin, K. D. *J. Am. Chem. Soc.* **1998**, *120*, 12960.
(124) Liang, H.-C.; Zhang, C. X.; Henson, M. J.; Sommer, R. D.; Hatwell, K. R.; Kaderli, S.; Zuberbühler, A. D.; Rheingold, A. L.; Solomon, E. I.; Karlin, K. D. *J. Am. Chem. Soc.* **2002**, *124*, 4170.
(125) Mirica, L. M.; Vance, M.; Rudd, D. J.; Hedman, B.; Hodgson, K. O.; Solomon, E. I.; Stack, T. D. P. *J. Am. Chem. Soc.* **2002**, *124*, 9332.
(126) Cole, A. P.; Mahadevan, V.; Mirica, L. M.; Stack, T. D. P. *J. Am. Chem. Soc.* **2003**, submitted.
(127) Itoh, S.; Taki, M.; Nakao, H.; Holland, P. L.; Tolman, W. B.; Que, L., Jr.; Fukuzumi, S. *Angew. Chem., Int. Ed.* **2000**, *39*, 398.
(128) Momenteau, M.; Reed, C. A. *Chem. Rev.* **1994**, *94*, 659.
(129) Schatz, M.; Becker, M.; Walter, O.; Liehr, G.; Schindler, S. *Inorg. Chim. Acta* **2001**, *324*, 173.
(130) Schatz, M.; Leibold, M.; Foxon, S. P.; Weitzer, M.; Heinemann, F. W.; Hampel, F.; Walter, O.; Schindler, S. *Dalton Trans.* **2003**, 1480.
(131) Wei, N.; Murthy, N. N.; Chen, Q.; Zubieta, J.; Karlin, K. D. *Inorg. Chem.* **1994**, *33*, 1953.
(132) Karlin, K. D. Private communication, work in progress.
(133) Börzel, H.; Comba, P.; Katsichtis, C.; Kiefer, W.; Lienke, A.; Nagel, V.; Pritzkow, H. *Chem. Eur. J.* **1999**, *5*, 1716.
(134) Chaudhuri, P.; Hess, M.; Weyhermüller, T.; Wieghardt, K. *Angew. Chem., Int. Ed.* **1999**, *38*, 1095.
(135) Trofimenko, S. *Chem. Rev.* **1993**, *93*, 943.
(136) Kitajima, N.; Tolman, W. B. *Prog. Inorg. Chem.* **1995**, *43*, 419.
(137) Egan, J. W.; Haggerty, B. S.; Rheingold, A. L.; Sendlinger, S. C.; Theopold, K. H. *J. Am. Chem. Soc.* **1990**, *112*, 2445.
(138) Zhang, X.; Loppnow, G.; Mcdonald, R.; Takats, J. *J. Am. Chem. Soc.* **1995**, *117*, 7828.
(139) Qin, K.; Incarvito, C.; Rheingold, A.; Theopold, K. *Angew. Chem., Int. Ed.* **2002**, *41*, 2333.
(140) Spencer, D. J. E.; Reynolds, A. M.; Holland, P. L.; Jazdzewski, B. A.; Duboc-Toia, C.; Le Pape, L.; Yokota, S.; Tachi, Y.; Itoh, S.; Tolman, W. B. *Inorg. Chem.* **2002**, *41*, 6307.
(141) Gubelmann, M. H.; Williams, A. F. *Struct. Bonding (Berlin)* **1983**, *55*, 1.
(142) Fredericq, L. *C. R. Acad. Sci.* **1878**, *87*, 996.
(143) Fredericq, L. *Arch. Zool. Exp.* **1878**, *7*, 535.
(144) Karlin, K. D.; Cruse, R. W.; Gultneh, Y.; Hayes, J. C.; Zubieta, J. *J. Am. Chem. Soc.* **1984**, *106*, 3372.
(145) Karlin, K. D.; Cruse, R. W.; Gultneh, Y.; Farooq, A.; Hayes, J. C.; Zubieta, J. *J. Am. Chem. Soc.* **1987**, *109*, 2668.
(146) Cruse, R. W.; Kaderli, S.; Karlin, K. D.; Zuberbühler, A. D. *J. Am. Chem. Soc.* **1988**, *110*, 6882.
(147) Karlin, K. D.; Hays, J. C.; Gultneh, Y.; Cruse, R. W.; Mckown, J. W.; Hutchinson, J. P.; Zubieta, J. *J. Am. Chem. Soc.* **1984**, *106*, 2121.
(148) Tyeklár, Z.; Karlin, K. D. *Acc. Chem. Res.* **1989**, *22*, 241.
(149) Suzuki, M.; Furutachi, H.; Okawa, H. *Coord. Chem. Rev.* **2000**, *200*, 105.
(150) Blackburn, N. J.; Strange, R. W.; Cruse, R. W.; Karlin, K. D. *J. Am. Chem. Soc.* **1987**, *109*, 1235.
(151) Pate, J. E.; Cruse, R. W.; Karlin, K. D.; Solomon, E. I. *J. Am. Chem. Soc.* **1987**, *109*, 2624.
(152) Karlin, K. D.; Cruse, R. W.; Gultneh, Y. *J. Chem. Soc., Chem. Commun.* **1987**, 599.
(153) Karlin, K. D.; Ghosh, P.; Cruse, R. W.; Farooq, A.; Gultneh, Y.; Jacobson, R. R.; Blackburn, N. J.; Strange, R. W.; Zubieta, J. *J. Am. Chem. Soc.* **1988**, *110*, 6769.
(154) Sorrell, T. N.; Vankai, V. A. *Inorg. Chem.* **1990**, *29*, 1687.
(155) Mahrooftahir, M.; Murthy, N. N.; Karlin, K. D.; Blackburn, N. J.; Shaikh, S. N.; Zubieta, J. *Inorg. Chem.* **1992**, *31*, 3001.
(156) Murthy, N. N.; Mahroof-Tahir, M.; Karlin, K. D. *Inorg. Chem.* **2001**, *40*, 628.
(157) Mahrooftahir, M.; Karlin, K. D. *J. Am. Chem. Soc.* **1992**, *114*, 7599.
(158) Nasir, M. S.; Karlin, K. D.; Mcgowty, D.; Zubieta, J. *J. Am. Chem. Soc.* **1991**, *113*, 698.
(159) Karlin, K. D.; Gan, Q. F.; Tyeklár, Z. *Chem. Commun.* **1999**, 2295.
(160) Baldwin, M. J.; Ross, P. K.; Pate, J. E.; Tyeklár, Z.; Karlin, K. D.; Solomon, E. I. *J. Am. Chem. Soc.* **1991**, *113*, 8671.
(161) Solomon, E. I.; Tuczek, F.; Root, D. E.; Brown, C. A. *Chem. Rev.* **1994**, *94*, 827.
(162) Ma, H.; Allmendinger, M.; Thewalt, U.; Lentz, A.; Klinga, M.; Rieger, B. *Eur. J. Inorg. Chem.* **2002**, 2857.
(163) Rockcliffe, D. A.; Martell, A. E.; Reibenspies, J. H. *J. Chem. Soc., Dalton Trans.* **1996**, 167.
(164) Rockcliffe, D. A.; Martell, A. E. *J. Chem. Soc., Chem. Commun.* **1992**, 1758.
(165) Asato, E.; Hashimoto, S.; Matsumoto, N.; Kida, S. *J. Chem. Soc., Dalton Trans.* **1990**, 1741.
(166) Ngwenya, M. P.; Chen, D.; Martell, A. E.; Reibenspies, J. *Inorg. Chem.* **1991**, *30*, 2732.
(167) Rockcliffe, D. A.; Martell, A. E. *Inorg. Chem.* **1993**, *32*, 3143.
(168) Rockcliffe, D. A.; Martell, A. E. *J. Mol. Catal. A: Chem.* **1995**, *99*, 101.
(169) Martell, A. E.; Motekaitis, R. J.; Menif, R.; Rockcliffe, D. A.; Llobet, A. *J. Mol. Catal. A: Chem.* **1997**, *117*, 205.
(170) Speier, G.; Tyeklár, Z.; Toth, P.; Speier, E.; Tisza, S.; Rockenbauer, A.; Whalen, A. M.; Alkire, N.; Pierpont, C. G. *Inorg. Chem.* **2001**, *40*, 5653.
(171) Henson, M. J.; Vance, M. A.; Zhang, C. X.; Liang, H. C.; Karlin, K. D.; Solomon, E. I. *J. Am. Chem. Soc.* **2003**, *125*, 5186.
(172) Uozumi, K.; Hayashi, Y.; Suzuki, M.; Uehara, A. *Chem. Lett.* **1993**, 963.
(173) Schatz, M.; Becker, M.; Thaler, F.; Hampel, F.; Schindler, S.; Jacobson, R. R.; Tyeklár, Z.; Murthy, N. N.; Ghosh, P.; Chen, Q.; Zubieta, J.; Karlin, K. D. *Inorg. Chem.* **2001**, *40*, 2312.
(174) Wei, N.; Murthy, N. N.; Tyeklár, Z.; Karlin, K. D. *Inorg. Chem.* **1994**, *33*, 1177.

(175) Halfen, J. A.; Young, V. G.; Tolman, W. B. *J. Am. Chem. Soc.* **1996**, *118*, 10920.
(176) Berreau, L. M.; Halfen, J. A.; Young, V. G.; Tolman, W. B. *Inorg. Chim. Acta* **2000**, *297*, 115.
(177) Bol, J. E.; Driessen, W. L.; Ho, R. Y. N.; Maase, B.; Que, L.; Reedijk, J. *Angew. Chem., Int. Ed. Engl.* **1997**, *36*, 998.
(178) He, C.; Dubois, J. L.; Hedman, B.; Hodgson, K. O.; Lippard, S. J. *Angew. Chem., Int. Ed.* **2001**, *40*, 1484.
(179) Foxon, S. P.; Walter, O.; Schindler, S. *Eur. J. Inorg. Chem.* **2002**, 111.
(180) Kamaraj, K.; Kim, E.; Galliker, B.; Zakharov, L. N.; Rheingold, A. L.; Zuberbühler, A. D.; Karlin, K. D. *J. Am. Chem. Soc.* **2003**, *125*, 6028.
(181) Schindler, S.; Hubbard, C. D.; Van Eldik, R. *Chem. Soc. Rev.* **1998**, *27*, 387.
(182) Hayashi, H.; Fujinami, S.; Nagatomo, S.; Ogo, S.; Suzuki, M.; Uehara, A.; Watanabe, Y.; Kitagawa, T. *J. Am. Chem. Soc.* **2000**, *122*, 2124.
(183) Hayashi, H.; Uozumi, K.; Fujinami, S.; Nagatomo, S.; Shiren, K.; Furutachi, H.; Suzuki, M.; Uehara, A.; Kitagawa, T. *Chem. Lett.* **2002**, 416.
(184) Chuang, C.; Lim, K.; Chen, Q.; Zubieta, J.; Canary, J. W. *Inorg. Chem.* **1995**, *34*, 2562.
(185) Comba, P.; Schiek, W. *Coord. Chem. Rev.* **2003**, *238*, 21.
(186) Comba, P.; Lienke, A. *Inorg. Chem.* **2001**, *40*, 5206.
(187) Becker, M.; Heinemann, F. W.; Knoch, F.; Donaubauer, W.; Liehr, G.; Schindler, S.; Golub, G.; Cohen, H.; Meyerstein, D. *Eur. J. Inorg. Chem.* **2000**, 719.
(188) Comba, P.; Hilfenhaus, P.; Karlin, K. D. *Inorg. Chem.* **1997**, *36*, 2309.
(189) Bode, R. H.; Bol, J. E.; Driessen, W. L.; Hulsbergen, F. B.; Reedijk, J.; Spek, A. L. *Inorg. Chem.* **1999**, *38*, 1239.
(190) Heirwegh, K.; Borginon, H.; Lontie, R. *Biochim. Biophys. Acta* **1961**, *48*, 517.
(191) Van Holde, K. E. *Biochemistry* **1967**, *6*, 93.
(192) Freedman, T. B.; Loehr, J. S.; Loehr, T. M. *J. Am. Chem. Soc.* **1976**, *98*, 2809.
(193) Ling, J. S.; Nestor, L. P.; Czernuszewicz, R. S.; Spiro, T. G.; Fraczkiewicz, R.; Sharma, K. D.; Loehr, T. M.; Sandersloehr, J. *J. Am. Chem. Soc.* **1994**, *116*, 7682.
(194) Gaykema, W. P. J.; Hol, W. G. J.; Vereijken, J. M.; Soeter, N. M.; Bak, H. J.; Beintema, J. J. *Nature* **1984**, *303*, 23.
(195) Kitajima, N.; Koda, T.; Hashimoto, S.; Kitagawa, T.; Moro-Oka, Y. *J. Chem. Soc., Chem. Commun.* **1988**, 151.
(196) Ross, P. K.; Solomon, E. I. *J. Am. Chem. Soc.* **1990**, *112*, 5871.
(197) Kitajima, N.; Koda, T.; Hashimoto, S.; Kitagawa, T.; Moro-Oka, Y. *J. Am. Chem. Soc.* **1991**, *113*, 5664.
(198) Kitajima, N.; Fujisawa, K.; Fujimoto, C.; Moro-Oka, Y.; Hashimoto, S.; Kitagawa, T.; Toriumi, K.; Tatsumi, K.; Nakamura, A. *J. Am. Chem. Soc.* **1992**, *114*, 1277.
(199) Thompson, J. S. *J. Am. Chem. Soc.* **1984**, *106*, 4057.
(200) Addison, A. W.; Rao, T. N.; Reedijk, J.; Van Rijn, J.; Verschoor, G. C. *J. Chem. Soc., Dalton Trans.* **1984**, 1349.
(201) Kodera, M.; Katayama, K.; Tachi, Y.; Kano, K.; Hirota, S.; Fujinami, S.; Suzuki, M. *J. Am. Chem. Soc.* **1999**, *121*, 11006.
(202) Lam, B. M. T.; Halfen, J. A.; Young, V. G.; Hagadorn, J. R.; Holland, P. L.; Lledos, A.; Cucurull Sanchez, L.; Novoa, J. J.; Alvarez, S.; Tolman, W. B. *Inorg. Chem.* **2000**, *39*, 4059.
(203) Hu, Z.; George, G. N.; Gorun, S. M. *Inorg. Chem.* **2001**, *40*, 4812.
(204) Hu, Z. B.; Williams, R. D.; Tran, D.; Spiro, T. G.; Gorun, S. M. *J. Am. Chem. Soc.* **2000**, *122*, 3556.
(205) Ross, P. K.; Solomon, E. I. *J. Am. Chem. Soc.* **1991**, *113*, 3246.
(206) Baldwin, M. J.; Root, D. E.; Pate, J. E.; Fujisawa, K.; Kitajima, N.; Solomon, E. I. *J. Am. Chem. Soc.* **1992**, *114*, 10421.
(207) Henson, M. J.; Mahadevan, V.; Stack, T. D. P.; Solomon, E. I. *Inorg. Chem.* **2001**, *40*, 5068.
(208) Lynch, W. E.; Kurtz, D. M.; Wang, S. K.; Scott, R. A. *J. Am. Chem. Soc.* **1994**, *116*, 11030.
(209) Sorrell, T. N.; Allen, W. E.; White, P. S. *Inorg. Chem.* **1995**, *34*, 952.
(210) Cvetkovic, M.; Batten, S. R.; Moubaraki, B.; Murray, K. S.; Spiccia, L. *Inorg. Chim. Acta* **2001**, *324*, 131.
(211) Sanyal, I.; Mahrooftahir, M.; Nasir, M. S.; Ghosh, P.; Cohen, B. I.; Gultneh, Y.; Cruse, R. W.; Farooq, A.; Karlin, K. D.; Liu, S. C.; Zubieta, J. *Inorg. Chem.* **1992**, *31*, 4322.
(212) Pidcock, E.; Debeer, S.; Obias, H. V.; Hedman, B.; Hodgson, K. O.; Karlin, K. D.; Solomon, E. I. *J. Am. Chem. Soc.* **1999**, *121*, 1870.
(213) Itoh, S.; Kumei, H.; Taki, M.; Nagatomo, S.; Kitagawa, T.; Fukuzumi, S. *J. Am. Chem. Soc.* **2001**, *123*, 6708.
(214) Itoh, S.; Nakao, H.; Berreau, L. M.; Kondo, T.; Komatsu, M.; Fukuzumi, S. *J. Am. Chem. Soc.* **1998**, *120*, 2890.
(215) Osako, T.; Tachi, Y.; Taki, M.; Fukuzumi, S.; Itoh, S. *Inorg. Chem.* **2001**, *40*, 6604.
(216) Karlin, K. D.; Nasir, M. S.; Cohen, B. I.; Cruse, R. W.; Kaderli, S.; Zuberbühler, A. D. *J. Am. Chem. Soc.* **1994**, *116*, 1324.
(217) Karlin, K. D.; Haka, M. S.; Cruse, R. W.; Gultneh, Y. *J. Am. Chem. Soc.* **1985**, *107*, 5828.
(218) Blackburn, N. J.; Strange, R. W.; Farooq, A.; Haka, M. S.; Karlin, K. D. *J. Am. Chem. Soc.* **1988**, *110*, 4263.
(219) Karlin, K. D.; Tyeklár, Z.; Farooq, A.; Haka, M. S.; Ghosh, P.; Cruse, R. W.; Gultneh, Y.; Hayes, J. C.; Toscano, P. J.; Zubieta, J. *Inorg. Chem.* **1992**, *31*, 1436.
(220) Pidcock, E.; Obias, H. V.; Abe, M.; Liang, H. C.; Karlin, K. D.; Solomon, E. I. *J. Am. Chem. Soc.* **1999**, *121*, 1299.
(221) Liang, H. C.; Karlin, K. D.; Dyson, R.; Kaderli, S.; Jung, B.; Zuberbühler, A. D. *Inorg. Chem.* **2000**, *39*, 5884.
(222) Karlin, K. D.; Haka, M. S.; Cruse, R. W.; Meyer, G. J.; Farooq, A.; Gultneh, Y.; Hayes, J. C.; Zubieta, J. *J. Am. Chem. Soc.* **1988**, *110*, 1196.
(223) Battaini, G.; De Carolis, M.; Monzani, E.; Tuczek, F.; Casella, L. *Chem. Commun.* **2003**, 726.
(224) Santagostini, L.; Gullotti, M.; Monzani, E.; Casella, L.; Dillinger, R.; Tuczek, F. *Chem. Eur. J.* **2000**, *6*, 519.
(225) Holland, P. L.; Cramer, C. J.; Wilkinson, E. C.; Mahapatra, S.; Rodgers, K. R.; Itoh, S.; Taki, M.; Fukuzumi, S.; Que, L.; Tolman, W. B. *J. Am. Chem. Soc.* **2000**, *122*, 792.
(226) Taki, M.; Teramae, S.; Nagatomo, S.; Tachi, Y.; Kitagawa, T.; Itoh, S.; Fukuzumi, S. *J. Am. Chem. Soc.* **2002**, *124*, 6367.
(227) Reger, D. L.; Collins, J. E.; Rheingold, A. L.; Liable-Sands, L. M. *Organometallics* **1996**, *15*, 2029.
(228) Karlin, K. D.; Gan, Q. F.; Farooq, A.; Liu, S. C.; Zubieta, J. *Inorg. Chem.* **1990**, *29*, 2549.
(229) Karlin, K. D.; Gultneh, V.; Hayes, J. C.; Zubieta, J. *Inorg. Chem.* **1984**, *23*, 519.
(230) Lee, S. C.; Holm, R. H. *Inorg. Chem.* **1993**, *32*, 4745.
(231) Zhang, C. X.; Liang, H. C.; Kim, E. I.; Shearer, J.; Helton, M. E.; Kim, E.; Kaderli, S.; Incarvito, C. D.; Zuberbühler, A. D.; Rheingold, A. L.; Karlin, K. D. *J. Am. Chem. Soc.* **2003**, *125*, 634.
(232) Ryan, S.; Adams, H.; Fenton, D. E.; Becker, M.; Schindler, S. *Inorg. Chem.* **1998**, *37*, 2134.
(233) Pidcock, E.; Obias, H. V.; Zhang, C. X.; Karlin, K. D.; Solomon, E. I. *J. Am. Chem. Soc.* **1998**, *120*, 7841.
(234) Jung, B.; Karlin, K. D.; Zuberbühler, A. D. *J. Am. Chem. Soc.* **1996**, *118*, 3763.
(235) Zhang, C. X.; Liang, H. C.; Kim, E.; Gan, Q. F.; Tyeklár, Z.; Lam, K. C.; Rheingold, A. L.; Kaderli, S.; Zuberbühler, A. D.; Karlin, K. D. *Chem. Commun.* **2001**, 631.
(236) Sayre, L. M.; Nadkarni, D. V. *J. Am. Chem. Soc.* **1994**, *116*, 3157.
(237) Mandal, S.; Macikenas, D.; Protasiewicz, J. D.; Sayre, L. M. *J. Org. Chem.* **2000**, *65*, 4804.
(238) Thompson, J. S. *J. Am. Chem. Soc.* **1984**, *106*, 8308.
(239) Tolman, W. B. *Acc. Chem. Res.* **1997**, *30*, 227.
(240) Cahoy, J.; Holland, P. L.; Tolman, W. B. *Inorg. Chem.* **1999**, *38*, 2161.
(241) Que, L., Jr.; Tolman, W. B. *Angew. Chem., Int. Ed.* **2002**, *41*, 1114.
(242) Mahadevan, V.; Hou, Z. G.; Cole, A. P.; Root, D. E.; Lal, T. K.; Solomon, E. I.; Stack, T. D. P. *J. Am. Chem. Soc.* **1997**, *119*, 11996.
(243) Mahadevan, V.; Dubois, J. L.; Hedman, B.; Hodgson, K. O.; Stack, T. D. P. *J. Am. Chem. Soc.* **1999**, *121*, 5583.
(244) Holland, P. L.; Rodgers, K. R.; Tolman, W. B. *Angew. Chem., Int. Ed.* **1999**, *38*, 1139.
(245) Mahadevan, V.; Henson, M. J.; Solomon, E. I.; Stack, T. D. P. *J. Am. Chem. Soc.* **2000**, *122*, 10249.
(246) Funahashi, Y.; Nakaya, K.; Hirota, S.; Yamauchi, O. *Chem. Lett.* **2000**, 1172.
(247) Straub, B. F.; Rominger, F.; Hofmann, P. *Chem. Commun.* **2000**, 1611.
(248) Mahapatra, S.; Halfen, J.; Wilkinson, E.; Pan, G.; Cramer, C. J.; Que, L., Jr.; Tolman, W. B. *J. Am. Chem. Soc.* **1995**, *117*, 8865.
(249) Mahapatra, S.; Young, V. G.; Kaderli, S.; Zuberbühler, A. D.; Tolman, W. B. *Angew. Chem., Int. Ed. Engl.* **1997**, *36*, 130.
(250) Henson, M. J.; Mukherjee, P.; Root, D. E.; Stack, T. D. P.; Solomon, E. I. *J. Am. Chem. Soc.* **1999**, *121*, 10332.
(251) Ottenwaelder, X.; Mahadevan, V.; Stack, T. D. P. Unpublished results.
(252) Halfen, J. A.; Mahapatra, S.; Wilkinson, E. C.; Kaderli, S.; Young, V.; Que, L., Jr.; Zuberbühler, A. D.; Tolman, W. B. *Science* **1996**, *271*, 1397.
(253) Mahapatra, S.; Halfen, J. A.; Tolman, W. B. *J. Am. Chem. Soc.* **1996**, *118*, 11575.
(254) Enomoto, M.; Aida, T. *J. Am. Chem. Soc.* **1999**, *121*, 874.
(255) Holland, P. L.; Rodgers, K. R.; Tolman, W. B. *Angew. Chem., Int. Ed.* **1999**, *38*, 1139.
(256) Taki, M.; Itoh, S.; Fukuzumi, S. *J. Am. Chem. Soc.* **2002**, *124*, 998.
(257) Taki, M.; Itoh, S.; Fukuzumi, S. *J. Am. Chem. Soc.* **2001**, *123*, 6203.
(258) Itoh, S.; Fukuzumi, S. *Bull. Chem. Soc. Jpn.* **2002**, *75*, 2081.
(259) Cramer, C. J.; Smith, B. A.; Tolman, W. B. *J. Am. Chem. Soc.* **1996**, *118*, 11283.
(260) Bérces, A. *Inorg. Chem.* **1997**, *36*, 4831.
(261) Flock, M.; Pierloot, K. *J. Phys. Chem. A* **1999**, *103*, 95.

(262) Siegbahn, P. E. M. *J. Biol. Inorg. Chem.* **2003**, *8*, 577.
(263) Cole, A. P.; Root, D. E.; Mukherjee, P.; Solomon, E. I.; Stack, T. D. P. *Science* **1996**, *273*, 1848.
(264) Mukherjee, P. Ph.D. Thesis, Stanford University, 2000.
(265) Root, D. E.; Henson, M. J.; Machonkin, T.; Mukherjee, P.; Stack, T. D. P.; Solomon, E. I. *J. Am. Chem. Soc.* **1998**, *120*, 4982.
(266) Machonkin, T.; Mukherjee, P.; Stack, T. D. P.; Solomon, E. I. *Inorg. Chim. Acta* **2002**, *341*, 39.
(267) Bérces, A. *Chem. Eur. J.* **1998**, *4*, 1297.
(268) Daul, C. A.; Fernandez-Ceballos, S.; Ciofini, I.; Rauzy, C.; Schläpfer, C.-W. *Chem. Eur. J.* **2002**, *8*, 4392.
(269) Ciofini, I.; Daul, C. *Coord. Chem. Rev.* **2003**, *238*, 187.
(270) Zumft, W. G. *Microbiol. Mol. Biol. Rev.* **1997**, *61*, 533.
(271) Brown, K.; Djinovic-Carugo, K.; Haltia, T.; Cabrito, I.; Saraste, M.; Moura, J. J. G.; Moura, I.; Tegoni, M.; Cambillau, C. *J. Biol. Chem.* **2000**, *275*, 41133.
(272) Brown, K.; Tegoni, M.; Prudencio, M.; Pereira, A. S.; Besson, S.; Moura, J. J. G.; Moura, I.; Cambillau, C. *Nat. Struct. Biol.* **2000**, *7*, 191.
(273) Reim, J.; Krebs, B. *Angew. Chem., Int. Ed. Engl.* **1994**, *33*, 1969.
(274) Reim, J.; Werner, R.; Haase, W.; Krebs, B. *Chem. Eur. J.* **1998**, *4*, 289.
(275) Meyer, F.; Pritzkow, H. *Angew. Chem., Int. Ed.* **2000**, *39*, 2112.

CR020632Z